Effect of hydrologic and hydraulic calculation approaches on pier scour estimates

by

Luis Fernando Castaneda Galvis

A thesis submitted to the Graduate Faculty of Civil and Environmental Engineering
Auburn University
in partial fulfillment of the
requirements for the Degree of
Master of Science in Civil and Environmental Engineering

Auburn, Alabama
December 9, 2023

HEC-HMS, RRE, SCS Curve Number, HEC-RAS, 1D- models, 2D models, Pier bridge Scour, HEC-18, Hydraulic Toolboox, Observation Method for Scour

Approved by

Dr. Jose G. Vasconcelos, Committee Chair, Professor of Civil Engineering
Dr. J. Brian Anderson, Committee member, Professor of Civil Engineering
Dr. Xing Fang, Committee member, Professor of Civil Engineering

Abstract

Bridge scour, a phenomenon characterized by the erosion and removal of sediment from the vicinity of bridge foundations, is a significant concern in the fields of civil engineering and infrastructure management. There are various hydrologic and hydraulic approaches to calculating the peak flow that are used to determine the water depth and velocity in the vicinity of a bridge, which are variables used for scour estimates. Depending on the assumptions, limitations, and boundary conditions, each approach can yield significantly different flow results that influence water depth and velocity estimates. Also, even when methods estimate similar flow magnitudes, different velocity distributions can result from bridge configurations between these methods. The extent to which these methods can influence pier scour depth estimation is not well understood due to a lack of systematic investigations. This research addresses this question by evaluating pier scour on four bridges with 12 combinations of hydrological and hydraulic approaches for a total of 48 simulations.

Each simulation was analyzed to assess the potential pier scour depth using the FHWA HEC-18 and the Observation Method for Scour methodologies. There are various alternatives to calculating the peak flow: Regional Regression Equations (RRE), Flood Frequency Analysis (FFA), and distributed models using HEC-HMS 4.9 were evaluated using the SCS Curve Number for abstractions and different antecedent moisture conditions.

The peak flow was estimated for a 100-yr event, and the hydrological models were simulated for one event-based. HEC-RAS 6.1/6.2 was utilized for the hydraulics analysis, and 1D-WSPRO, 1D-Energy, 2D SA connection, and 2D terrain modification with raised piers were used as bridge modeling approaches. The models in HEC-RAS were created using Lidar data with a resolution of 1 meter x 1 meter (3.28 x 3.28 ft). The results showed that the

regression equations, often used by state DOT's, do not always yield the worst-case hydrological scenario when compared with hydrological models' simulation. The results of the 1D models are very similar, and in most cases, they produce less scour depth. The 2D approaches better represent the approach channel for the bridges with complex configurations and depict large velocities and therefore more scour depth than the 1D models. Lastly, it was found that the moisture conditions can influence determining the worst-case scenario for peak flow determinations, which in turn impact the scour calculations.

Acknowledgments

I would like to give special thanks to my wife, Wendy, for her support. She has been with me despite the difficulties, and I want to say that I love her. My son Daniel is my best friend, and now he has become a strong, brave man. To my little daughter, María Alejandra, because it was love at first sight and God had a perfect plan for her.

I would like to thank my parents, who always supported me despite the decisions that I made, which were not always the best. I love them, and I hope they continue to give me their wisdom.

I would like to acknowledge and give my warmest thanks to my advisor, Jose Goes Vasconcelos Neto, who gave me the confidence and the opportunity to be here and make this work possible. I appreciate all his support during these two years.

I would also like to thank God, the God of the impossible "Here I am". He knows despite the proof I stood firm believing in the promises that he wants to me. "I will instruct you and teach you the way you should go; I will counsel you with my loving eye on you"- Psalms 32-8

I would like to say thanks to the Alabama DOT for supporting this project and all the help that they gave us during these two years.

Table of Contents

List of Tables

List of Figures

List of Abbreviations

AASHTO	American Association of State Highway Transportation Officials
ALDOT	Alabama Department of Transportation
DEM	Digital Elevation Models
FHWA	Federal Highway Administration
HEC-RAS	Hydrologic Engineering Center – River Analysis System
HEC-HMS	Hydrologic Engineering Center – Hydrologic Modeling System
OMS	Observation method for scour
TxDOT	Texas Department of Transportation
USGS	United States of Geological Survey
TRB	Transportation Research Board
RRE	Regional Regression Equations
FFA	Flood Frequency Analysis

1. INTRODUCTION AND OBJECTIVES

According to Wang and Liang (2017), scour is a natural occurrence that results from the erosive action of a flowing stream on erodible beds. Scour is a common problem where water, soil, and structure interact (Prendergast and Gavin, 2014). It is the digging up and removal of material from the bed and banks of streams caused by the erosive action of moving water (Hamill, 1999).

Bridge scour is a pressing concern in civil engineering and infrastructure management, posing a significant threat to the safety and stability of bridges worldwide (Melville and Sutherland, 1988). This phenomenon, characterized by the erosive removal of sediment from the vicinity of bridge foundations, has been responsible for numerous catastrophic bridge failures, leading to substantial economic and human losses (Richardson and Davis, 2001). The prediction and assessment of bridge scour are paramount in ensuring the resilience and longevity of bridge structures (Froehlich and Pilarczyk, 2017)

Hydraulic Engineering Circular No. 18 (HEC-18), is a reference for designing, evaluating, and inspecting bridges for scour (Anerson et al., 2012), and provides a deterministic procedure to calculate the scour depth near the bridge site using the median particle size (D50) and a peak flow, usually based on a 100-year design flood event. The magnitude of the flood event is specified by the watershed characteristics and the rainfall distribution (Chow et. al, 1988). There are different ways to calculate the peak flow which are, Rational Method (Mulvaney, T. J.,1851), SCS Curve Number Method (Mockus, V.,1972), Unit Hydrograph Method (Clark, C.O. 1945; Snyder, W. M., 1938; Mockus, V.,1972), Flood frequency Analysis (Chow et al, 1953), distributed hydrological models (Fleming, M. J., & Doan, J. H., 2009: Rossman, 2010; Neitsch et al, 2009) and Regional

Regression Equations (Ries et al., 2007). The most common method used by state's Department of Transportation is the Regional Regression Equations (RRE), because of their simplicity and the ease of data collection to determine peak flows associated with a given interval recurrence interval.

For the state of Alabama, there are different technical documents related to RRE, for peak flow (Anderson, B. T., 2020) (Hedgecock, 2004) and (Hedgecock and Lee, 2010), for low flow, and annual flow statistics (Feaster et al., 2020). Alternatively, the distributed hydrological models (Fleming, M. J., & Doan, J. H., 2009; Rossman, 2010; Neitsch et al., 2009) can be used to estimate the abstractions characterizing the hydrological processes, including interception, evapotranspiration, infiltration, runoff formation, and movement at both the cell and basin scales. These methods are physically based models, and the results are more representative of local conditions in watersheds.

Once the peak flow is calculated, it is necessary to develop the bridge scour calculations to estimate the velocity and the water depth in the vicinity of the bridge. Usually, there are different hydraulic modeling approaches to estimate the head losses associated with the bridge structure, and they can be one-dimensional (1D) or two-dimensional (2D). Depending on the method used to calculate velocity and the water depth, the values of these variables present differences in magnitude, direction, and distribution (Brunner et al., 2020). Those differences result in a given peak flow value. Even though there are several alternatives to calculate the peak flow and different bridge modeling approaches, there is not a systematic study to evaluate the differences in results for combinations of different alternatives to calculate the peak flow and different bridge modeling approaches based on 1D and 2D models. The research question that this study aims to address is:

To what extent can pier scour estimates be influenced by varying alternatives to hydrologic and hydraulic computational approaches?

1.1. Objectives

This research aims to address the research question by performing a systematic study in which different hydrologic and hydraulic approaches are used for scour estimates on four bridges in Alabama. Specifically, this study proposes:

- To calculate the peak flow for four selected bridges in Alabama using Regional Regression Equations (RRE) and distributed models using HEC-HMS 4.9 for different antecedent soil moisture conditions and a 100-yr flood event.
- To evaluate for the four selected Bridges, four different bridge modeling approaches using HEC-RAS 6.1/6.2 and models in 1D and 2D (1D WSPRO, 1D Energy, 2D SA connection, 2D Terrain modification with raised piers)
- To use these hydrological and hydraulic results to conduct scour calculations using Hydrologic Engineering Circular HEC-18 and the Observation Method for Scour and analyze these results.

2. LITERATURE REVIEW

2.1. Hydrological methods for peak flow rates

Peak flow estimates are often used for the design of conveyance systems in open channels. There are different ways to estimate peak flows depending on whether the watershed is gauged or ungauged. In gaged sites, it is common to use Flood Frequency Analysis (FFA), considering that there exists an inverse relationship between the magnitude of an extreme event and its frequency of occurrence, according to Chow et al. (1988). In ungauged sites, methods such as Regional Regression Equations (RRE) are used to calculate peak flows along with hydrological modeling results. The difference between these methods in ungauged watersheds is that the latter consider abstractions or losses, which are linked to physical processes such as infiltration (Green and Ampt, 1911), interception (Goudriaan and Monteith, 1990), evaporation (Penman, 1948; Priestley and Taylor, 1972), and evapotranspiration (Monteith and Unsworth, 2013). In addition, there is a method to calculate the direct runoff and quantify the abstractions developed by the Soil Conservation Service (SCS) (Mockus, 1972), known as the SCS method for abstractions, that is based on land cover, land use, area, and hydrological conditions.

This research compares peak flow predictions using FFA, RRE, and hydrological models for gauged sites and RRE and hydrological models for ungauged sites. The subsequent section presents a brief description of the hydrological methods used in this study.

2.1.1 Flood Frequency Analysis (FFA)

The primary aim of conducting a frequency analysis on hydrologic data is to establish the relationship between the occurrence of severe events and their corresponding magnitudes, utilizing probability distributions. Typically, the values used in this approach refer to the annual maximum discharge, denoting the highest instantaneous peak flow observed at any given point throughout the year. It is assumed that consecutive measurements of this variable across different years are statistically independent (Chow, 1953).

The observed data should typically be adjusted to an extreme value (EV) probability distribution, considering the goodness of fit product of the null hypothesis that the data are distributed as expected. If the goodness of fit test indicates that the data does not follow the expected distribution, then an alternative extreme value probability distribution may need to be considered. This adjustment ensures that the observed data adequately represents the extremes and allows for more accurate analysis and predictions. The most common extreme value distributions are the Gumbel extreme value distribution and the log-Pearson Type III distribution. The log-Pearson Type III distribution is a three-parameter gamma distribution with a logarithmic transform of the independent variable (Chow et al., 1988).

Flynn et al. (2006) describe PeakFQ, a software application developed by the United States Geological Survey (USGS) that integrates the principles outlined in Bulletin 17B (B17B) of the Interagency Advisory Committee on Water Data (IACWD, 1982). In accordance with B17B, annual peak-flow data must be fitted to a log-Pearson Type III distribution using the Expected Moments Algorithm (EMA) (Cohn et al., 1997) and a generalized version of the Grubbs-Beck test for low outliers (Cohn et al., 2013).

2.1.2 Regional Regression Equations (RRE)

Regression equations are used to estimate peak flows at ungagged or limited sites. The United States Geological Survey (USGS) has created and compiled regional regression equations, which are incorporated in computer software called the National Streamflow Statistics software (NSS) (Ries III et al., 2007), which is the foundation for StreamStats (Ries III et al., 2004) and allows quick estimation of peak flows throughout the US.

Brown et al. (2009) mention how the rural equations were built for all the states based on a series of studies conducted by the USGS, State Highway, and other agencies. Those equations are based on watershed and climatic characteristics within specific regions of each state that can be obtained from topographic maps, rainfall reports, and atlases. These regression equations are generally referred to as Equation 1.

$$RQ_T = a\ A^b\ B^C\ C^d \quad \textbf{(1)}$$

Where:

RQ_T=T- year rural peak flow

A= Regression constant

b, c, d= Regression coefficients

A, B, C= Basin characteristics

Brown et al. (2009) describe how the USGS developed seven-parameter nationwide urban regression equations to convert rural peak flows to urban peak flows. The urban equations are based on data from 269 basins across 56 cities and 31 states. These equations have been systematically evaluated and shown to provide accurate estimates of peak flows with recurrence intervals ranging from 2 to 500 years, with findings errors that may still be

on the order of 35 to 50% when compared to field measurements. Those errors can be too large for bridge scour estimates.

In Alabama, there are different documents to estimate the magnitude of flood frequencies. Most of them are focused on the size of the watershed's characteristics, stream size (small and large), and the magnitude of the analyzed event. Those documents can be split into three types of references related to peak flow (Anderson, 2020) (Hedgecock, 2004) (Hedgecock and Lee, 2010), low flow, and annual flow statistics (Feaster et al., 2020), and are used to estimate annual exceedance probability flows at ungauged locations. They were developed by using current geospatial data, new analytical methods, and annual peak flow (Anderson, 2020).

In those reports, Alabama is divided into four flood regions that were delineated based upon review of residual plots, previous reports, eight-digit hydrologic unit code maps, geologic maps, and physiographic maps (Anderson, 2020). The four flood regions are depicted in Figure 1.

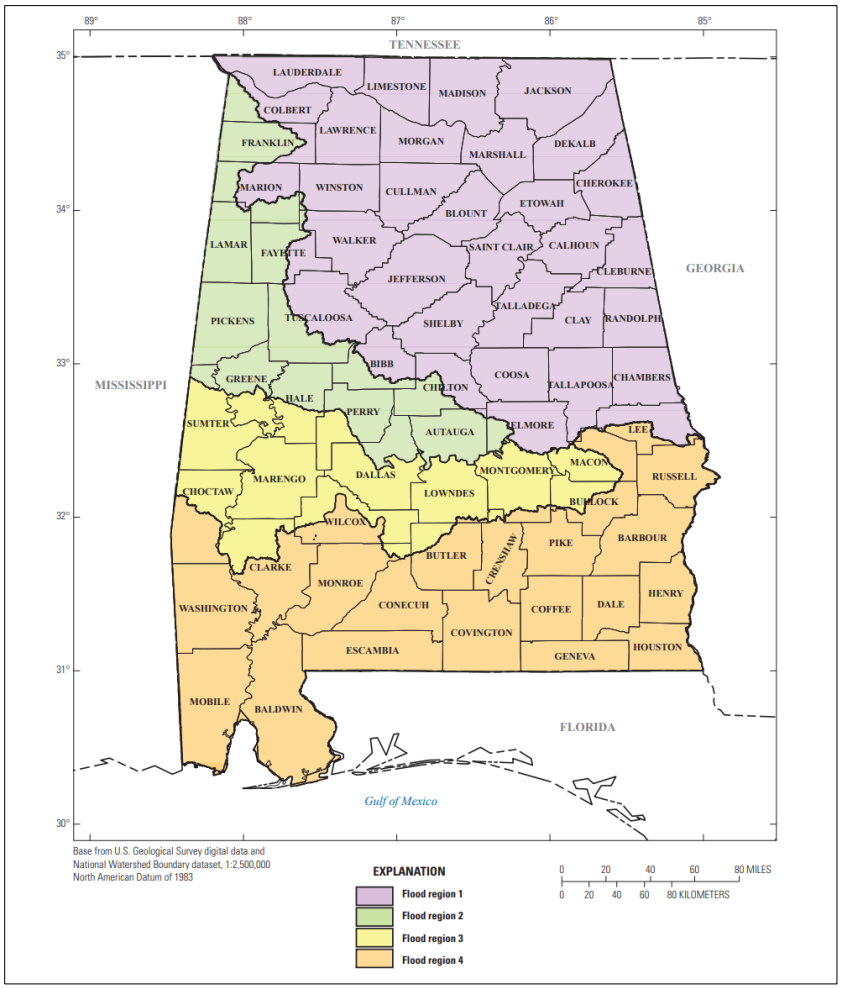

Figure 1. Locations of the Flood regions in Alabama (Anderson, 2020)

2.1.3 Hydrological models

Hydrological models were created to simulate and understand the movement and distribution of water in various natural systems, such as watersheds, rivers, and groundwater aquifers (Chow et al., 1988). There are different types of hydrological models, among which we can highlight empirical and physical-based models, and they differ in their approaches to simulating and predicting hydrological processes. The empirical models are primarily based on historical data and observations, and they do not explicitly consider the underlying physical processes that govern hydrology. On the other hand, the physical-based models are

designed to represent the fundamental physical processes that govern the movement of water in the hydrological cycle. They consider principles of fluid dynamics, conservation of mass, energy, and momentum (Maidment, 1993). Those hydrological models, in turn, can be classified into lumped and distributed models and their difference lies in that lumped models simplify the watershed into a single unit (Chow et al., 1988)., while distributed models consider the spatial variability of hydrological processes (Beven, K. J., & Kirkby, M. J.,1979)

Chen, Y. (2018) defines the distributed hydrological models are a type of hydrological model that divides the terrain of an entire studied basin into numerous cells and then characterizes the hydrological processes, including interception and evapotranspiration, snowmelt, infiltration, and runoff formation and movement at both the cell and basin scales. Some examples are SWWM (Rossman, 2010), SWAT (Neitsch et al, 2009) and HEC-HMS (Feldman, 2000). In this study, the hydrological peak flow was determined using HEC-HMS, and a brief description of these models is presented below.

The Hydrologic Engineering Center (HEC) from the U.S. Army Corps of Engineers developed the Hydrologic Modeling System software, which intends to reproduce hydrological analysis procedures such as event infiltration, unit hydrographs, and hydrologic routing loss models, direct runoff models, hydrologic routing models, naturally occurring confluences and bifurcations, water-control strategies, and an automated calibration package. HEC-HMS also includes procedures necessary for continuous simulation including evapotranspiration, snowmelt, and soil moisture accounting (Feldman, 2000).

In this study, the models were event-based simulations, and thus the effect of evapotranspiration was not considered. In addition, to compute the abstractions was used a method known as SCS curve number developed by the Natural Resources Conservation Services (NRCS), which calculates the peak flow as a function of drainage basin area,

potential watershed storage, and the time of concentration (Mockus, 1972). The rainfall runoff separates total rainfall into direct runoff, retention, and initial abstraction to yield using Equation 2 (Brown et al., 2009).

$$Q_D = \frac{(P - 0.2 \cdot S_R)^2}{P + 0.8 \cdot S_R} \quad \textbf{(2)}$$

Where:

Q_D = Depth of direct runoff (in)

P = depth of 24-hour precipitation (in)

S_R= Potential maximum retention (in)

The potential maximum retention SR is calculated with Equation 3.

$$S_R = \left(\frac{1000}{CN} - 10\right) \quad \textbf{(3)}$$

Where:

CN: Curve Number. CN depends on the Land cover and the hydrological soil groups. The value considered in Equation 3 corresponds to AMC II or normal antecedent moisture conditions. The antecedent moisture conditions (AMC) are the level of saturation that the soil has when the rainfall starts. Exist three different levels of Antecedent Moisture Conditions as is shown in Table 1.

Table 1. CN's correction by antecedent runoff condition (AMC)

Antecedent Moisture Condition	Antecedent Moisture Condition (5-days before)	CN Equation
I	Less than 0.5 in	$CN_I = \frac{4.2 \cdot CN_{II}}{10 - 0.058 \cdot CN_{II}}$
II	0.5 to 1.1 in	CN_{II}
III	Above 1.1 in	$CN_{III} = \frac{23 \cdot CN_{II}}{10 + 0.13 \cdot CN_{II}}$

The antecedent moisture conditions (AMC) were a key part of the hydrological simulations used in this study. This is because different AMC conditions were simulated in each watershed to find the worst-case scenario for bridge scour calculations.

A calibration process was conducted in this research, following the methodological steps proposed by Feldman (2000), which are based on the search optimization parameter values and are illustrated below.

- The process starts with data collection, and each process requires different types of data collection. For instance, rainfall-runoff models require rainfall data and flow time series. Routing models require inflow and outflow data from the routing reach.
- The program uses initial parameter estimates and observed boundary conditions to create models for watershed runoff hydrographs and channel outflow hydrographs. The goal is to compare the model's fit with the real hydrologic system. If the fit isn't satisfactory, the program adjusts the parameters and repeats. The optimal parameter values are reported when the fit is satisfactory, which can be used for flood runoff analyses, such as runoff or routing computations. Figure 2 shows the calibration process diagram used by HEC-HMS.

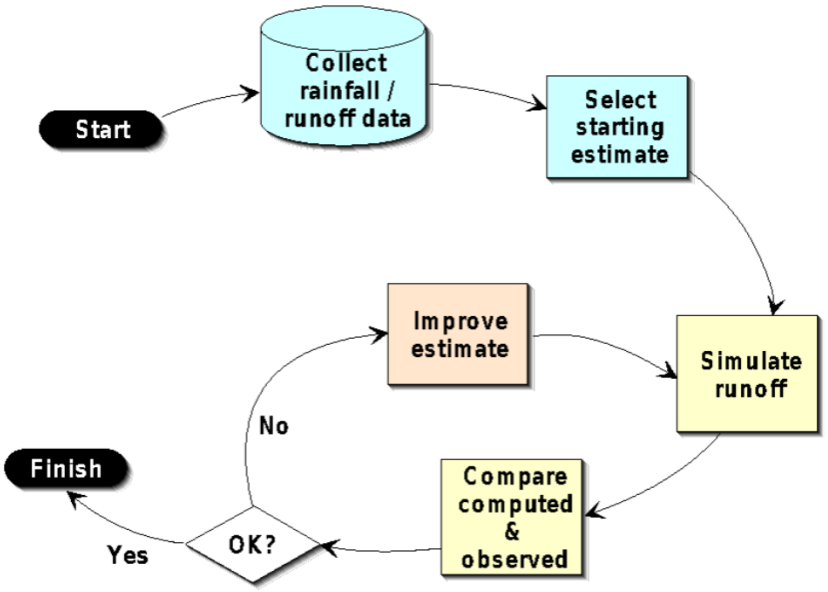

Figure 2. Calibration process diagram used by HEC-HMS. Feldman (2000)

Feldman, (2000) explains how HEC-HMS compares a computed hydrograph to an observed one by computing goodness-of-fit indexes. It uses algorithms to find model parameters that yield the best value of an objective function. The goal is to find reasonable parameters that minimize the objective function's minimum value. The objective functions that HEC-HMS can evaluate in the calibration process are, sum of absolute errors, sum of squared residuals, percent error to peak and peak-weighted root mean square error function. In this research the objective function evaluated was percent error in peak and is shown in Equation 4.

$$Z = 100\,\frac{q_{s(peak)} - q_{O(Peak)}}{q_{O(Peak)}} \qquad \textbf{(4)}$$

2.2. Hydraulics models for stream depth and velocity calculations

Hydraulic models are simplified representations of complex systems like water, vegetation, sediment, and the atmosphere (Robinson et al., 2019). Hydraulic models are simplifications of reality and provide accurate solutions to basic conservation equations when applied correctly (conservation of energy, mass, and momentum). Those models are used for various purposes, including quick answers, detailed planning, structure design, real-time modeling, and predicting dam or levee failure (Brunner et al., 2020). There are many such models (e.g., FLO-2D, TUFLOW, HEC-RAS-2D, and SHR-2D), but this thesis was focused on HEC-RAS as this was the one used in the research.

Brunner and CEIWR-HEC, (2020) illustrate that the River Analysis System (HEC-RAS) developed by the Hydrologic Engineering Center from the U.S. Army Corps of Engineers is a software tool designed for conducting various hydraulic analyses. It enables users to perform calculations related to one-dimensional steady flow hydraulics, as well as one and two-dimensional unsteady flow river hydraulics. Additionally, HEC-RAS facilitates the modeling of sediment transport and mobile bed dynamics in both quasi-unsteady and full unsteady flow scenarios. Furthermore, the software allows for the analysis of water temperature and provides capabilities for generalized water quality modeling, specifically in relation to nutrient fate and transport.

2.2.1 Governing Equations 1D vs 2D models

Brunner and CEIWR-HEC (2016) introduce the governing principles that govern the flow of water in streams are continuity and the conservation of momentum. These principles are theoretically described as partial differential equations. Those principles are employed in the derivation of unsteady flow equations in one and two dimensions, commonly referred to

as shallow water equations. These assumptions include the assumption that water behaves as an incompressible fluid, the pressure distribution follows hydrostatic principles, the vertical acceleration can be considered negligible, the bed slope is relatively mild (less than 10%), the boundary friction can be accounted for using flow resistance laws such as Manning's equation for steady flows, and the Boussinesq approximation is valid, thereby disregarding forces resulting from variations in water density.

One-Dimensional Equations (1D)

Brunner et al. (2020) illustrate that the partial differential equations for the 1D continuity and momentum equations with respect to depth (h) and velocity (u) (See Equation 5 and 6) and the symbols used for motion and mass conservation equations are shown in Figure 3. Those equations are only for 1D flows, and there is a variation for 2D flows which are presented in the next page.

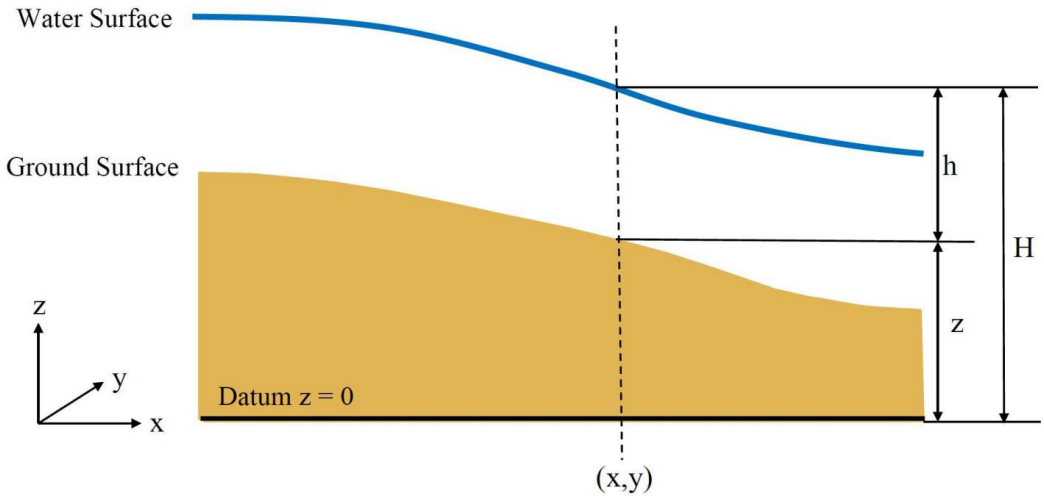

Figure 3. Symbols used. Equations for motion and mass conservation (Brunner et al., 2020)

$$\frac{\partial h}{\partial t} + \frac{\partial (hu)}{\partial x} - q = 0 \quad \textbf{(5)}$$

$$\frac{\partial u}{\partial t} + u\frac{\partial u}{\partial x} + g\left(\frac{\partial h}{\partial x} + S_0 + S_f + S_h\right) = 0 \quad \textbf{(6)}$$

Where:

u = velocity in the x direction

h = depth of water

g = gravity

t = time

x = distance in the direction of flow (x plane)

q = Lateral inflow term (source/sink)

S_0 = Bed slope

S_f = Friction slope, from Manning's equation.

S_h = added force term (Minor Losses)

Two-Dimensional Equations (2D)

Brunner et al. (2020) presents a version of the two-dimensional vertically and laterally average continuity (Equation 7 and 8) and vertically averaged momentum (Equation 9 and 10) and laterally averaged Momentum (Equation 11 and 12) can be written in partial differential equation form, with respect to depth (h)) and velocity (u, v, U, V) as is shown below.

$$\frac{\partial H}{\partial t} + \frac{\partial (hu)}{\partial x} + \frac{\partial (hv)}{\partial y} - q = 0 \quad \textbf{(7)}$$

$$\frac{\partial \mathrm{UB}}{\partial \mathrm{x}} + \frac{\partial \mathrm{WB}}{\partial \mathrm{z}} - qB = 0 \quad \textbf{(8)}$$

$$\frac{\partial u}{\partial t} + u\frac{\partial u}{\partial x} + v\frac{\partial u}{\partial y} = -g\frac{\partial H}{\partial x} + v_t\left(\frac{\partial^2 u}{\partial x^2} + \frac{\partial^2 u}{\partial y^2}\right) - c_f u + fv \quad \textbf{(9)}$$

$$\frac{\partial v}{\partial t} + u\frac{\partial v}{\partial x} + v\frac{\partial v}{\partial y} = -g\frac{\partial H}{\partial x} + v_t\left(\frac{\partial^2 v}{\partial x^2} + \frac{\partial^2 v}{\partial y^2}\right) - c_f v + fu \quad \textbf{(10)}$$

$$\frac{\partial UB}{\partial t} + U\frac{\partial UB}{\partial x} + W\frac{\partial UB}{\partial z} = -g\frac{\partial BH}{\partial x} + \frac{B}{\rho}\frac{\partial P}{\partial x} + \frac{1}{\rho}\frac{\partial B\tau_{xx}}{\partial x} + \frac{1}{\rho}\frac{\partial B\tau_{xz}}{\partial z} \quad \textbf{(11)}$$

$$\frac{1}{\rho}\frac{\partial P}{\partial z} = -g\frac{\partial H}{\partial z} \quad \textbf{(12)}$$

Where:

v = velocity in the y direction

y = distance in the lateral direction (y plane)

H = water surface elevation (z + Depth)

v_t = horizontal eddy viscosity coefficient

c_f = bottom friction coefficient

f = Coriolis parameter

U = laterally averaged velocity in x direction

W = laterally averaged velocity in z direction

B = width

P = laterally averaged pressure

τ_{xx},τ_{xz} = turbulent stresses in the xx, and xz directions, respectively

q = lateral inflow per unit volume

2.2.2 1D and 2D Hydraulics models, assumptions and limitations

Robinson et al., 2019 mention that 1D models have some advantages over 2D models in certain applications. For instance, 1D models are computationally less demanding and require fewer resources compared to their 2D counterparts. Additionally, they can provide a simplified representation of complex systems, making them easier to interpret and analyze. However, 1D models have inherent assumptions and limitations such as:

- Flow direction, flow path and flow splits
- Spacing between cross sections
- Ineffective flow areas and flow contraction and expansion coefficients at bridges
- Boundary conditions and roughness parameters
- Channel slope limitation and gradually varied flow

These assumptions can lead to erroneous results in projects with high hydraulic complexity.

On the other hand, 2D models have distinct physical assumptions and limitations compared to 1D models, which are often neglected in hydraulic analyses of river systems, those assumptions include:

- Dimensional limitations (no vertical velocity components for velocity, flow diffusion and flow turbulence)
- Boundary conditions in all open boundaries (can produce sources of error),
- Wetting and drying limitations (can vary depends on the modeled scheme),
- Turbulence accounting (internal momentum transfers is using eddy viscosity, can result in unrealistic patterns)
- Issues with model stability and converge.

Brunner et al. (2020) also discusses the computational differences between 1D and 2D unsteady flow modeling. In the context of the HEC-RAS model, the information below relates to major 1D and 2D unsteady flow modeling.

- **Water Surface and Velocities** The main difference lies in that 1D models compute a single water surface elevation at each cross section, while 2D models compute unique water surfaces for every cell/face, with detailed water surfaces and velocities varying based on the number of cells used.

- **Friction Losses** In 1D models, friction losses are calculated by multiplying an averaged friction slope (S_f) by the distance between cross sections. For 2D models, the friction slope is also calculated at each face of the cells, but it is typically not averaged over the cell because the direction of the flow is in two dimensions.
- **Conveyance Calculations** Conveyance in 2D models is computed separately for each cell face, while in 1D models, conveyance is calculated for the main channel Brunner et al. (2020) as a separate flow area. This can result in different findings, with the highest discrepancies found in steep banks.
- **Contraction and Expansion Losses** In 1D models, losses due to contraction and expansion are determined by multiplying empirical coefficients by velocity head, while 2D models include pressure forces and spatial acceleration terms.
- **Ineffective Flow Areas** Due to the fact that 1D models require conveyance across sections, requiring "ineffective flow" areas. 2D models calculate recirculation zones automatically, but turbulence modeling and coefficients can influence their size and water velocity.

2.2.3 Modeling Bridges in HEC-RAS

Brunner (2016) explains that HEC-RAS have four different ways to compute losses through the bridges in 1D are: Energy Equation, Momentum balance, Yarnell equation and FHWA WSPRO method. This research makes a comparison using two of those methods using 1D models, Energy Equation and WSPRO method.

- Energy equation This approach considers a bridge as a natural river cross-section. It involves removing the area below the water surface and raising the wetted perimeter to the points where the water meets the structure. The approach employed in this

method incorporates Manning's n values to account for friction losses, as well as contraction and expansion coefficients to address transition losses.

- WSPRO method is an iterative solution that calculates the water surface profile through a bridge by solving the energy equation. It is performed from the exit cross section (1) to the approach cross-section (4), with the energy balance being performed in steps from the exit section (1) to the cross section just downstream (2) of the bridge, inside of the bridge at the downstream end (BD), inside of the bridge at the upstream end (BU) to just upstream of the bridge (3), and from just upstream of the bridge (3) to the approach section (4). An illustration of the channel profile and the cross sections used for modeling losses through the bridges are shown in Figure 4 and Figure 5.

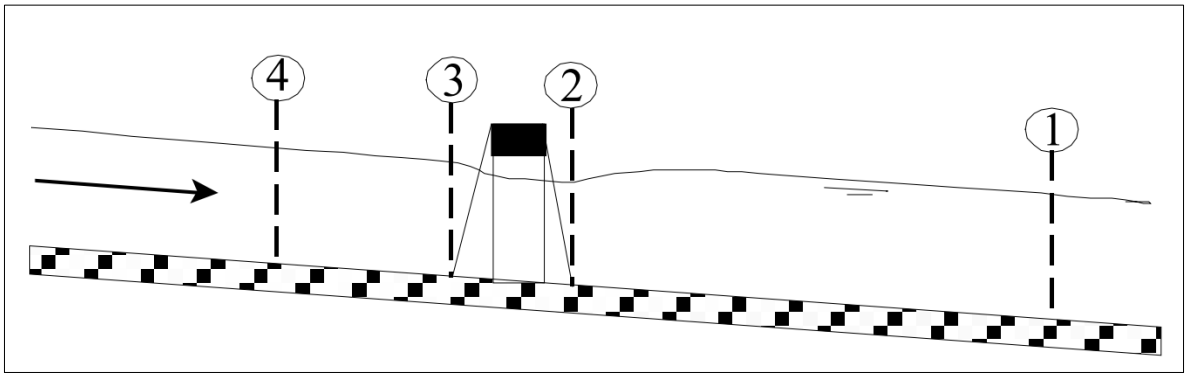

Figure 4. Channel Profile and cross section locations (Brunner and CEIWR-HEC, 2020)

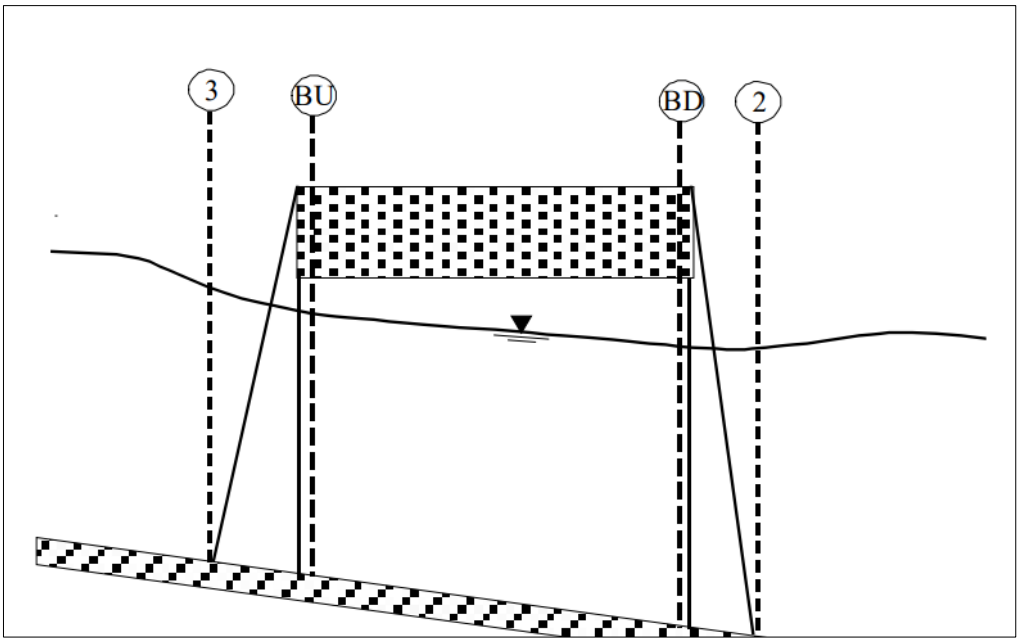

Figure 5. Cross Sections Near and Inside the Bridge (Brunner and CEIWR-HEC, 2020)

Similarly, there are two different ways to model compute losses through the bridges in HEC-RAS 2D: 1) Create an SA 2D connection (Brunner and CEIWR-HEC, 2020) and, 2) terrain modification with raised piers (Hydrologic Engineering Center, 2023).

- SA 2D connection HEC-RAS has a tool that allows to model roadway crossing bridges and culverts inside of 2D flow areas. This tool can handle the full range of flow regimes, from low flow to pressure flow, combined pressure flow, and flow going over the top of the bridge deck or roadway. The HEC-RAS software takes the user input bridge data and modeling approaches, then develops a family of rating curves for the bridge, just as it does for 1D modeling. However, for 2D modeling, the bridge's curves are used to obtain a water surface difference through the bridge for each set of cells being used to model the bridge. This water surface difference is then equated to a force. That force is distributed and put into a special version of the momentum equation for each set of cells spanning the bridge centerline. So instead

of calculating friction forces, pressure forces, and spatial acceleration forces, these forces are obtained from the bridge curves. Then the 2D equations are solved as they are normally solved at any cell/face in the model**.** (Brunner and CEIWR-HEC, 2020)

- 2D Terrain modification with raised piers To model piers in bridges rising the terrain elevation in HEC-RAS, it can use the Terrain Modification tool in RAS Mapper to improve the terrain by adding channel information, adding high ground (such as a road), adding features that impede flow (such as piers), or otherwise modifying the terrain elevations. Then 2D equations are then resolved as they would be at any cell-face in the model. the 2D equations (Hydrologic Engineering Center, 2023).

2.3. Bridge Scour calculations

Bridge scour is the result of modifications to water flow patterns, such as bends or constrictions, which can increase water turbulence. (Richardson et. al, 1993). There are three main components in the total scour in bridges: Long-term aggradation and degradation, contraction scour at the bridge and local scour at the pier or abutments (Richardson and Davis, 2001). Those components are described below:

- Aggradation and degradation are long-term changes in the elevation of the streambed, affecting the river section where the bridge is located. Aggradation is the deposition of eroded material upstream of the bridge, while degradation lowers the streambed and contributes to overall scour.
- Contraction scours occur when a bridge's placement constricts the stream flow region, often during flood events. This can cause increased flow velocities and higher shear stresses, potentially leading to erosion.

- Local scour is a phenomenon that occurs close to a specific bridge pier, abutment, spur, or embankment and causes sediment removal as a result of vortices created by flow-obstructing objects.

2.3.1 Parameters related to Bridge Scour estimates

Critical shear stress refers to the minimum shear stress required to initiate erosion in cohesionless soils. In other words, it is the threshold at which the soil particles start to detach and move. Understanding the critical shear stress is crucial because it helps determine the stability of the soil and its resistance to erosion. If the shear stress acting on the soil exceeds the critical shear stress, erosion will occur. On the other hand, if the shear stress is below the critical shear stress, no erosion will take place. Arneson et al. (2012) defines shear stress as the force per unit area applied to the channel boundary by flowing water. Equation 13 shows the definition of shear stress.

$$\tau = K_b . \Upsilon . R . S_f \quad \textbf{(13)}$$

Where:

τ = Design shear stress, lb/ft^2 (N/m2)

K_b = Bend coefficient (dimensionless)

Υ = Unit weight of water, lb/ft^3

R = Hydraulic radius (area divided by wetted perimeter), ft (m)

S_f = Slope of the energy grade line, ft/ft (m/m)

Another important parameter is the critical velocity, which is the lowest velocity required to begin sediment transport and erosion at a pier. When the flow velocity reaches critical velocity, sediment particles from the bed can be displaced and transported (Richardson and Davis, 2001).

Considering these factors, bridge scour can happen through two different mechanisms limited to sediment motion: (1) when the water is clear, which means that there is no movement of sediment in the bed of the approach channel, and (2) when there is sediment motion in the approach flow. Under clear water conditions ($V_c > V$), sediment remains stationary in the bed of the approach channel due to a low or equal bed shear stress compared to the critical bed shear stress required for sediment motion. On the other hand, under live bed conditions ($V_c < V$), there is a generalized movement of the bed sediment caused by a higher bed shear stress exceeding the critical threshold (Arneson et al, 2012)

In addition, there is another important parameter to consider is the erosion rate. Briaud et al. (1999) found that the erosion rate in scour processes depends on the critical shear stress, the soil and water temperatures, the chemical makeup of the soil and water, the soil water content, the plasticity index, the soil unit weight, the soil undrained shear strength, and the average grain size. Briaud et al. (2011) presents a graph shown Figure 6 that related the critical shear stress with the particle grain size as a function of D_{50} (mm) with the critical shear stress (N/m^2). This V-shaped graph also illustrates that particle size controls the erosion threshold of coarse-grained soils, while particle size does not correlate with the erosion threshold of fine-grained soils. This effect is due to the cohesive nature of fine-grained (i.e., silt and clay) soils (Anerson et al., 2012) .

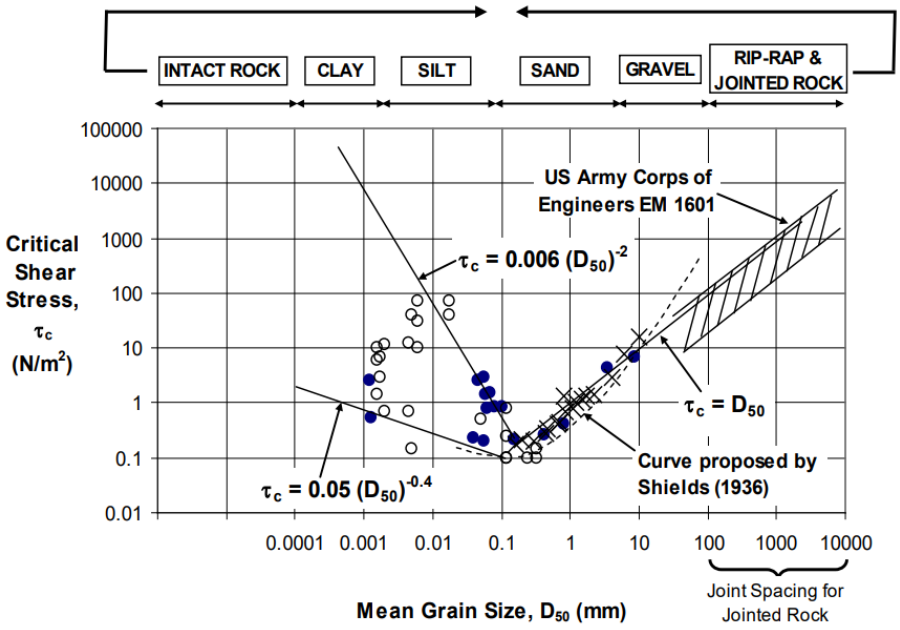

Figure 6. Critical shear stress vs particle grain size (Briaud et al. 2011)

Usually, in scour analysis, we assume that the soil is uniform. Nevertheless, in reality, the soil can involve multiple layers with characteristics that can vary significantly with depth. For this situation, a multilayer analysis can be conducted (Pokharel, S., 2017; Briaud et al., 2011). This type of analysis assumes different layers in the channel bottom bed with specific thicknesses (y_i). Each layer, which has a different D_{50}, can be removed for flood events with constant velocity during a period (t_i). When the scour depth Y_{si} exceeds the thickness Y_i, the following layer is involved (Y_{i+1}), eroding its thickness during a specific time (ti+1). Geotechnical borings provide the necessary stratigraphic information, distribution particle size, and D50 for each stratum required for this multilayer analysis. This type of analysis is common in cohesive soils, where the erosion rate of the material can support long periods of time and several flood events (Anerson et al., 2012). It is important to mention in this type of method that there is a large variability in the D50 around the cross section and the stratigraphic profile that influences in a significant way the scour estimates.

2.3.2 Practical guidelines for scour calculations

There are several reference documents related to Bridge scour and are mentioned below.

- *HEC 18 Evaluating Scour at Bridges (2012):* This document state of knowledge and practice for the design, evaluation, and inspection of scour-critical bridges includes policy and regulatory basis for the FHWA Scour Program, risk-based evaluations, developing Plans of Action (POAs), countermeasure design philosophy (new vs. existing bridges), and a section on contraction scour in cohesive materials (Anerson et al., 2012)
- *HEC 20 Stream Stability at Highway Structures (2012):* This document contains recommendations for identifying stream instability issues at highway stream crossings. The HEC-20 manual discusses geomorphic and hydraulic elements that influence stream stability and gives a step-by-step analysis technique for assessing stream stability issues. (Lagasse et al., 2012).
- *HEC 23 Bridge Scour and Stream Instability Countermeasures: Experience, Selection and Design Guidance (2009):* The objective of this document is to ascertain and provide design principles for mitigating bridge scour and stream instability, as observed in the practices adopted by different State departments of transportation (DOTs) within the United States (Lagasse et al., 2009).
- *HDS 7 Hydraulic Design of Safe Bridges (2012):* This guidance provides technical information and recommendations on bridge hydraulic design. Bridges should be constructed to be as safe as feasible while keeping costs low and the impact on property and the environment to a minimum. This guidance also covers regulatory issues, specialized methodologies for bridge hydraulic modeling, hydraulic model

selection, the effects of bridge design on scour and stream instability, and sediment transport (Zevenbergen et al. 2012).

- *Observation method for estimating future scour depth at existing bridges (2013):*

  This method uses charts that extrapolate or interpolate measured scour depths at the bridge to obtain the scour depth corresponding to a specified future flood event. It was designed to be used as a first-order assessment in conjunction with a routine bridge inspection program (Briaud et al. 2011) (Govidasamy et al., 2013)

This research is focused on HEC 18: Evaluating Scour at Bridges (Anerson et al., 2012) and most specifically on pier scour calculations. Nevertheless, pier scour calculations using the Observation Method for Scour (Govidasamy et al., 2013) were conducted to compare results.

2.3.3 Worst-Case scour scenario

Sharp et al. (2021) describe two definitions for the worst-case scour scenario: one created by FHWA, which recommended the use of 100-year and 500-year exceedance discharges as the scour design flood and scour check flood, and the second proposed by AASHTO LRFD, which recognizes that the worst-case scour depth may not occur at the highest flow rate that the scour design flood or scour check flood may have (i.e., Q_{100} and Q_{500} events). As a result, the scour design flood may include some flood magnitude less than Q_{100}, resulting in increased scour at the bridge. If that is the case, the standards provide for that discharge to be used as the scour design flood. Similarly, if a flood event less than the Q_{500} creates the worst-case scour depth at the bridge, it should be used as the scour check flood. Another way to put it is that the scour design flood should be the worst-case scour for all floods up to and including Q_{100}.

The FHWA included risk-based approaches in their bridge program goals, including the scour program, in a recommendation to the United States Congress in 2010. This analysis addresses the significance of the structure, the need for reliable crossings, and the economic effects of a collapse. All bridges used to be planned for scour using Q_{100} flood events, then double-checked using Q_{500}, before the advent of risk-based approaches. The recommended minimum scour design and check flood frequencies based on hydraulic design flood frequencies defined by FHWA in HEC-18 (Anderson et al., 2012) are shown in Table 2.

Table 2. Hydraulic design, scour design and scour design check flood frequencies

Hydraulic design Flood Frequency, Q_D	Scour design Flood Frequency, Q_s	Scour design check Flood Frequency, Q_c
Q_{10}	Q_{25}	Q_{50}
Q_{25}	Q_{50}	Q_{100}
Q_{50}	Q_{100}	Q_{200}
Q_{100}	Q_{200}	Q_{500}

Briaud et al. (2011) proposed a methodology to determine the scour rate in cohesive soils. This method allows the user to predict the scour depth as a function of time. This method is based on two parameters: the maximum scour depth and the maximum shear stress. Those methods require determining the scour depth using a given set of sequential daily discharge values. In addition, Briaud et al. (2011) also established a method for preparing daily discharges based on the recorded previous hydrographs (Q_{100} and Q_{500}) for predictions of possible scour depths in the future. To calculate the daily discharges, Montecarlo assumed that the hydrograph was modeled as a stochastic process. The methodology uses a theoretical distribution (log-normal) and the future daily stream flow as the exponential of a normally distributed variable. At the same time, Briaud et al. (2011) developed another approach based on Q_{100} and Q_{500} that utilized the cumulative density function (CDF) of the lognormal

distribution of Q evaluated at Q_{100} and Q_{500} to calculate daily stream discharges. It is important to mention that these methods are useful for scour predictions in cohesive soils.

This study is based on the premise that the maximum scour will happen for an event with an exceedance probability of 1% or a 100-yr return period.

2.3.3 Pier scour

Pier scour is a type of local scour and occurs around individual bridge piers and abutments. Downward flow is induced at the upstream end of bridge piers, leading to very localized erosion in the direct vicinity of the structure (Hamill, 1999). This research is focused on pier scour comparison, so more emphasis will be placed on this type of scour. To contextualize the phenomenon of pier scours, it is important to describe the flow field on a single pier. Pier scours are caused by resulting vortices induced by the objects obstructing the flow. In this process, the downward flow is induced at the upstream of the bridge pier leading to a localize erosion in the vicinity of the structure; horseshoes vortices are then created at the base of the pier due to the acceleration of the flow around the nose of the pier and the subsequent flow movement at the edge of the scour hole. Finally, wake vortices are created when the flow at the side of the pier is separated (Prendergast and Gavin 2014).

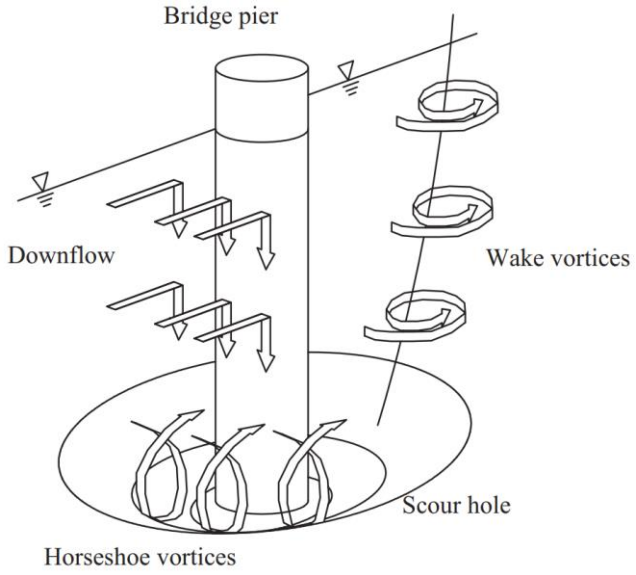

Figure 7. Flow around a single pier (Prendergast and Gavin, 2014)

Despite the lack of field data, local scours at piers have been thoroughly studied in the lab. Most studies have been conducted on simple piers as such as Ettema (1976, 1980) Sheppard, (1999); Melville and Coleman (2000); Richardson and Davis (1995, 2001) and Sheppard and Renna (2010) and Anerson et al., (2012), others conducted in complex piers as such as Jones and Sheppard (2000), Salim and Jones (1995,1996, 1999) and Sheppard, (2001), and some in cohesive materials as Briaud et al., (2009, 2011) and others in coarse bed as Lagasse et. al., (2012). Also, there are methods based on scour observations as THE Observation Method for scour (Govindasamy et al., 2013). This research is focused on HEC-18 calculations (Anerson et al., 2012) and the Observation method for scour (OMS) (Govindasamy et al., 2013)., for that reason their origin and formulations are presented below.

2.3.4 HEC- 18 equations for pier scour

Liu et. al (1961) and Chang and Yevdjevich (1962) conducted studies in the Colorado state university when describes the physical hydrodynamic and physical description an aspect of contraction and local scour; and prepared a logical outline of future research procedures into the study of the local scour phenomenon, those equation products of that work are known as Colorado State University Equations. Those equations were based on preliminaries studies conducted by Einstein (1950), Laursen (1956) and Chabert and Engeldinger (1956).

Studies performed by Jones (TRB, 1983) shown that the Colorado State University Equation (CSU) covered the condition for most equations developed for local pier scour. Using the recommendations from this study, the FHWA recommended the CSU equation in the interim procedures that came with the FHWA's Technical Advisory T5140.20 (1988).

The CSU equation was also recommended, with some changes, in earlier editions of HEC-18. In addition, studies conducted by Mueller (1996) compared 22 scour equations with field measurements and concluded that the HEC-18 (CSU) equation was appropriate for design because it rarely underestimated measured scour depth but frequently overpredicted the actual scour. Figure 8 illustrates the comparison of scour equations for variable depth ratios (y/a) according with Jones (TRB, 1983).

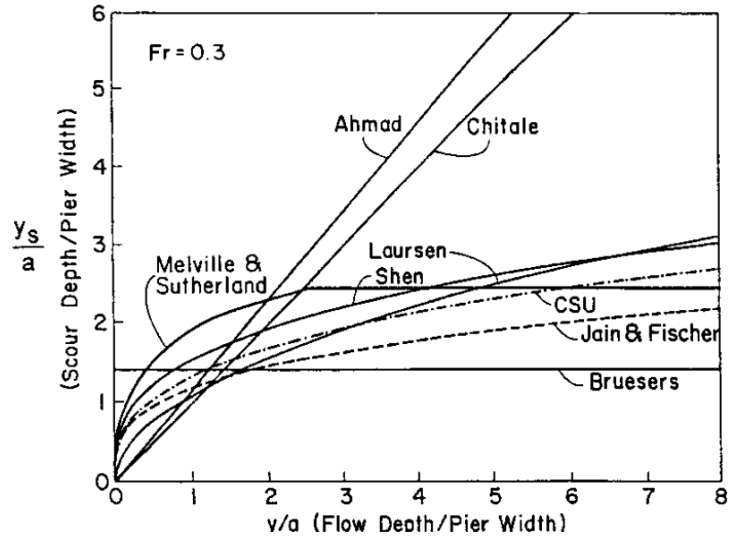

Figure 8. Comparison of scour equations for variable depth ratios (y/a) according with Jones (TRB, 1983)

The HEC-18 pier scour equation (based on the CSU equation) is recommended for both live bed and clear-water pier scour in cohesionless soils. Figure 9 shows the Pier scour sketch according to HEC-18 and its respectively equation is shown in Equation 14 (Anerson et. al, 2012).

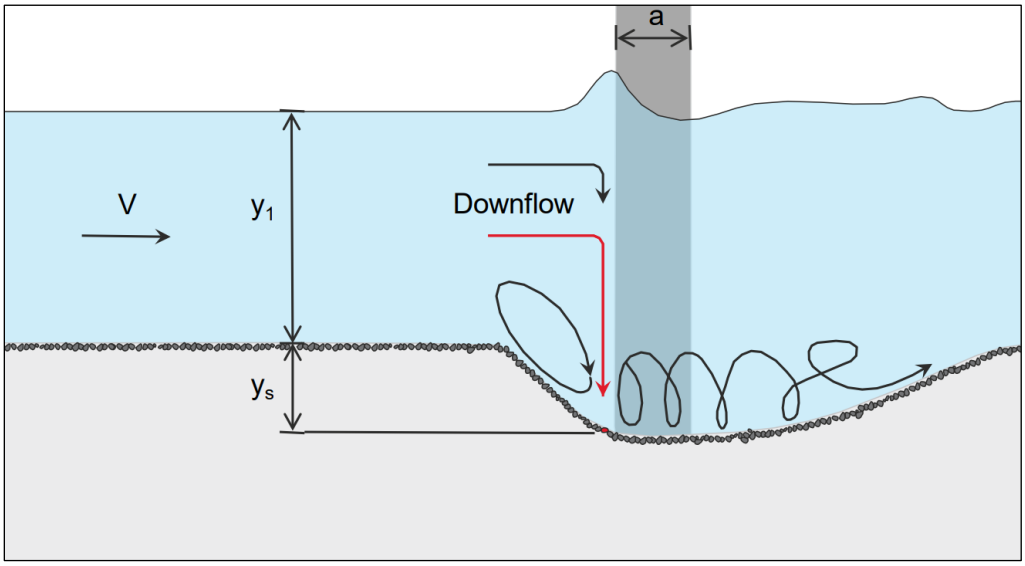

Figure 9. Pier scour sketch (Anerson et al., 2012)

$$\frac{y_s}{y_1} = 2.0\ K_1\ K_2\ K_3\ \left(\frac{a}{y_1}\right)^{0.65}\ Fr_1^{043} \quad \textbf{(14)}$$

where:

y_s = Scour depth (ft)

y_1 = Flow depth directly upstream of the pier (ft)

K_1, K_2 and K_3 are correction factors for pier nose shape, for angle of attack of flow and for bed condition respectively.

a = Pier width (ft)

L = Length of pier (ft)

Fr_1 = Froude Number directly upstream of the pier = $V_1/(gy_1)^{1/2}$

V_1 = Mean velocity of flow directly upstream of the pier (ft/s)

g = Acceleration of gravity (32.2 ft/s^2)

Anerson et al., 2012 defines as a rule of thumb that the maximum scour depth for round nose piers aligned with the flow is:

$y_s \leq 2.4$ times the pier width (a) for Fr ≤ 0.8

$y_s \leq 3.0$ times the pier width (a) for Fr > 0.8

2.3.5 Observation method for scour (OMS)

OMS, presented by Briaud et al. (2009), Briaud et al. (2011) and Govindasamy et al. (2013), is a method for estimating future scour depth of existing bridges without site-specific erosion testing. It was developed as a first-order assessment for bridge inspection programs like the Texas Department of Transportation (TxDOT). The method uses observations at existing bridges to determine scour depth for a specified future flood event. This information is

obtained from scour depth observations and charts that relate the future scour depth ratio (Z_{fut}=Zmo) to the future velocity ratio (V_{fut}=V_{mo}).

Govindasamy et al. (2013) explains that OMS has four methodological steps which are: (1) Observe the maximum scour depth at the bridge (2) Determine the maximum flow velocity the bridge has been subjected to since its construction (3) Determine scour depth for a future flood using Z-future charts (4) Compare the future scour depth to the allowable (threshold) scour depth of the foundation. The description of those methodological steps are shown below:

(1) Maximum Observed Scour Depth (Z_{mo}) This value is obtained directly from routine bridge inspection reports and other records of measurements.

(2) Determine the maximum flow velocity the bridge has been subjected to since its construction (V_{mo}). To estimate V_{mo} and, consequently, V_{fut}, there are two possible cases depending on whether there is flow data available from gauge stations. If flow data is available, after obtaining annual instantaneous flow peaks series at the bridge or somewhere nearby, a flood frequency analysis is performed seeking the flow corresponding to the selected future peak flow magnitude (Q_{fut}). Then, Q_{mo} must be determined, as the maximum deserved peak flow has occurred at the station since the day of the bridge construction. Then, Q_{mo} must be determined as the maximum deserved peak flow that has occurred at the station since the day of the bridge construction. However, if flow data is not available, V_{mo} and V_{fut} must be inferred from flow data near the bridge by developing maps of historical flow recurrence intervals to determine the maximum flow observed at the bridge (RIQ_{mo}) and by the relationship between RIQ_{mo} and Q_{mo}/Q_{fut}. Alternatively, the estimated V_{mo}/V_{fut} can be determined by converting Q_{mo}/Q_{fut} using

hydrological and hydraulic tools such as HEC-HMS and HEC-RAS (Brunner, 2020) or TAMU-FLOW (Briaud et al., 2009)

(3) Determine scour depth for a future flood This step requires the use of charts that relate Z_{fut}/Z_{mo} to V_{fut}/V_{mo} (Briaud et al., 2011; Govindasamy et al., 2013) which in turn obeys the relationship shown in Equation 15.

$$Z_{fut} = Z_{mo} \times f(V_{fut}/V_{mo}) \quad \textbf{(15)}$$

(4) Compare the future scour depth to the allowable (threshold) scour depth of the foundation This step Z_{fut} is now compared with the allowable scour depth (Z_{thresh}). If Zfut is less than Zthresh, the bridge is considered to have minimal risks and should undertake regular monitoring, otherwise, the bridge is considered requiring further analysis Govindasamy et al. (2013).

3. METHODOLOGY

Peak flow rates, approach velocities and depths, as well as scour calculations, were conducted using a combination of hydrological and hydraulic methods at four bridges in Alabama. The selection of these bridges was based on previous reviews of the AASHTOWare Bridge Management software (BrM) system, in which events between inspections that could have caused significant scour were sought. All the selected bridges here were identified using the same identifier recorded in BrM, which matches the state's Bridge Identification Number (BIN). The methodology used to perform the calculations mentioned is divided into four sections, which are described below:

- Sites description: Section provides a brief description of the geographical location of the sites where the bridges are situated, the type of structure, the number of piers, and the area of the watershed associated with them.
- Hydrological analysis: Section provides details about the input information used to feed the hydrological models, including some details about their construction, such as the digital terrain models, watershed delineation, land use, hydrological soil types, and the incorporated processes. The input information related to rainfall and the type of simulated event is also outlined, as well as the steps taken to perform the FFA and the calibration process for sites that had streamflow and precipitation data. This part also includes the final models developed in HEC-HMS 4.9, which served as the foundation for estimating the input flow in the hydraulic models.
- Hydraulic Analysis: Section presents the parameters used for the creation and simulation of hydraulic models using HEC-RAS 6.1/6.2 and some of the constraints depending on the type of model, whether it is in 1D (WSPRO, Energy) or in 2D (SA 2D connection, 2D terrain modification with raised piers). Additionally, it illustrates

how sections and points were created for comparing velocities to ensure they were the same in all the models.

- Bridge Sour Calculations and comparisons: Section describes the procedure followed for calculating scour, considering the results of the approach velocity from the previous section, and using the HEC-18. Similarly, the methodology used to estimate scour using OMS is also described. Finally, the results are compared, and a peak-to-average metric calculation is used for comparing scour, velocity, and depth values among methodologies. Additionally, the results of each model were compared to a benchmark model, which was the 2D terrain modification with raised piers using HEC-HMS estimates of peak flow. The selection of this model as a reference model is due to its advantages, considerations, and results, as it better represents the physical phenomenon with fewer assumptions and limitations, as demonstrated in section 2.2 of this document. Figure 10 shows a flowchart of this thesis methodology.

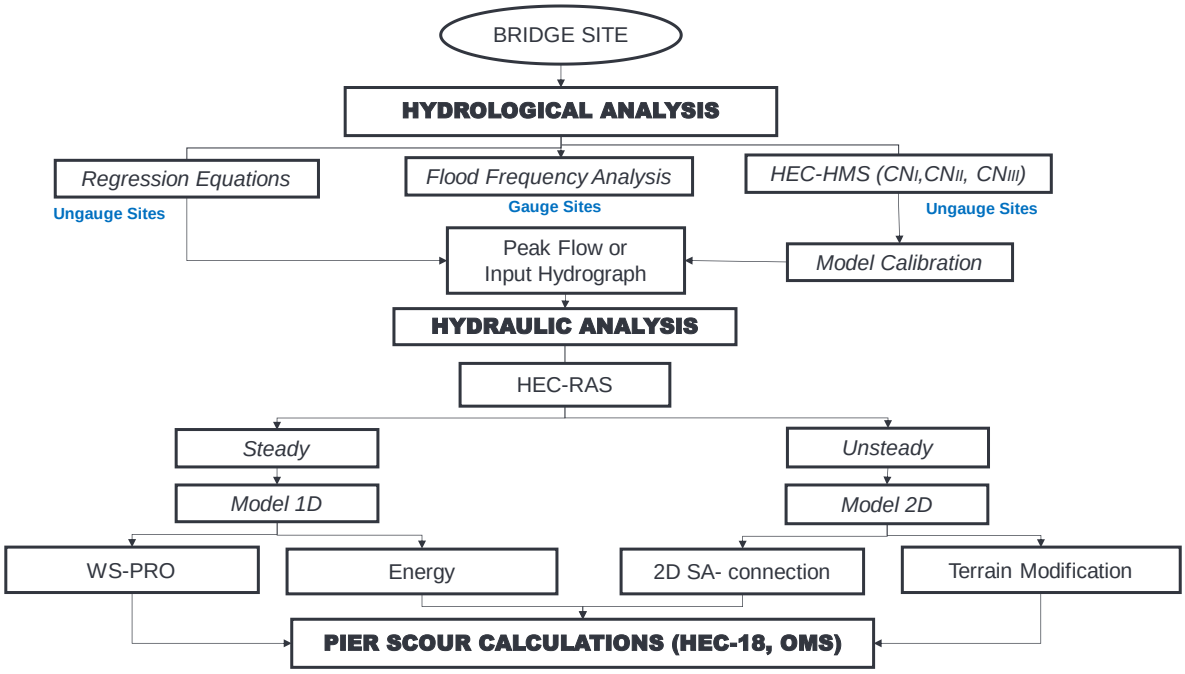

Figure 10. Methodology Flowchart

3.1 Study Sites

The four studied bridges are located in the state of Alabama, and for this study, they were identified using the same AASTHOWare BrM identifier and pier nomenclature within of the hydraulic models. The general location in the state of Alabama for the four selected bridges is shown in

Figure ***11***.

- BrM No 015002. Little Double Bridges Creek and County Road 606
- BrM No 010738. Blue Creek and Meriwether Trail
- BrM No 013310. Conecuh River and County Road 2243
- BrM No 007070. French Creek and CO RT No 62

The identifiers shown here are, as mentioned earlier, the same as those used in BrM.

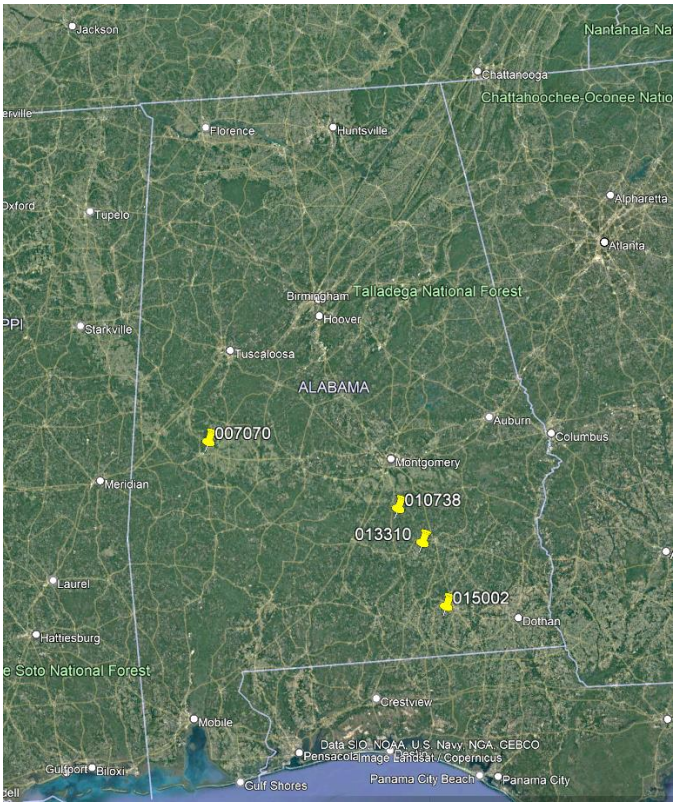

Figure 11. Location of the selected Bridges in the State of Alabama (Google Earth, 2023)

3.1.1 BrM No 015002. Little Double Bridges Creek and County Road 606

The first bridge studied corresponds to BrM No. 015002, which is sited in Coffee County, near Enterprise, Alabama, over County Road 606 at the intersection with Little Double Bridges Creek**.** The watershed under consideration covers an estimated area of 21.33 square miles and its geographical limits are delineated by latitudes extending over from 31.383° to 31.271° and eastern longitudes ranging from -86.014° to -85.941°. This bridge has the particularity of having a USGS streamflow gauge station, which is identified as No. 02362240. Figure 12 illustrates the bridge's structure and its location. Likewise, Figure 13 shows the USGS station and a screenshot of the data that can be extracted from its website.

Figure 12. Location of Bridge No 015002. (Google Earth, 2023)

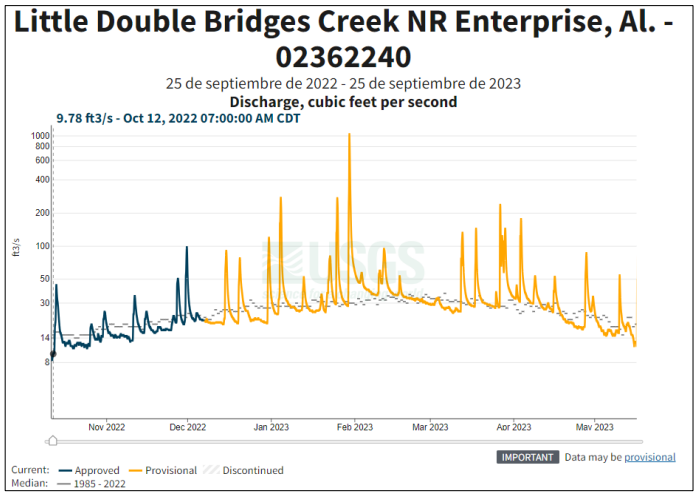

Figure 13. USGS station No. 02362240 is located at the Bridge entrance. (USGS, 2023)

The bridge is supported with four intermediate square piers aligned in groups of five and has an approximate span of 170 feet between abutments. Figure 14 shows the bridge configuration taken from BrM.

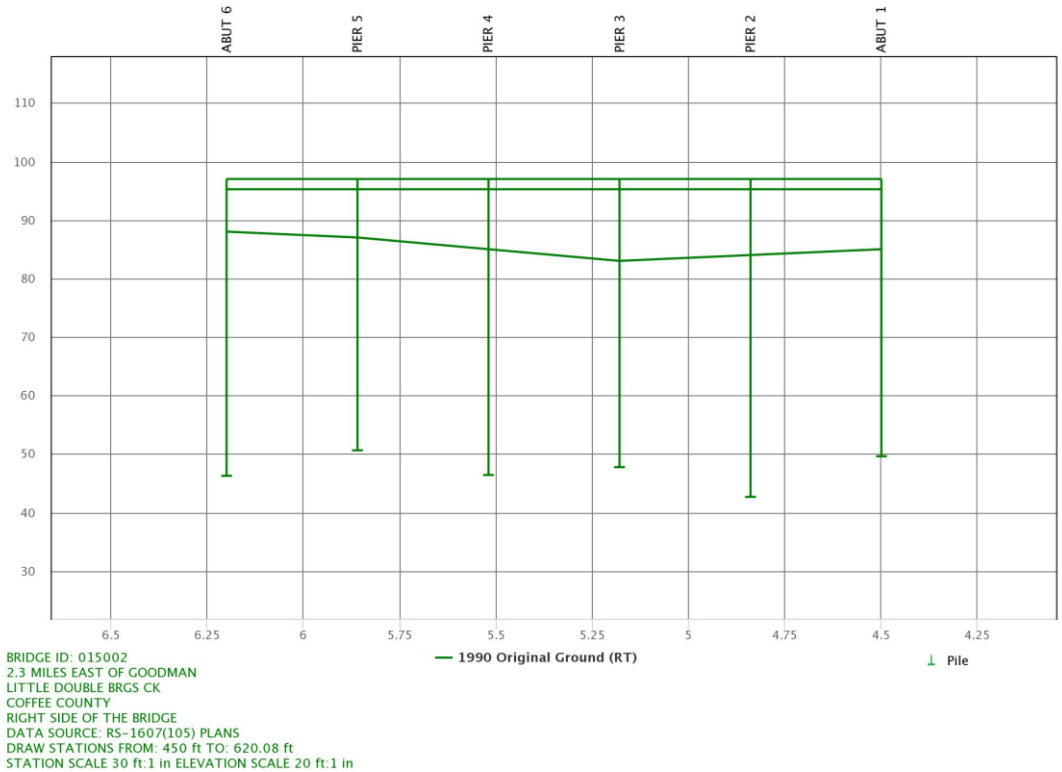

Figure 14. Bridge No 0150002 configuration. (AASHTOWare BrM, 2023)

3.1.2 BrM No 010738. Blue Creek and Meriwether Trail

The second Bridge, identified as BrM No. 010738, is located in Montgomery County at the intersection of Blue Creek and the Meriwether Trail. This watershed is defined by latitudes ranging from 32.0007° to 32.0023° and east longitudes ranging from -86.2813° to -86.2822°, covering an area of approximately 4.53 square miles being the smallest watershed in this study. The bridge is supported with a span of 102 feet and two rows of intermediate square piers aligned in groups of five. Figure 15 presents the bridge location. Also, the Figure 16 illustrates the bridges configuration extracted from AASHTOWare BrM.

Figure 15. Location of Bridge No 010738. (Google Earth, 2023)

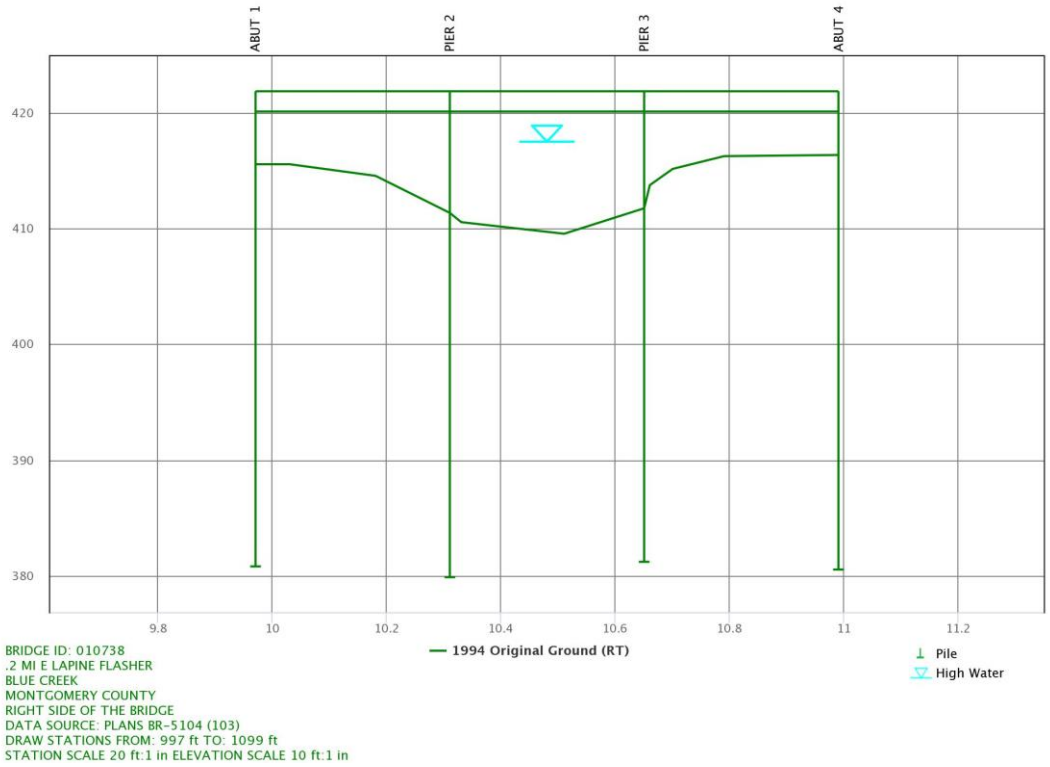

Figure 16. Bridge No 010738 configuration. Source: AASHTOWare BrM

3.1.3 BrM No 013310. Conecuh River and County Road 2243

The third bridge, identified as BrM No. 013310, is situated in Pike County, near to Goshen at the point of intersection of the Conecuh River and County Road 2243. The watershed area is about 369 square miles and is the largest one of this study. Its boundaries are defined by latitudes ranging from 31.7814° to 32.1275° and eastern longitudes spanning from -85.7115° to -86.1051°. This bridge has an approximate length of 737 feet and features 16 rows of intermediate piers, of which four of them have larger sections aligned in pairs, unlike the other smaller ones that are aligned in groups of three. Figure 17 displays the bridge location. Also, the Figure 18 shows the bridges configuration extracted from AASHTOWare BrM.

Figure 17. Location of Bridge No 013310. (Google Earth, 2023)

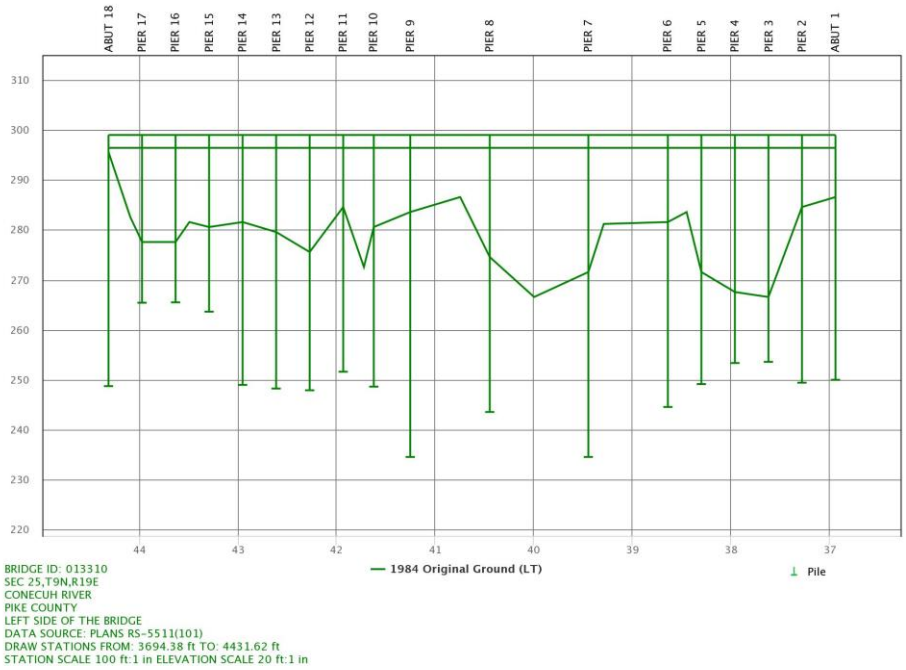

Figure 18. Bridge No 013310 configuration. (AASHTOWare BrM, 2023)

3.1.4 BrM No 007070. French Creek and CO RT No 62

The fourth Bridge No. 007070 is located in Marengo County, close to Demopolis at the point of intersection of French Creek and CO RT No. 62. The total area of this watershed is around 12.3 square miles bounded by latitudes that range from 32.5059° to 32.4832° and eastern longitudes ranging from -87.7770° to -87.7724°. The bridge length is 225 feet with three

rows intermediate circular piers in groups of four and two lines in groups of eight. Figure 19 depicts the location and Figure 20 illustrates the configuration for the Bridge No 013310.

Figure 19. Location of Bridge No 013310. (Google Earth, 2023)

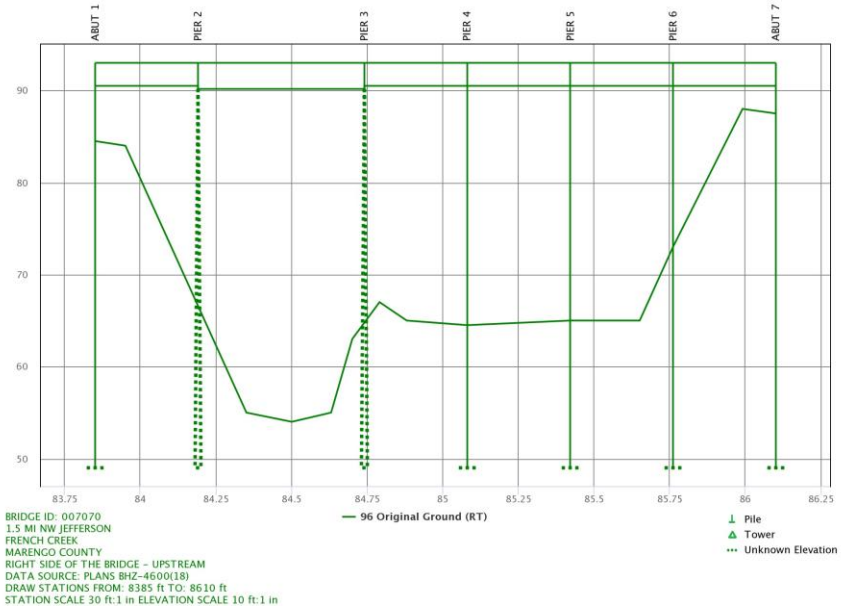

Figure 20. Bridge No 013310 configuration. Source: AASHTOWare BrM

3.2 Hydrological methods

3.2.1. Regional Regression Equation (RRE)

For all the selected bridges, peak flow calculations were carried out (Hedgecock and Lee, 2010; Anderson, 2020) using RRE, taking into account the flood zones corresponding

to each bridge as illustrated in Section 2.1.2 of this document and considering the characteristics of each watershed associated with these bridges. The steps to perform this analysis were three and are described below:

i. Determine the watershed area using StreamStats considering the bridge as the point of analysis (POA) (https://streamstats.usgs.gov/ss/) (Ries III et al., 2004). To carry out this process, it is necessary to generate a report in StreamStats and extract the area contributing to the POA (Point of Analysis). Figure 21 provides a screenshot of the report and the area, for an example watershed.

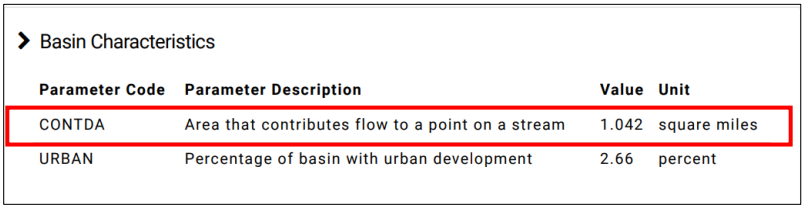

Basin Characteristics

Parameter Code	Parameter Description	Value	Unit
CONTDA	Area that contributes flow to a point on a stream	1.042	square miles
URBAN	Percentage of basin with urban development	2.66	percent

Figure 21. Area extracted from Streamstats for an example watershed.

ii. Determine the flood region as proposed by (Anderson, 2020), presented in Figure 1. Each bridge was categorized based on its respective watershed location within each region. Bridges No. 015002 and 010738 are classified under Flood Region No. 4, while bridges No. 007070 and 013310 are classified under Flood Region No. 3.

iii. Use RRE for peak flows with the area calculated in step 1 and the size and level of urbanization recommendations provided by (Hedgecock and Lee, 2010) (Anderson, 2020) and considering a return period of 100-yr event.

3.2.2. Flood Frequency Analysis (FFA)

For those bridges that featured USGS streamflow gauges was conducted an FFA. Within the context of this specific study, it is important to mention that only bridge No 015002 is equipped with a stream gauge. The procedure to conduct this analysis is describe below:

i. Download multiannual peak streamflow data for the USGS National Water Information System (https://waterdata.usgs.gov/nwis) for the site of analysis. Figure 22 provides an example of the information that can be obtained for those bridges with streamflow data. The information corresponds to the Bridge No 015002.

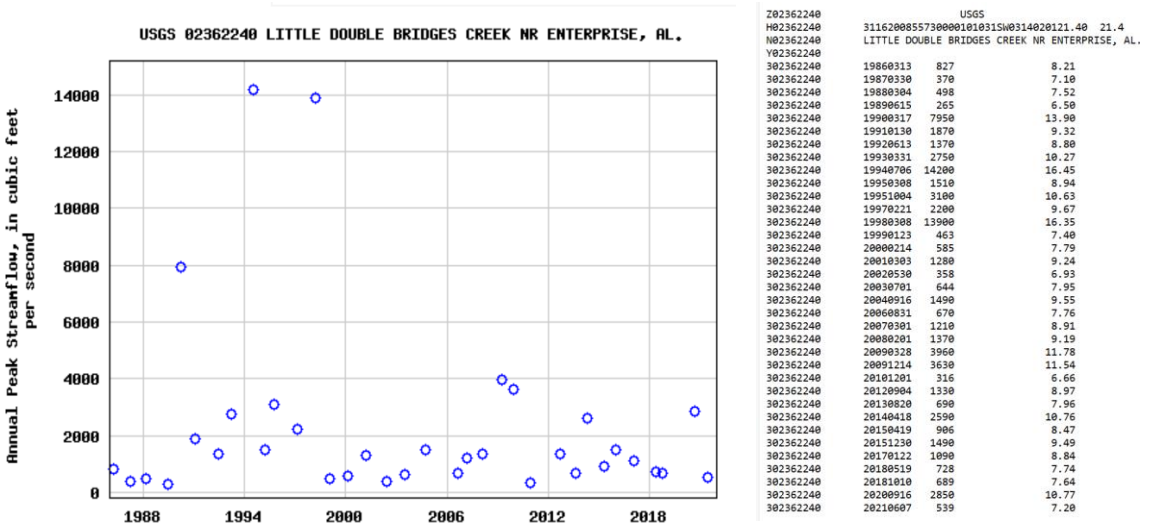

Z02362240		USGS	
H02362240	31162008557300001010315W0314020121.40 21.4		
N02362240	LITTLE DOUBLE BRIDGES CREEK NR ENTERPRISE, AL.		
Y02362240			
302362240	19860313	827	8.21
302362240	19870330	370	7.10
302362240	19880304	498	7.52
302362240	19890615	265	6.50
302362240	19900317	7950	13.90
302362240	19910130	1870	9.32
302362240	19920613	1370	8.80
302362240	19930331	2750	10.27
302362240	19940706	14200	16.45
302362240	19950308	1510	8.94
302362240	19951004	3100	10.63
302362240	19970221	2200	9.67
302362240	19980308	13900	16.35
302362240	19990123	463	7.40
302362240	20000214	585	7.79
302362240	20010303	1280	9.24
302362240	20020530	358	6.93
302362240	20030701	644	7.95
302362240	20040916	1490	9.55
302362240	20060831	670	7.76
302362240	20070301	1210	8.91
302362240	20080201	1370	9.19
302362240	20090328	3960	11.78
302362240	20091214	3630	11.54
302362240	20101201	316	6.66
302362240	20120904	1330	8.97
302362240	20130820	690	7.96
302362240	20140418	2590	10.76
302362240	20150419	906	8.47
302362240	20151230	1490	9.49
302362240	20170122	1090	8.84
302362240	20180519	728	7.74
302362240	20181010	689	7.64
302362240	20200916	2850	10.77
302362240	20210607	539	7.20

Figure 22. Peak flow streamflow data for Bridge No 015002

ii. Using the multiannual peak flow data extracted, use the USGS PeakFQ software (Flynn et al., 2006), which is derived from Bulletin 17b (England et al., 2019).

iii. Find the regional skew option and a standard error recommended by (Hedgecock and Lee, 2010) (Anderson, 2020) to run the analysis.

iv. Use the result charts to find the 1% annual exceedance probability that corresponds to a 100-year streamflow event and get the peak flow. Figure 23 displays the mentioned result graph for one of the analysis watersheds using the PeakFQ software

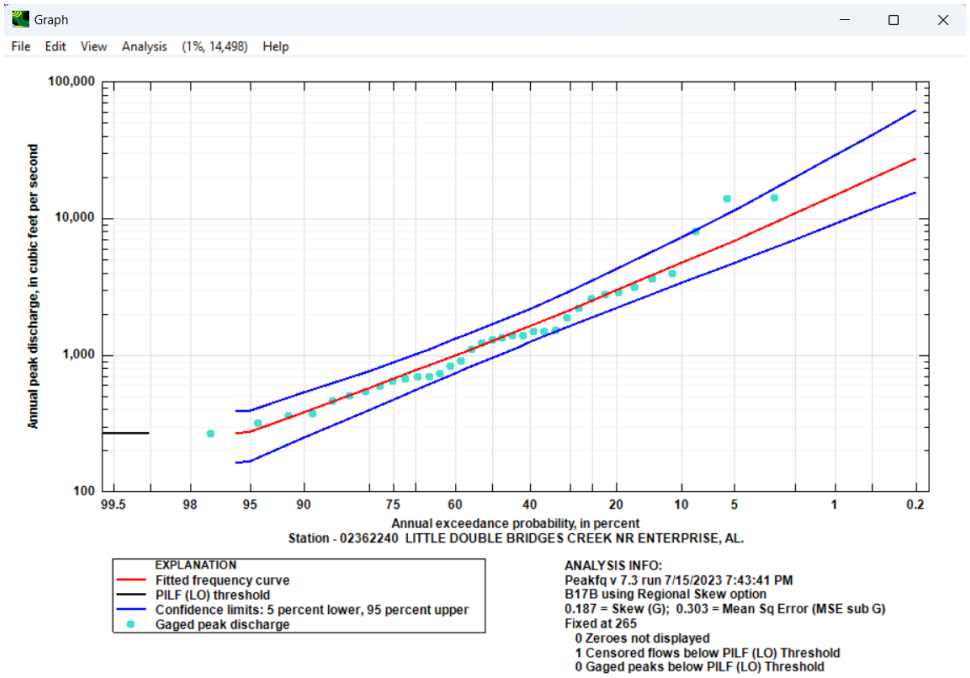

Figure 23. Resulted chart using the software PeakFQ

3.2.3. Hydrological models

In order to analyze all the watersheds associated with each of the studied bridges, hydrological models were developed using HEC-HMS 4.9 software and HEC-GeoHMS for ArcGIS Desktop 10.x. All the watershed characteristics were calculated using USGS Digital Elevation Models (DEM). The methodological steps for creating the hydrological models are described below:

i. Delineate the watershed for each model using the tool delineate in Streamstats (https://streamstats.usgs.gov/ss/) (Ries III et al., 2004) and download the area in shapefile (*.shp) format. Figure 24 displays the analyzed watersheds delineated in StreamStats.

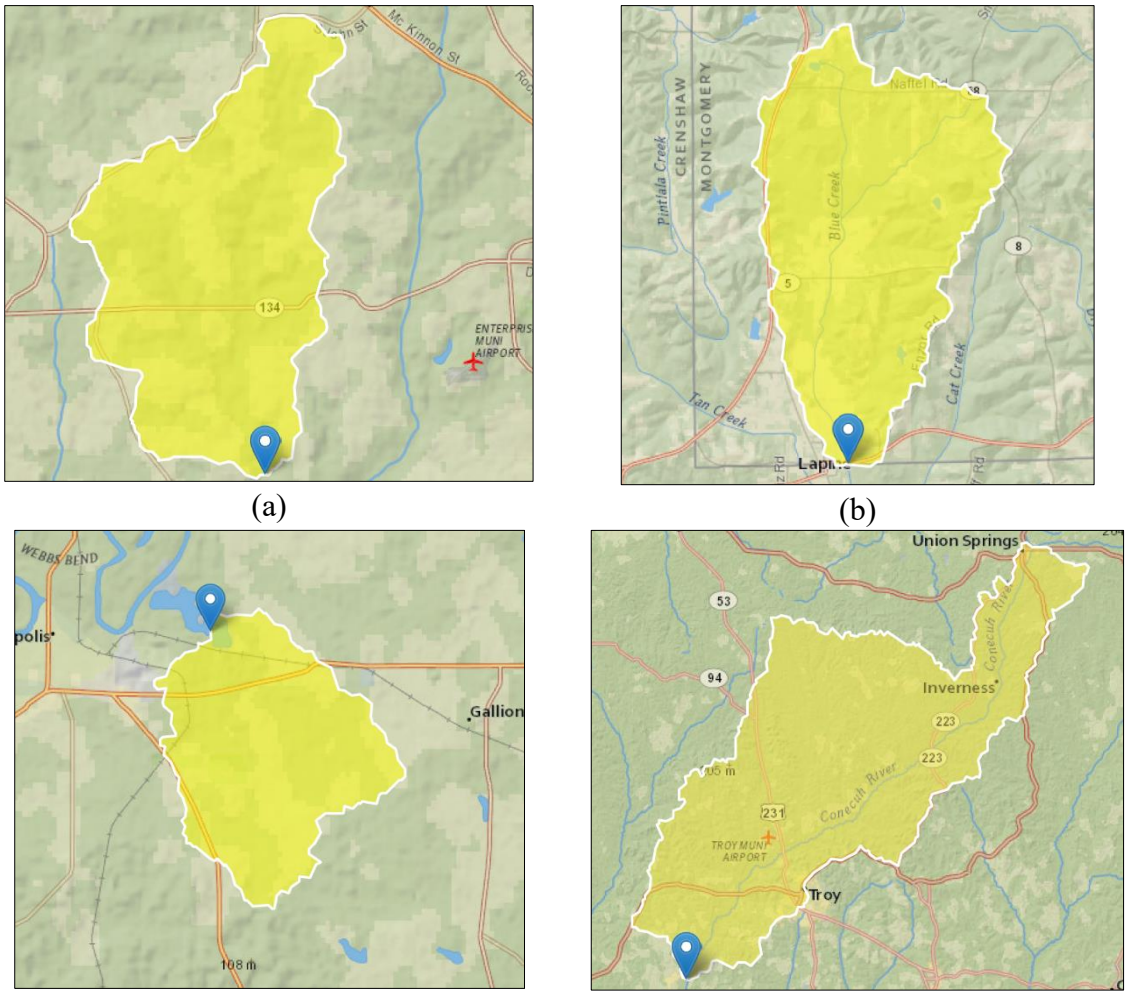

(a) (b)

(c) (d)

Figure 24. Watershed associated with the analyzed bridges (a) BrM No 015002 (b) BrM No 010738 (c) BrM No 007070 (d) BrM 013310

ii. Download the DEM from USGS National Maps (Carswell Jr., & William J., 2013). To perform this procedure, it is necessary to go to the website (https://apps.nationalmap.gov/downloader/#/), select the area of interest, check the available information, and download it. Sometimes, it is necessary to create a mosaic of several DEMs to complete the required information for each watershed. Figure 25 depicts the DEMs used to conduct the analysis for the four watersheds.

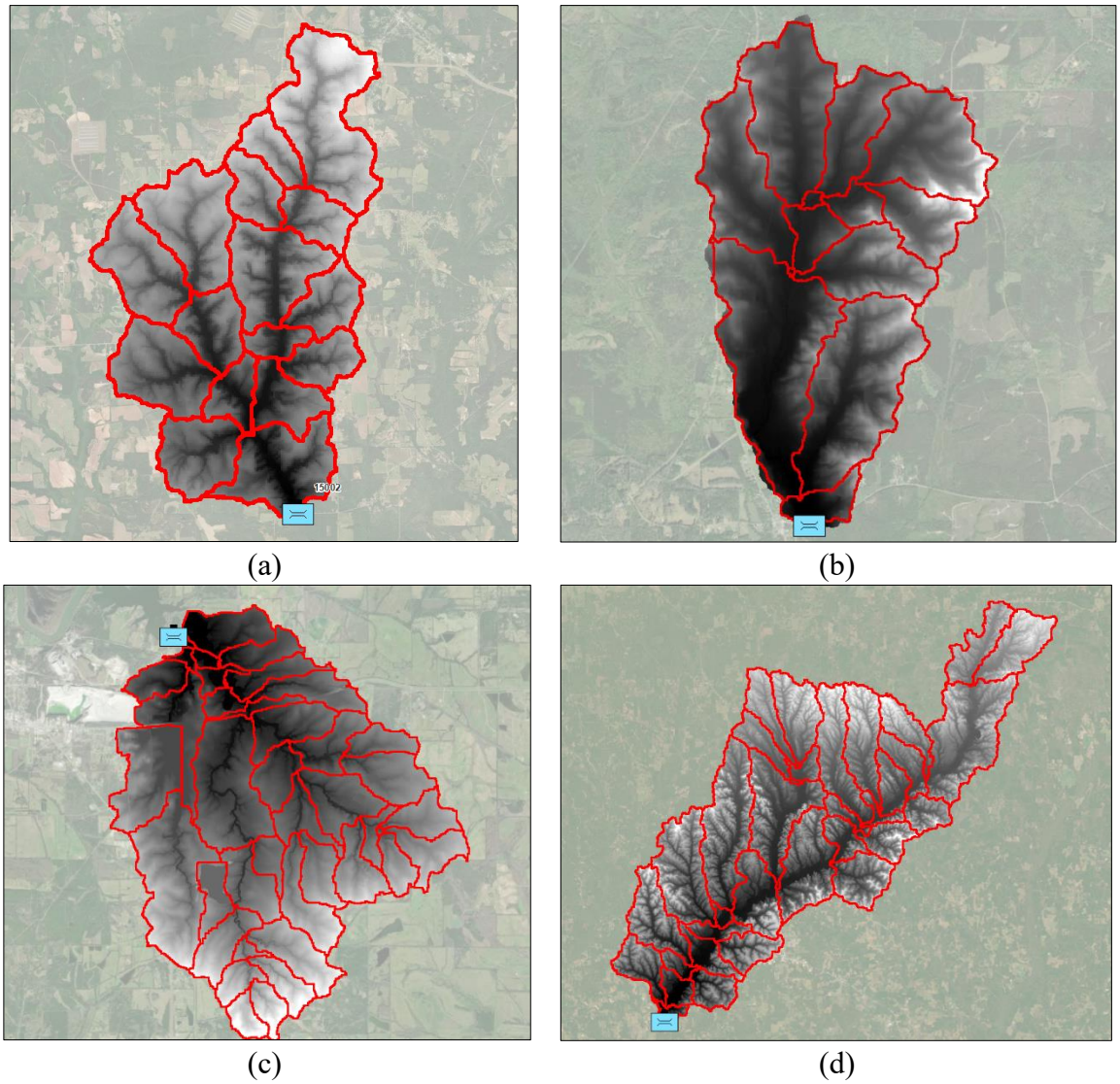

Figure 25. DEMs for the watersheds associated with the selected bridges (a) BrM No 015002 (b) BrM No 010738 (c) BrM No 007070 (d) BrM 013310

iii. Process the DEM using HEC-GeoHMS using the recommendations by Fleming and Doan (2009). This process is associated with the catchment and stream definition based on flow direction and accumulation. Also, this process defines a slope map for the watersheds.

iv. Define the watershed characteristics using the post-processed DEM using HEC-GeoHMS using the guidelines proposed by Fleming and Doan, 2009. Those

characteristics are related to river length, river and basin slope and definition of the longest flow path.

v. Define the hydrological methods to be simulated in HEC-HMS in terms of losses, transformations, base flow, and routing methods. Additionally, it is necessary to specify the required parameters for each method, depending on the chosen one. Typically, these methods have different parameters and necessary information. In this specific case, the Natural Resources Conservation Service curve number was used as a loss method. A fully composite CN_{II} is determined by using geoprocessing analysis in ArcGIS 10.x, integrating data from the National Land Cover Dataset (NLCD) (Dewitz, J., and U.S. Geological Survey 2021) and the Soil Survey Geographic Database (Soil Survey Staff, NRCS, USDA 2015) as reference tables. In addition, values for other initial moisture contents, CN_I and CN_{III}, are also obtained. Figure 26 illustrates the land coverage for the analyzed watersheds.

vi. Extract the rainfall from Atlas 14 (Perica et al., 2013) and configure the other methods necessary to run HEC-HMS. In these specific simulations, as a rainfall transformation method, the SCS dimensionless synthetic hydrograph (Mockus, 1972) was used for each of the sub-basins. The base flow value was not considered in the analysis. Other processes, such as evaporation or recharge, were considered negligible because the simulations were event-based and thus not continuous.

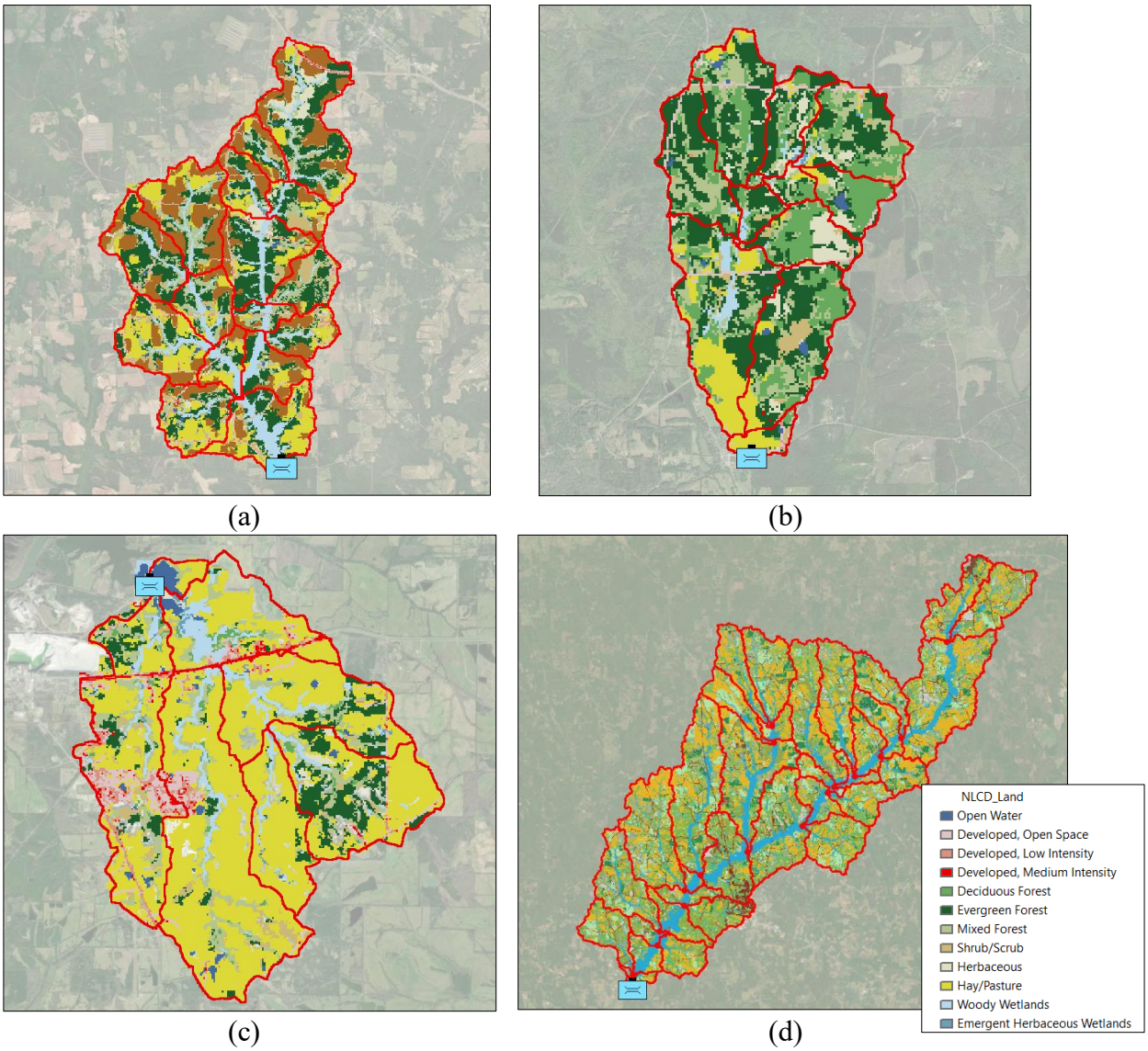

Figure 26. Land cover values for the analyzed watersheds related with the bridges (a) BrM No 015002 (b) BrM No 010738 (c) BrM No 007070 (d) BrM 013310

vii. Export the model to HEC-HMS from HEC-GeoHMS following the recommendations by (Fleming and Doan, 2009). Figure 27 shows the models created in HEC-HMS.

viii. Run the models and obtain the output hydrographs. These hydrographs correspond to CN_{II} or normal antecedent moisture conditions.

ix. Create models for dry antecedent moisture conditions CN_I and wet antecedent moisture conditions $CN_{III,}$ taking as a reference the models constructed for CNII and using the equations from Table 1 for each of the sub-basins belonging to each of the hydrological models.

x. Run the models for CN_I and CN_{III} and obtain the additional output hydrographs for each watershed.

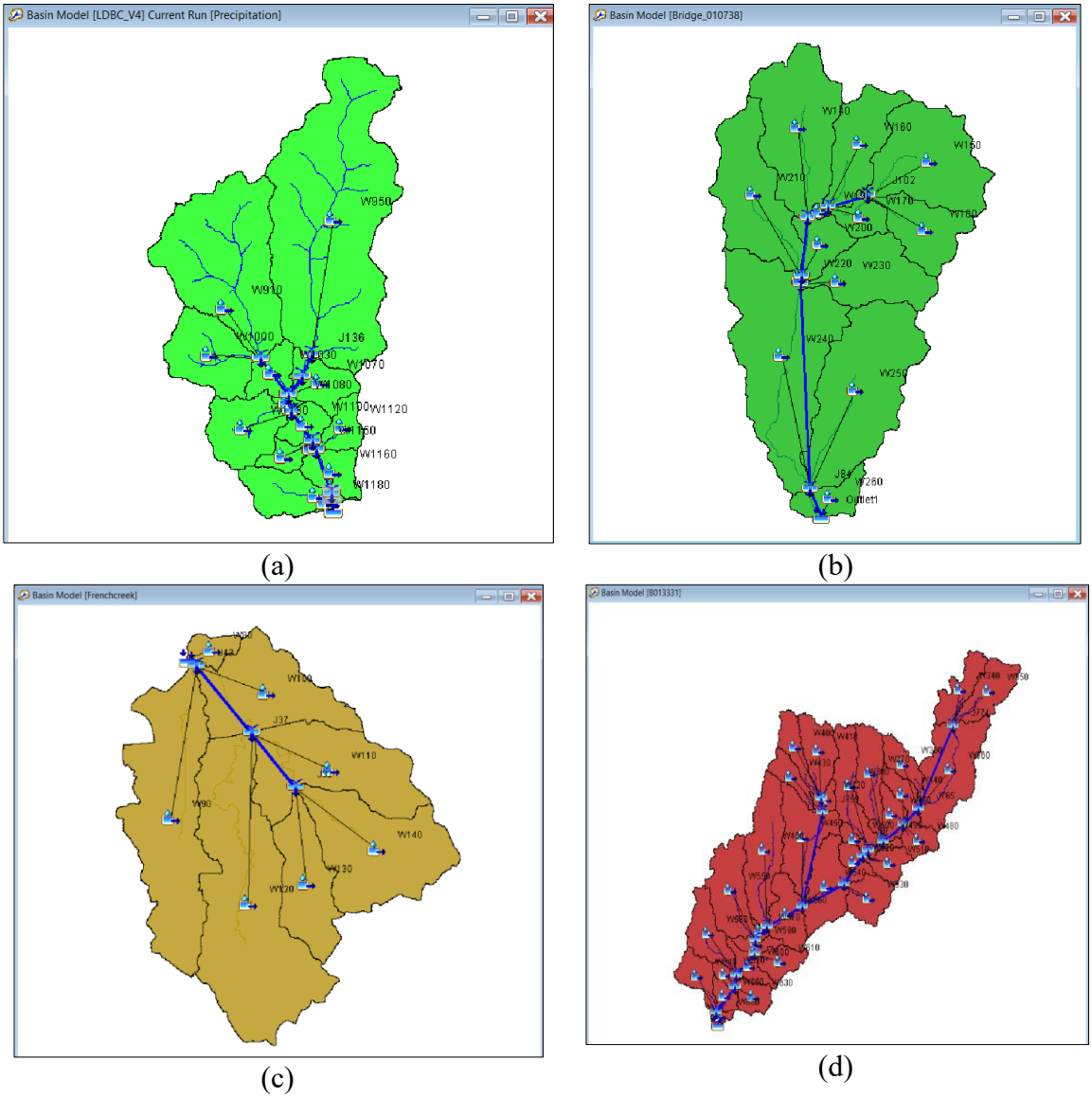

Figure 27. Models created in HEC-HMS for the watersheds associated with the bridges (a) BrM No 015002 (b) BrM No 010738 (c) BrM No 007070 (d) BrM 013310

3.2.4. Hydrological Calibration

For Bridge No 015002, which is the site of a USGS station. A calibration effort was performed for the HEC-HMS model. During an interval of 15 months, a rain gauge (see Figure 27) was deployed and utilized to collect and record information. The rain gauge data was utilized when combined with the stream flow measurements obtained from the USGS station to establish the calibration of a relatively strong rainfall event that occurred on March 18, 2022, which had a return period of 5 years. The calibration process was conducted taking into account the recommendations by Felman (2000) and using as objective function the percent error in peak and (Equation 4) presented in subsection 2.1.3 of this document.

Figure 28. Rain gage deployed in Bridge BrM No 015002

3.3. Hydraulic modeling approaches

Four different hydraulic modeling approaches were employed in order to determine the velocity in the proximity of the bridge. The velocities used for pier scour predictions were consistently applied at the same locations and over the same paths, ensuring consistency in the analysis. Two 1D steady models in which energy losses in bridges were simulated in HEC-RAS 6.1/6.2, one using WSPRO (Arneson and Shearman, 1998) and the other using

Energy Equation (Brunner, 1995) (Brunner and CEIWR-HEC, 2020). Similarly, two 2D unsteady models were tested using different bridge approaches, one using an SA/2D connection (Brunner et al., 2020) and the second using a terrain modification with raised piers (Hydrologic Engineering Center, 2023). These models aimed to analyze the impact of the bridge structure on flow patterns and water levels during unsteady flow conditions. The Courant number method, as described by Bruner (2021), was used in the implementation of the 2D models to ensure accurate and stable numerical simulations. The maximum Courant number used was 2.0 and the minimum 0.5. This method accounts for the time step size and grid spacing to maintain stability and avoid numerical instabilities. Because HEC-RAS uses an implicit solution scheme, courant numbers can be greater than one and still maintain a stable and accurate solution (Brunner et al., 2020).

Three types of geometries were created for the simulation of each bridge. The first corresponds to geometry used for the 1D models (WSPRO and Energy), which was the same; the difference lay in the bridge modeling approach and the number of cross sections that each method used to solve energy losses (Arneson and Shearman, 1998) (Brunner et al., 2020). The second type corresponds to the SA 2D connection, and the third type uses terrain modifications with raised piers. The mesh for this type of model is similar to the SA 2D connection, but it was discretized more finely in the areas near to the bridge approach and piers. Typically, cell values equal to or smaller than the pier size were considered to ensure variation in velocity between adjacent cells.

Below are presented the methodological steps for constructing the hydraulic models.

i. Download the terrain using RAS-Mapper in HEC-RAS. The Digital Elevations Models used for hydraulic calculations were Lidar data with a resolution of 1 meter x 1 meter (3.28 ft x 3.28 ft).

ii. Draw the 1D geometry (cross-sections) or 2D geometry according to the hydraulic model to be modeled (Define grid, grid size, mesh errors, computational points, and necessary breaklines).

iii. Define the bridge section for 1D models or the SA 2D connection for 2D models with this type of connection or modify the terrain by raising the piers.

iv. Define boundary conditions (Based on input hydrograph extracted from HEC-HMS, time step, and computational interval and other necessary parameters to set the model). The boundary conditions typically used for unsteady flow were flow hydrograph upstream and normal depth downstream.

v. Run each of the bridge modeling approach using HEC-RAS (WSPRO, Energy, 2D SA connection, 2D terrain modification with raised piers) for each analyzed flow (RRE, CN_I, CN_{II}, CN_{III})

vi. Verify warnings, errors, and results.

The following discussion provides more details of the methodological steps above and illustrates the geometry of the models used for each of the four analyzed bridges.

3.3.1. BrM No 015002. Little Double Bridges Creek and County Road 606

This section displays the geometry for the hydraulic models developed for Bridge BrM No. 015002, which is located over County Road 606 and crosses Little Double Bridges Creek. Figure 29 (a) and Figure 29 (b) display the geometry created for the 1D models (WSPRO and Energy) and the bridge cross section, respectively. Also, Figure 30 (a) shows the 2D geometry and Figure 30 (b) shows the SA 2D connection.

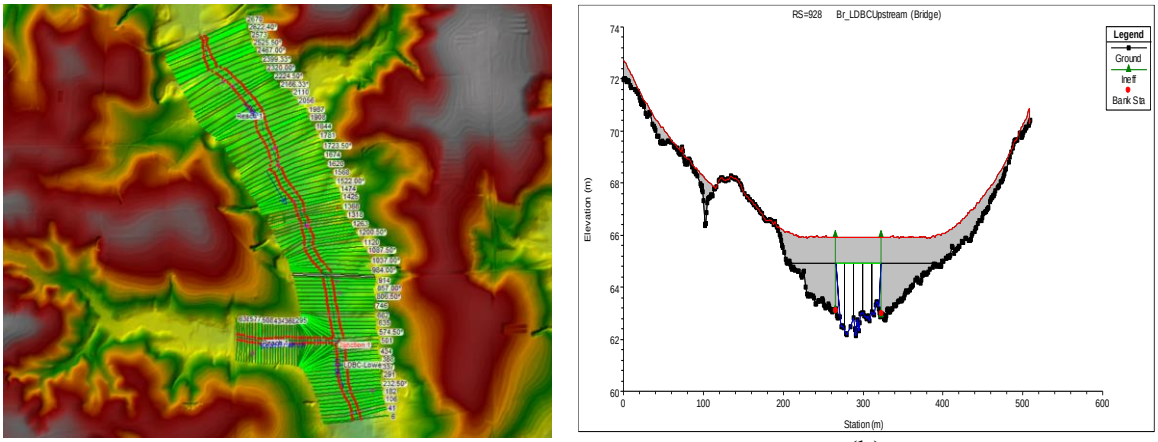

(a) (b)

Figure 29. Geometry 1D Hydraulic model in HEC-RAS and bridge cross section

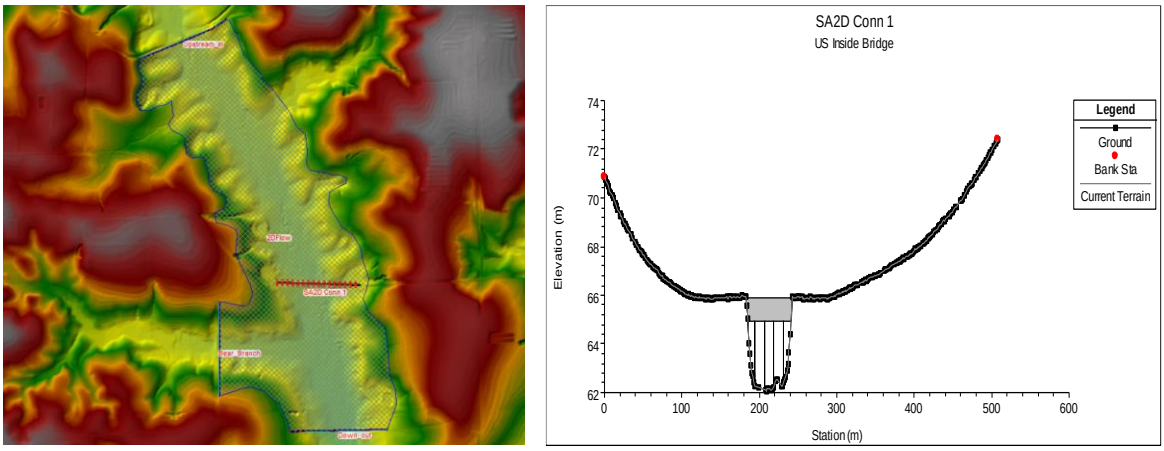

(a) (b)

Figure 30. Geometry 2D Hydraulic model in HEC-RAS and bridge and SA 2D connection

Similarly, Figure 31 (a) shows the set of 16 piers that were stamped into the DEM represent of the 2D terrain model with raised piers and Figure 31 (b) illustrates a bridge cross section with four columns caused by the modified terrain.

(a) (b)

Figure 31. Terrain modification with raised piers

3.3.2. BrM No 010738. Blue Creek and Meriwether Trail

The geometries for the hydraulic models generated for Bridge BrM No. 010738, which crosses the Blue Creek and Meriwether Trail, are shown in this section. Figure 32 (a) and Figure 32 (b) show the geometry developed for the bridge cross section and the 1D models (WSPRO and Energy), in that order. Additionally, Figure 33 (a) depict the 2D geometry and Figure 33 (b) SA 2D connection.

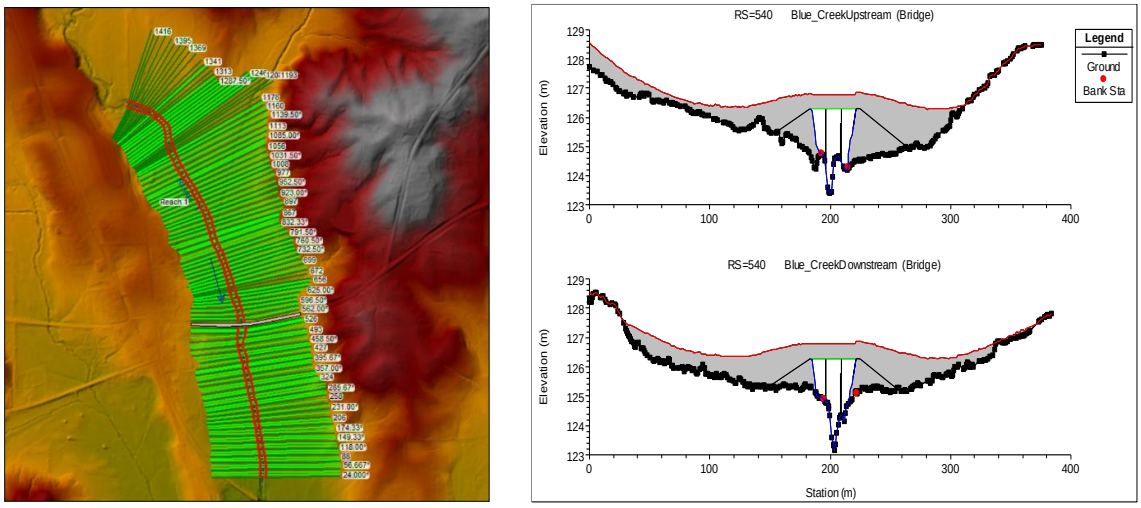

(a) (b)

Figure 32. Geometry 1D Hydraulic model in HEC-RAS and bridge cross section

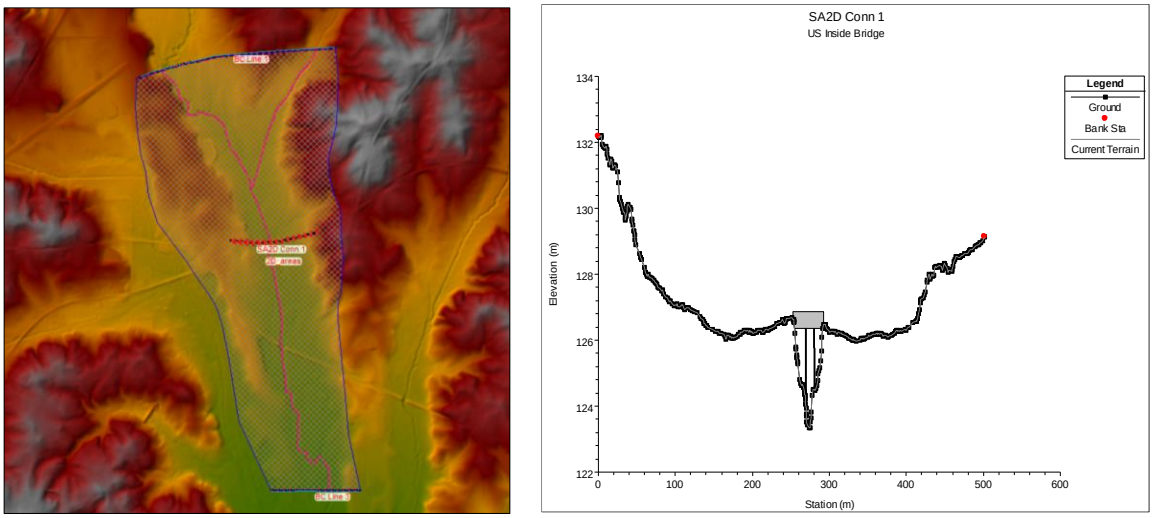

(a) (b)

Figure 33. Geometry 2D Hydraulic model in HEC-RAS and bridge and SA 2D connection

Finally, Figure 34 (a) displays a total of 10 piers that were incorporated into the DEM of the 2D terrain model with raised piers and Figure 34 (b) illustrates a bridge cross section with two columns as a result of the modified terrain.

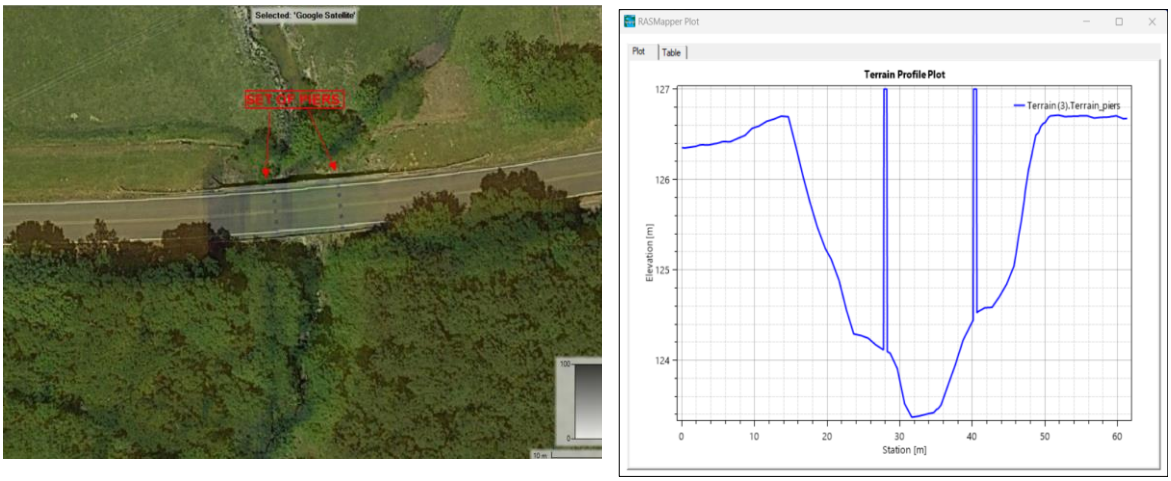

(a) (b)

Figure 34. Terrain modification with raised piers

3.3.3. Bridge BrM No 013310 Conecuh River and CR 2243

In this part, the geometries for the hydraulic models created for the Bridge BrM No. 013310, which intersects the Conecuh River and County Road 2243, are shown. In this subsection Figure 35 (a) show the geometry developed for the 1D models (WSPRO and Energy) and Figure 35 (b) the bridge cross section. Additionally, Figure 36 (a) depicts the 2D geometry and Figure 36 (b) SA 2D connection.

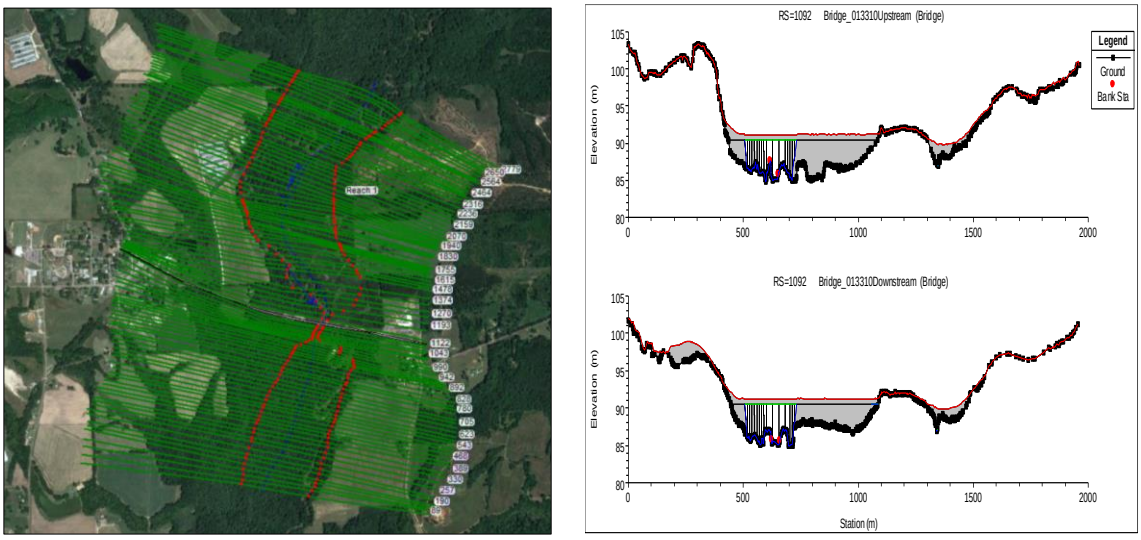

(a) (b)

Figure 35. Geometry 1D Hydraulic model in HEC-RAS and bridge cross section

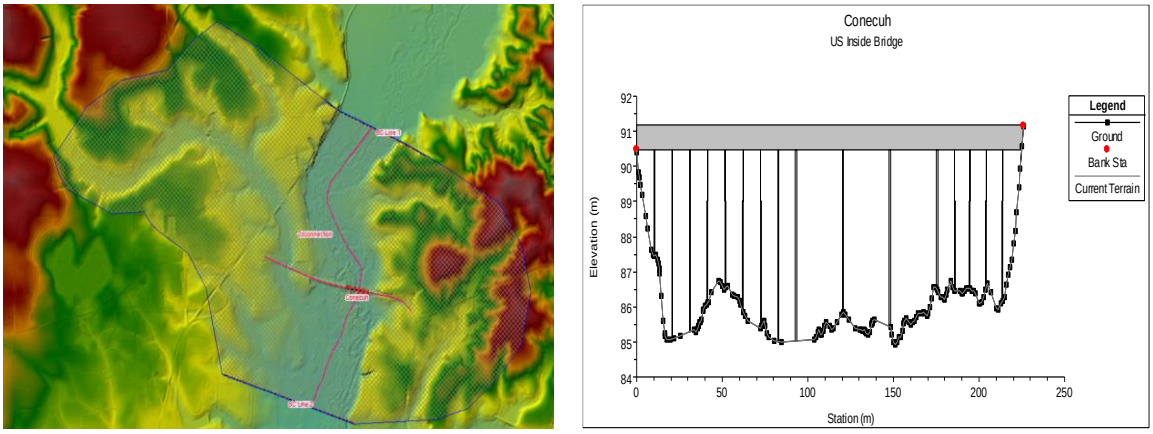

(a) (b)

Figure 36. Geometry 2D Hydraulic model in HEC-RAS and bridge and SA 2D connection

Finally, Figure 37 (a) displays a total of 58 piers were included into the terrain for the 2D model with raised piers and Figure 37 (b) depicts a bridge cross section with sixteen columns after the terrain DEM modification.

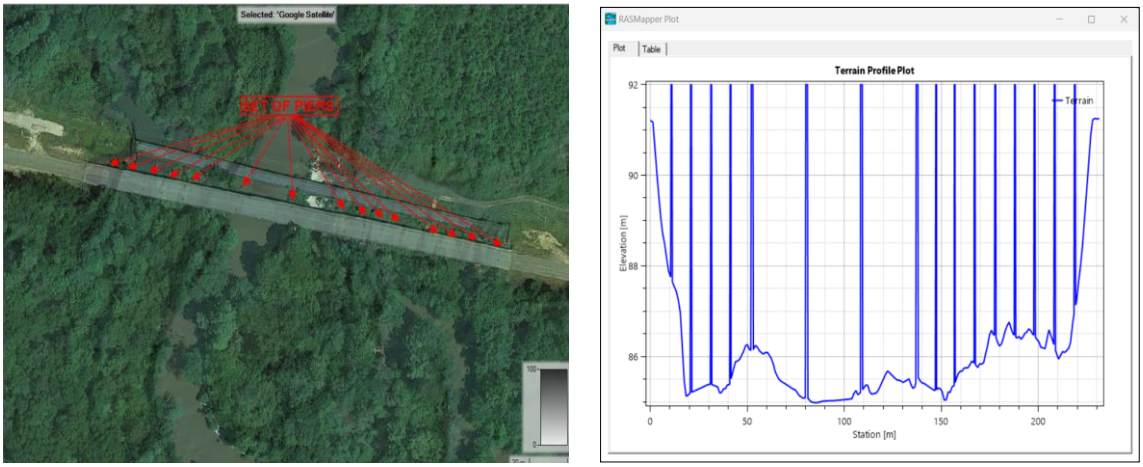

Figure 37. Terrain modification with raised piers

3.3.4. BrM No 007070. French Creek and CO RT No 62

The geometric details of the hydraulic models implemented for Bridge BrM No. 007070, which is over County Road 2243 and intersects the Conecuh River, are presented.

In this subsection Figure 38 (a) displays the geometry created for the 1D models (WSPRO and Energy), while Figure 38 (b) provides an illustration of the bridge cross-section. Furthermore, Figure 39 (a) showcases the 2D geometry, and Figure 39 (b) demonstrates the SA 2D connection.

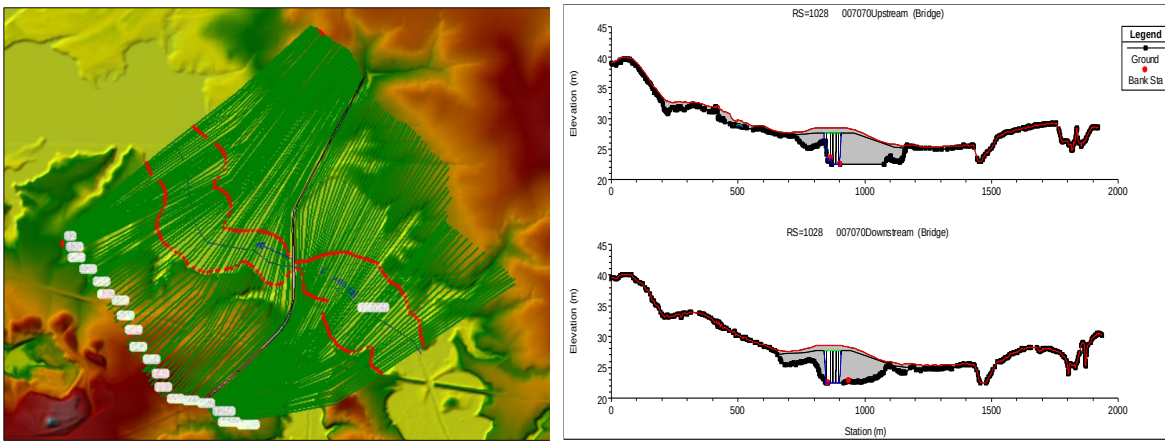

(a) (b)

Figure 38. Geometry 1D Hydraulic model in HEC-RAS and bridge cross section

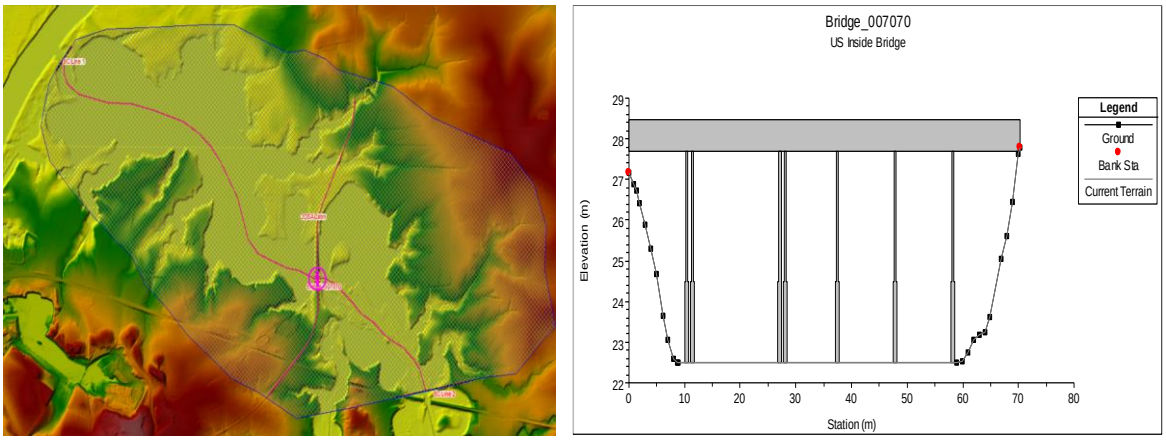

(a) (b)

Figure 39. Geometry 2D Hydraulic model in HEC-RAS and bridge and SA 2D connection

Figure 40 (a) presents the incorporation of 20 piers into the terrain for the 2D model with raised piers, while Figure 40 (b) presents a bridge cross-section featuring seven columns following the terrain adjustments.

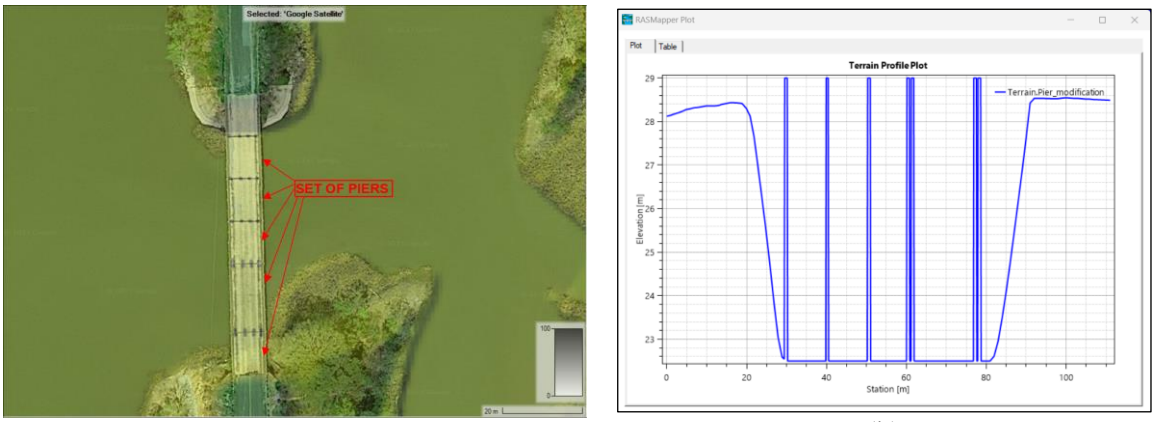

(a) (b)

Figure 40. Terrain modification with raised piers

3.4. Scour Calculations

This section provides an overview of the methodology associated with pier scour calculations for the four analyzed bridges. These calculations were divided into two parts, which are: scour calculation using the HEC-18 method and scour calculation using the OMS method. The methodological steps for both methods are described below.

3.4.1. Pier scour calculations using HEC-18 method.

The methodological steps used to perform scour calculations using the HEC-18 equation, based on CSU (Anerson et al., 2012) are outlined as follows:

i. Extract the depth and velocity values from HEC-RAS (Brunner et al, 2020) for each of the columns comprising the bridges, using each of the analyzed approximation methods (WSPRO, Energy, 2D SA connection, 2D terrain modification with raised piers).

ii. Extract the directions of the velocity vectors in RAS-Mapper (Brunner et al, 2020) for each of the approximation methods and determine the flow approach angle to the columns.

iii. Define values for K1, K2, and K3 factors for pier nose shape, angle of flow attack, and bed condition, respectively (Anerson et al., 2012).

iv. Estimate the particle distribution size of the soil for each bridge. It is necessary to take samples from the riverbed of the bridge and conduct this type of analysis in the lab to obtain $D_{50.}$

v. Perform calculations for each of the bridge piers using Equation 14 (See subsection 2.3.3) (Anerson et al., 2012). Use Hydraulic Toolbox 5.3 to solve hydraulic calculations (Bergendahl and Arneson, 2014), (Ghelardi, 2021). Hydraulic Toolbox was used instead of HEC-RAS because the bridge scour calculations in HEC-RAS are based on the fourth edition of HEC-18 (Richardson and Davis, 2001). Brunner (2020) mentions that the scour calculations in HEC-RAS have not been modified to keep the changes that are included in the fifth edition of HEC-18 (Anerson et al., 2020).

3.4.2. Pier scour calculations using OMS.

The methodology used to perform scour calculations using OMS (Govidasamy et al., 2013) (Briaud et al., 2011) is described below:

i. Determine the maximum observed scour $Z_{mo.}$ This value is determined using the inspections recorded in BrM, considering Zmo as the value of the original profile compared to the current profile. Additionally, the pile with the greatest scour is identified, and its value is recorded.

ii. Calculate the recurrence interval using TAMU Flood (Briaud et. al, 2011) based on nearby stream gages and rain gages.

iii. Obtain the ratio Q_{mo}/Q_{fut} as a function of the recurrence interval. Calculate the valor Q_{mo} y Q_{fut}=Q_{100} usando RRE

iv. Estimate the ratio between the maximum future velocity V_{max} and the maximum observed velocity V_{mo} through the local recurrence interval. Convert Q_{mo} to V_{mo} and Q_{fut} to V_{fut} using Manning equation HEC-RAS (1D or 2D)

Estimate future scour as a ratio between the maximum future scour Z_{max} and the maximum observed scour Z_{mo}

3.5. Comparison between scour results

The approaches used to compare the different alternatives for calculating the peak flow used for scour calculations through various bridge approximation models is presented below:

i. Direct comparison between the results and the different alternatives to calculate peak flow and scour. It was considered that the approach using HEC-HMS and HEC-RAS 2D with raised piers was the reference for comparison.

ii. Calculation of peak to average for scour. This value corresponds to the maximum calculated scour depth in one of the columns divided by the average scour depth of all columns in the cross-section of the bridge.

4. RESULTS

In this chapter, the results of the differences found among the various alternatives used to calculate peak flow for the scour analysis in bridge piers through hydraulic models for four bridges in Alabama are presented.

4.1 Hydrological Results

The information provided below presents the results of the different hydrological alternatives used to calculate peak flow in the selected bridges. These alternatives include RRE, FFA, and hydrological models.

RRE values for a 100-year event were calculated for the sites where the bridges are located, using the bridge as the watershed outlet. The values were computed in accordance with the guidelines provided by (Hedgecock and Lee, 2010) and (Anderson, 2020). The results of the values obtained using RRE are presented in Table 3**.**

Table 3. Peak using RRE for 100-yr return period values for the four analyzed bridges

BrM ID	River	Area (sq.mi)	PeakFlow (cfs)
015002	Little Double Bridges Creek	21.6	7,682
010738	Blue Creek	4.5	3,221
007070	French Creek	12.5	7,616
013310	Conecuh River	373.3	38,017

4.1.1 BrM No 015002. Little Double Bridges Creek and County Road 606

For the bridge BrM ID 015002, which has a USGS streamflow gauge station, it was performed an FFA analysis. Analyzing 37 years of peak streamflow data covering from 1986 to 2022, and utilizing the USGS software PeakFQ 7.4, a 100-year streamflow event was calculated obtaining a value of 14,570 cfs. This result is 89% longer than the corresponding RRE results.

In order to identify the cause of this difference, we searched for extreme events that occurred around the time when the peak instantaneous flow value was recorded and it was found that the record corresponded to Tropical Storm Alberto, which hit the area around Enterprise, Alabama, and BrM id 015002 on July 7, 1994. This situation shows that the value recorded at USGS Station No. 02362240 is real and illustrates that, in some cases, values calculated using RRE may not represent the worst scenario for peak flow calculation.

Using data collected from the rain gauge installed at Bridge No. 015002 and stream flow data recorded in the USGS Station No. 02362240, parameter calibration was performed for the Little Double Bridges Creek watershed, which drains into that bridge. The calibration process was carried out in HEC-HMS 4.9, aiming to minimize percent error in peak discharge (Equation 4) for a significant event-based that occurred on March 18, 2022. The optimization results for minimizing the percent error in peak discharge for Little Double Bridges is shown in Figure 41 and the comparison between the two resultant outflow hydrographs is illustrated in Figure 42. In the calibration process, the values of the composite CN remained constant, while the roughness coefficient for overland flow planes and channels values were varied for a simplex optimization in each sub-basin of the watershed. After the calibration process it was found a difference in the peak flow discharge between the observed and the calibrated data corresponding to 10 cfs, which is equivalent to a value of 0.5% of percent error in peak discharge. The roughness parameters adjusted during the calibration process were used in models representing different antecedent soil moisture conditions for the watershed associated with the mentioned bridge and considering that the other bridge watersheds share similar land use characteristics, urbanization percentages, and rural predominance; these parameters served as references for developing the other watershed models.

Objective Function Results for Trial "Optimization 1"

Project:Project 4 Optimization Trial:Optimization 1

Start of Trial: 17mar.2022, 00:00 Basin Model: dbcreek9
End of Trial: 20mar.2022, 23:45 Meteorologic Model:dbcreek9
Compute Time:18ene.2023, 20:08:40

Statistic at Basin Element "Outlet10"

Goal: Minimization
Statistic: Percent Error In Peak Discharge
Start of Function:17mar.2022, 00:00
End of Function: 20mar.2022, 23:45
Value: 0.10

Volume Units: (•) IN ( ) ACRE-FT

Measure	Simulated	Observed	Difference	Percent Difference
Volume (IN)	0.73	1.35	-0.62	-45.86
Peak Flow (CFS)	2060.5	2070.0	-9.5	-0.5
Time of Peak	18mar.2022, 15:45	18mar.2022, 17:30		

Figure 41. Calibration results for minimizing the percent error in peak discharge in Little Double Bridges Creek (BrM No 015002)

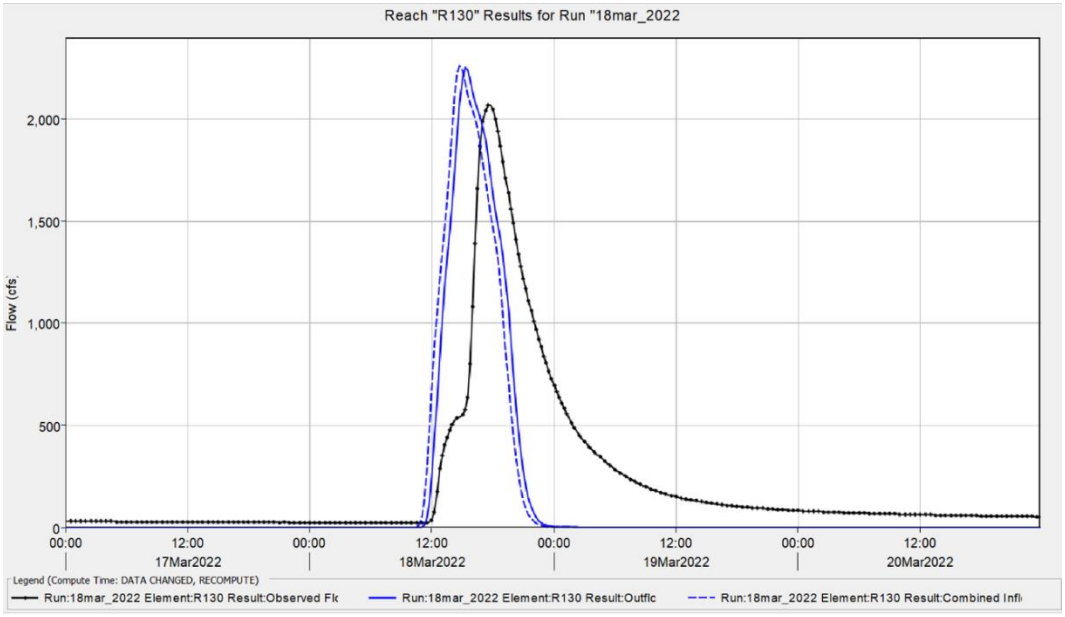

Figure 42. Comparison between the two resultant outflow hydrographs. Observed discharge (Black line) and Calibrated discharge (Blue line)

Hydrological models were created for 100-year rainfall events and evaluated for each watershed associated with the analyzed bridges. Due to the lack of calibration, the same setting for the hydrologic simulations on 015002 was used for the other bridges. In each case, different scenarios of antecedent moisture conditions (AMC), dry conditions (CN_I), normal conditions (CN_{II}), and wet conditions (CN_{III}) was used to facilitate the comparison of

results to make it easier to compare the results visually and assess how antecedent soil conditions affected the peak flow used for scour calculation, the results of the outflow hydrographs by watershed for each of the antecedent soil moisture conditions CN_I, CN_{II}, and CN_{III} are presented in groups. The value of CN_I is presented but hydraulic computations were not performed for these cases because flows were small, and scour would be minimum.

The outflow hydrographs are presented in Figure 43 for the watershed associated with the bridge BrM No 015002. In addition, Table 8 shows the peak flow value for each outflow hydrograph.

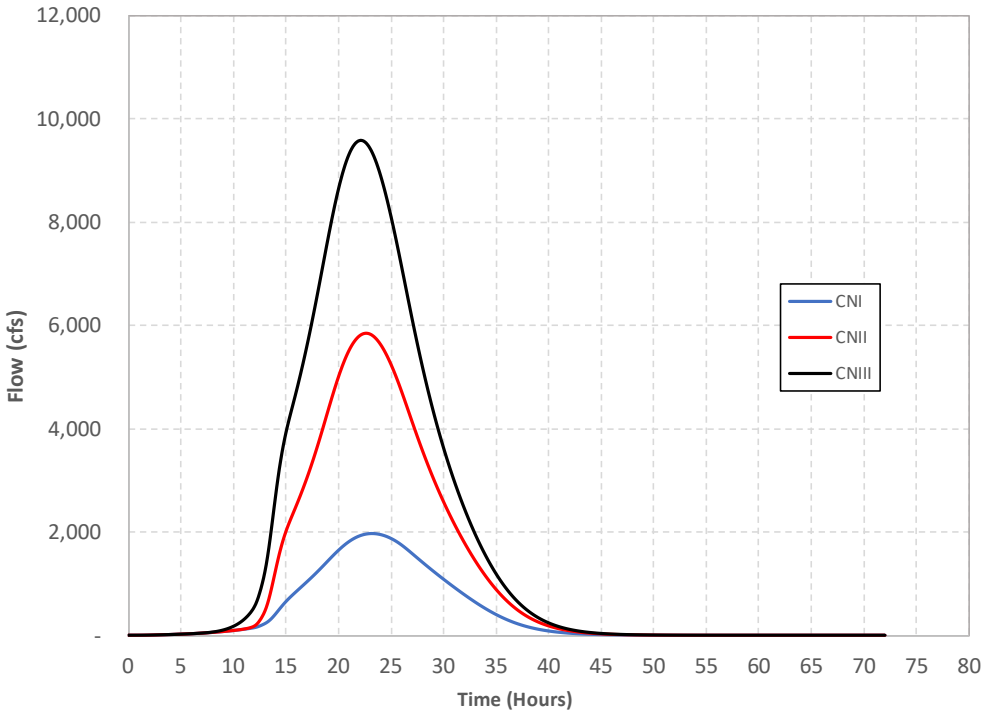

Figure 43. Outflow hydrographs for watershed associated BrM No 015002 and different antecedent soil moisture conditions, CN_I, CN_{II} and CN_{III}

Table 4. Peak flow for different antecedent moisture conditions. BrM No 015002 watershed

BrM ID	River	Peak flow AMC (cfs)		
		CN_I	CN_{II}	CN_{III}
015002	Little Double Bridges Creek	1,981	5,900	9,689

The results shown in Figure 46 and Table 4 reveal a difference of 3,789 cfs between the values of CN_{II} and CN_{III}, which corresponds to a difference of 64% percent. Additionally, it was observed that the value associated with CN_{II} does not represent the worst-case scenario in the calculation of peak flows that were modeled.

When comparing the peak flow of the RRE with CN_{II} and CN_{III}, the RRE is approximately 30% higher than CN_{II} and 26% lower than CN_{III}. Finally, when compared RRE and CN_{III} with FFA, RRE is 89% and CN_{III} is 50% lower than FFA. In this specific case, due to the presence of the extreme event Tropical Storm Alberto in 1994, neither the values of RRE nor those of the models using CN_{II} or CN_{III} correspond to the worst-case scenario recorded for this bridge. However, the value from the model using CN_{III} (wet antecedent moisture conditions) could be the scenario to use in the absence of data.

4.1.2 BrM No 010738. Blue Creek and Meriwether Trail

Similarly, scenarios using different antecedent soil moisture conditions were created and modeled for the Blue Creek watershed associated with Bridge BrM No 010738. The outflow hydrographs for this watershed are presented in Figure 44 and the peak flows for the different antecedent moisture conditions are presented in Table 5.

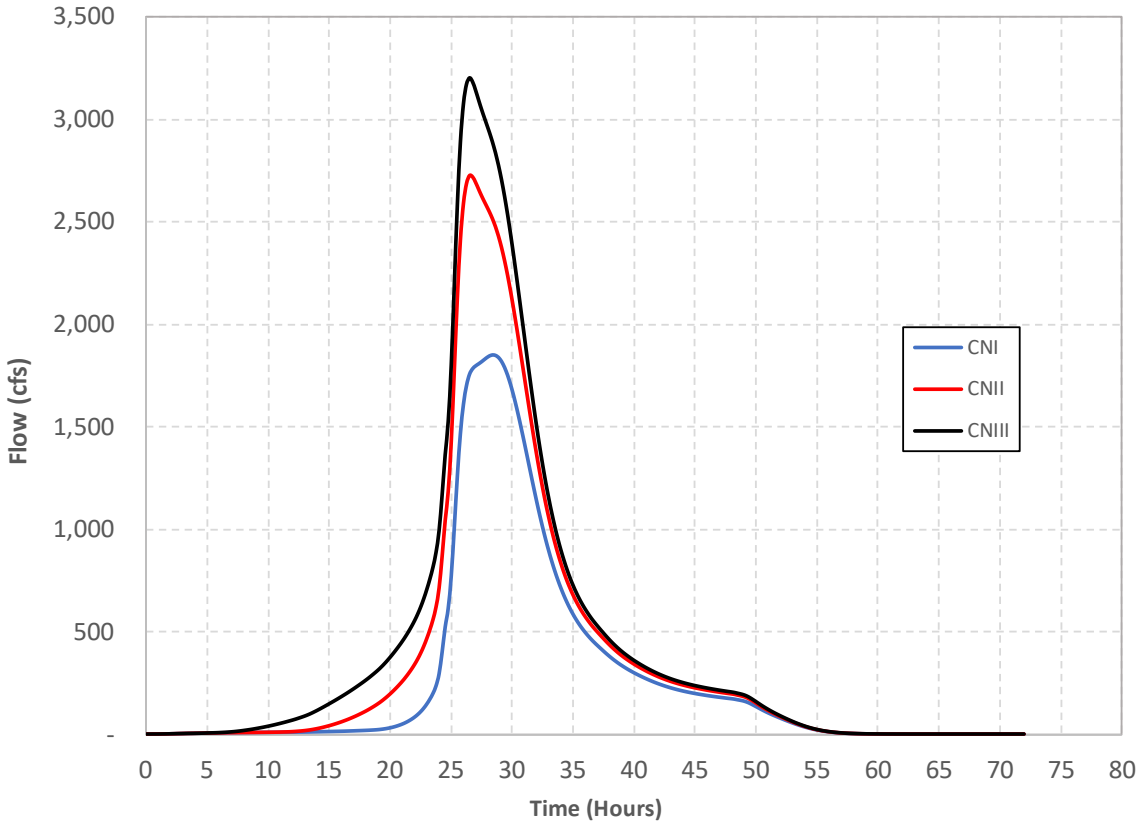

Figure 44. Outflow hydrographs for watershed associated BrM 0107038 and different antecedent soil moisture conditions, CN_I, CN_{II} and CN_{III}

The results provided in and Table 5 demonstrate a 16% difference in the values of the models employing CN_{II} and CN_{III}. Furthermore, when the peak flows modeled are compared to the RRE, it is found that the RRE value is greater by 0.6% and 16.9% than the models using CN_{III} and CN_{II}, respectively.

Table 5. Peak flow for BrM No. 010738 watershed using different antecedent moisture conditions.

BrM ID	River	Peak flow (cfs)		
		CN_I	CN_{II}	CN_{III}
010738	Blue Creek	1,849	2,756	3,202

4.1.3 BrM No 013310. Conecuh River and County Road 2243

In the same way, similar outflow hydrographs were made for BrM No. 013310 over Conecuh River using the same previous soil moisture conditions. These hydrographs are presented in Figure 45 and the peak flows associated with those hydrographs are presented in Table 6.

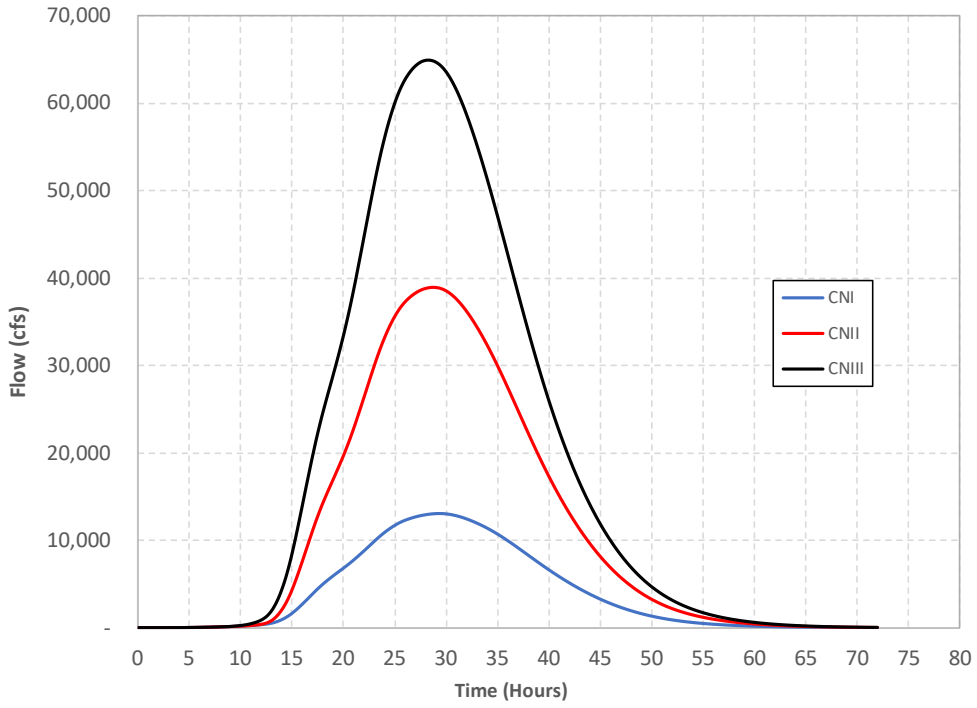

Figure 45. Outflow hydrographs for watershed associated BrM 013310 and different antecedent soil moisture conditions, CN_I, CN_{II} and CN_{III}

For this case, Table 6 shows a difference 66.8% between the peak flows calculated using CN_{II} and CN_{III}, and when these values are compared with RRE, CN_{II} is 2.39% greater than the RRE, and the CN_{III} is 70.8% higher. In this case, it is observed that the RRE values are closer to CN_{II}.

Table 6. Peak flow for BrM No. 007070 watershed using different antecedent moisture conditions.

BrM ID	River	Peak flow AMC (cfs)		
		CN_I	CN_{II}	CN_{III}
13310	Conecuh River	13,072	38,926	64,934

4.1.4 BrM No 007070. French Creek and CO RT No 62

Finally, models were constructed for the watershed associated with bridge BrM No 007070 under different antecedent soil moisture conditions. These hydrographs are shown in Figure 46, and the peak flows related with those hydrographs are presented in Table 7.

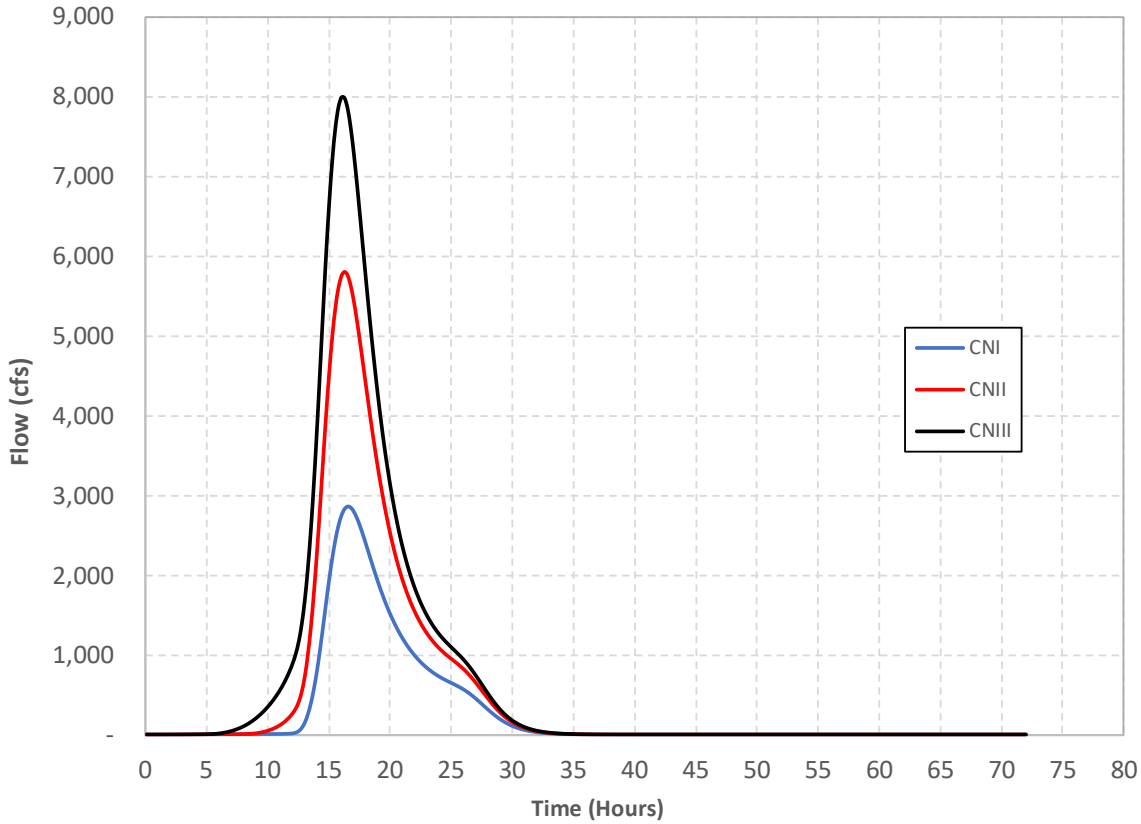

Figure 46. Outflow hydrographs for watershed associated BrM 007070 and different antecedent soil moisture conditions, CN_I, CN_{II} and CN_{III}

For this case, Table 7 shows a difference 36.8% between the peak flows calculated using CN_{II} and CN_{III}, and when these values are compared with RRE, CN_{II} is 31% lower than the

RRE, and the CN_{III} is 4.8% higher. In this case, it is observed that the RRE values are closer to CN_{III}.

Table 7. Peak flow for BrM No. 007070 watershed using different antecedent moisture conditions.

BrM ID	River	Peak flow AMC (cfs)		
		CN_I	CN_{II}	CN_{III}
007070	French Creek	2,867	5,811	7,986

For this case, Table 7 shows a difference 36.8% between the peak flows calculated using CN_{II} and CN_{III}, and when these values are compared with RRE, CN_{II} is 31% lower than the RRE, and the CN_{III} is 4.8% higher. In this case, it is observed that the RRE values are closer to CN_{III}.

4.1.5 Summary of the Hydrological Results

As a summary of the results described above, Table 8 presents the obtained peak flows for the hydrological methods used.

Table 8. Peak flow using hydrological models for a 100-yr return period for the four analyzed bridges

BrM ID	River	Peak flow RRE (cfs)	HEC-HMS estimates Peak flow AMC (cfs)		
			CN_I	CN_{II}	CN_{III}
015002	Little Double Bridges Creek	7,682	1,981	5,900	9,689
010738	Blue Creek	3,221	1,849	2,756	3,202
007070	French Creek	7,616	2,867	5,811	7,986
013310	Conecuh River	38,017	13,072	38,926	64,934

4.2. Hydraulic Results

In this section, the results of the four different bridge modeling approaches used to obtain the velocity in the vicinity of the bridge are presented. A total of 48 hydraulic models, 12 per bridge, were constructed as a result of the combinations between various hydrological modeling. The alternatives to estimate peak flows, included RRE, different antecedent soil moisture conditions (CN_{II} and CN_{III}), each combined with different bridge modeling approaches. These hydraulic models included: 1D WSPRO, 1D Energy, 2D SA Connection, and 2D terrain modification with raised piers. The CN_I model was not considered for scour analysis because it did not represent a worst-case scenario in scour calculations (low flow rates). To understand and visualize the differences that occur in the different bridge modeling approaches, maps are presented as an example using as a selected hydrological alternative, the antecedent soil moisture condition CN_{II}.

Typically, the results for each bridge are presented in two types of figures. The first type corresponds to velocity maps for the bridge modeling approaches, and the second type corresponds to water depth maps using the same approaches. For the first type of map, equal velocity ranges were created for comparing the velocity results. The depth and velocity ranges varied for each of the bridges, with low velocity values represented in shades of blue-green, medium velocities in yellow-orange, and high velocities in red. Similarly, water depth ranges were represented using low water depth values in green, medium values in yellow-orange, and high values in red-magenta. As a rule, the figures are labeled from (a) to (d), where: (a) corresponds to 1D WSPRO, (b) 1D Energy Equation, (c) 2D/SA connection, and (d) to 2D terrain modification with raised piers.

In addition, figures and tables were created for velocities and water depth as a comparison of the parameters among the different bridge modeling approaches to visualize

the differences between each approach. The tables show the percentage differences for velocity and water depth between each approach against the benchmark modeling approach, which is 2D terrain modification with raised piers model (Brunner et al, 2020) (Robinson, 2019). The equations used for those calculations are shown in Equation 16 and 17.

$$\%\ \text{Difference Velocity} = \left(1 - \frac{\text{Velocity Value in each method}}{\text{Velocity value in the benchmark}}\right) \text{x } 100 \tag{16}$$

$$\%\ \text{Difference Water depth} = \left(1 - \frac{\text{Water depth value in each method}}{\text{Water depth value in the benchmark}}\right) \text{x } 100 \tag{17}$$

4.2.1 BrM No 015002. Little Double Bridges Creek and County Road 606

Figure 47 shows the velocity map for the different bridge modeling approaches for Bridge BrM No. 015002, when the alternative to calculate the peak flow is antecedent moisture condition CN_{II}. In general terms, the approach models, 1D WSPRO (a) and 1D Energy (b), look very similar, conversely with the 2D models, which have higher velocities at the bridge entrance. When the 2D models are compared to each other, the 2D/SA connection model (c) exhibits lower velocities than the 2D terrain modification with raised piers model (d).

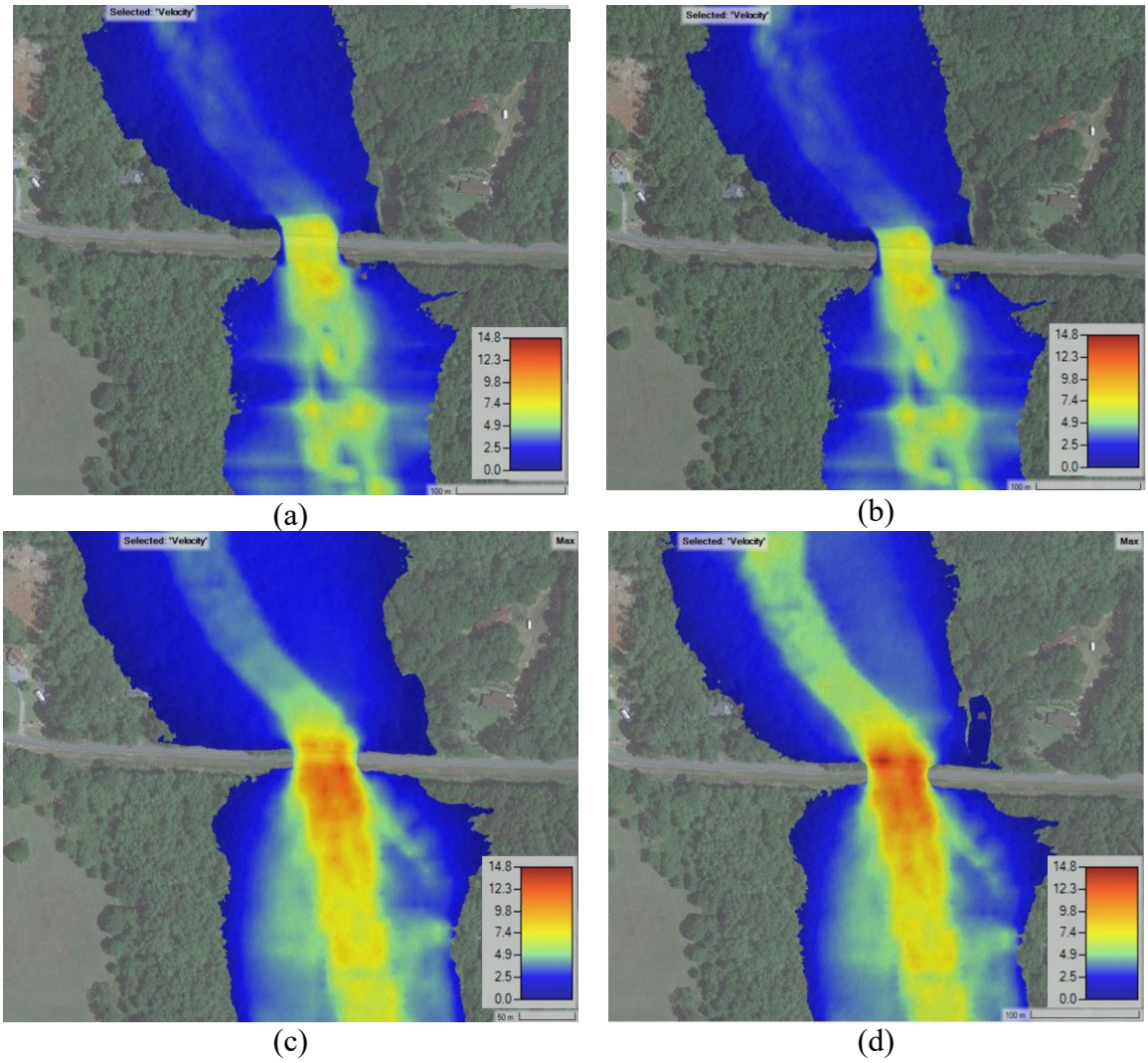

Figure 47. Velocities for different bridge modeling approaches, Bridge BrM No 015002. (a) WSPRO (b) Energy (c) 2D/SA connection (d) 2D terrain modification with raised piers

Figure 48 shows the velocity differences in each pier according to each bridge modeling approaches, showing the higher velocity in the benchmark model (2D terrain modification with raised piers) followed 2D-SA connection, WSPRO and energy, respectively. The percentage velocity differences between the benchmark and the other approaches vary depending on each approach and the method to calculate the peak flow. Table 9 shows the velocity comparison between the benchmark and the other methods, finding percentage velocity average differences below the benchmark ranging from 17.1%

to 24.1% according to each method, implying similar flow regimen conditions and velocity magnitude upstream the bridge entrance for the 1D models and the 2D SA connection model.

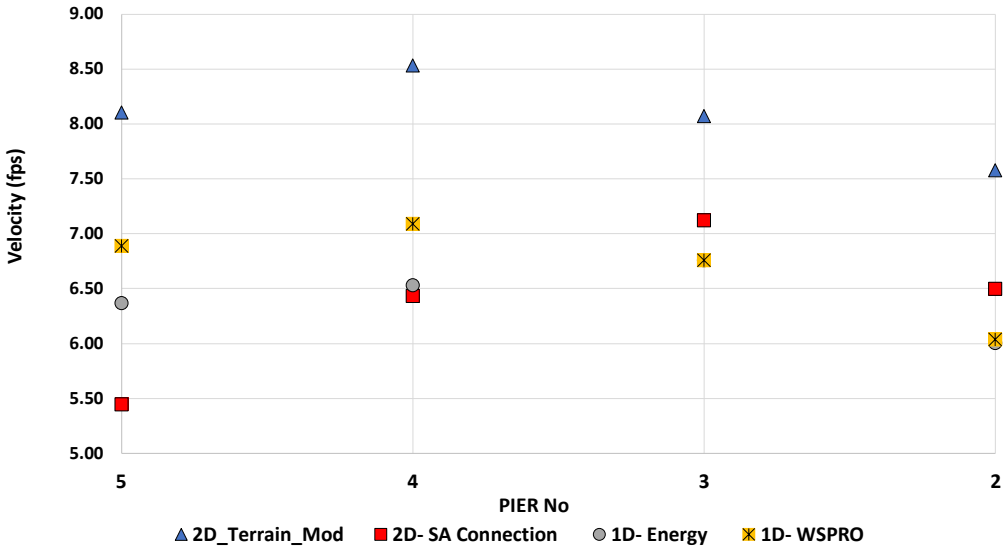

Figure 48.Velocities comparison for the bridge modeling approaches. Bridge BrM015002

Table 9. Velocity comparison between the benchmark model and other approaches for different alternatives to calculate peak flow. Bridge BrM 015002

Method	RRE	CN_{II}	CN_{III}
1D WSPRO	24 %	17.1%	23.5%
1D Energy	24.1%	20.5%	23.5%
2D Connection	21.7%	20.9%	23.5%

Similarly, Figure 49 shows that the water depth and floodplain results for the 1D models WSPRO (a) and 1D Energy (b) are very similar, contrary with the two-dimensional Models (c) (d), which display a broader floodplain and deeper water depths compared to the one-dimensional models.

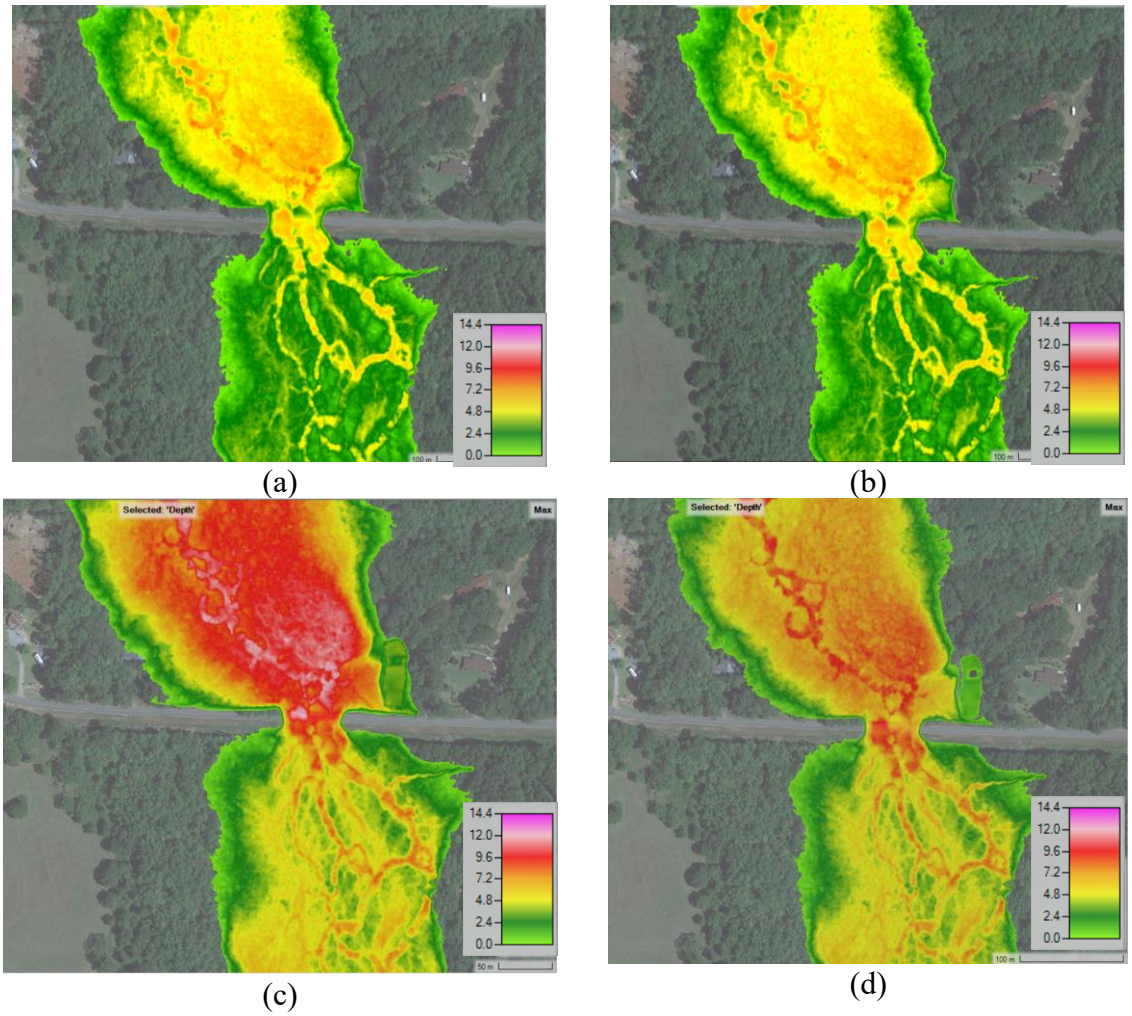

(a) (b)

(c) (d)

Figure 49. Water depth results for different bridge modeling approaches, Bridge BrM No 015002. (a) WSPRO (b) Energy (c) 2D/SA connection (d) 2D terrain modification with raised piers

When the 2D models are compared, the 2D-SA connection (c) shows a deep-water depth upstream of the bridge than the 2D terrain modification with raised piers model (d), which means low velocities upstream of the bridge. It seems that the flow is pooled at the bridge entrance in the 2D-SA connection model (c), creating a control section, a condition that may not be representative when compared to the benchmark model (2D terrain modification with raised piers), which does not represent this behavior in the results (d).

Figure 50 also shows the results for the water depths. It shows that the water depths were high for the 2D-SA connection and low for the 2D terrain modification with raised piers.

Table 10 shows the water depth comparison between modeling approaches, finding the percentage water depth average differences above the benchmark ranging from 11.6% to 55.5% according to each method. In this specific case, the negative value indicates that the average water depth percentage is above the benchmark.

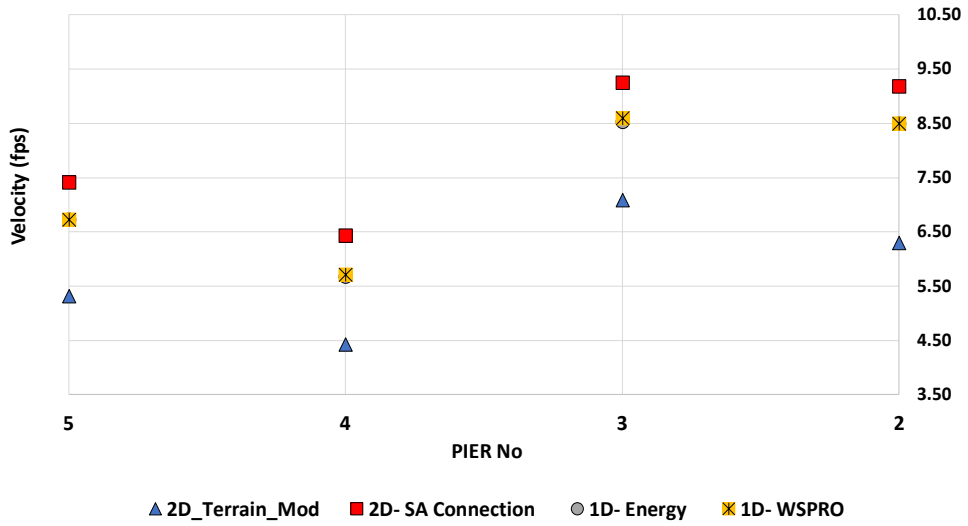

Figure 50.Water depth for the different bridge modeling approach. Bridge BrM015002

Table 10. Water depth comparison between the benchmark model and other bridge modeling approaches for different alternatives to calculate peak flow. BrM 015002

Method	RRE	CN_{II}	CN_{III}
1D WSPRO	-11.6%	-18.9%	-27.9%
1D Energy	-11.6%	-19.2%	-27.5%
2D Connection	-55.5%	-42%	-40.3%

4.2.2 BrM No 010738. Blue Creek and Meriwether Trail

Figure 51 shows the results of velocities for the different bridge modeling approaches for Bridge BrM No. 010738 over Blue Creek. Once again, the 1D velocity results for 1D models as WSPRO (a) and energy (b) are almost identical to each other, unlike the models in 2D models that show significant differences in velocity at the bridge entrance. Comparing the two 2D models, it was discovered that the 2D-SA connection model (c) has slower velocities upstream (bluer) than the 2D terrain modification model (d) (more yellow).

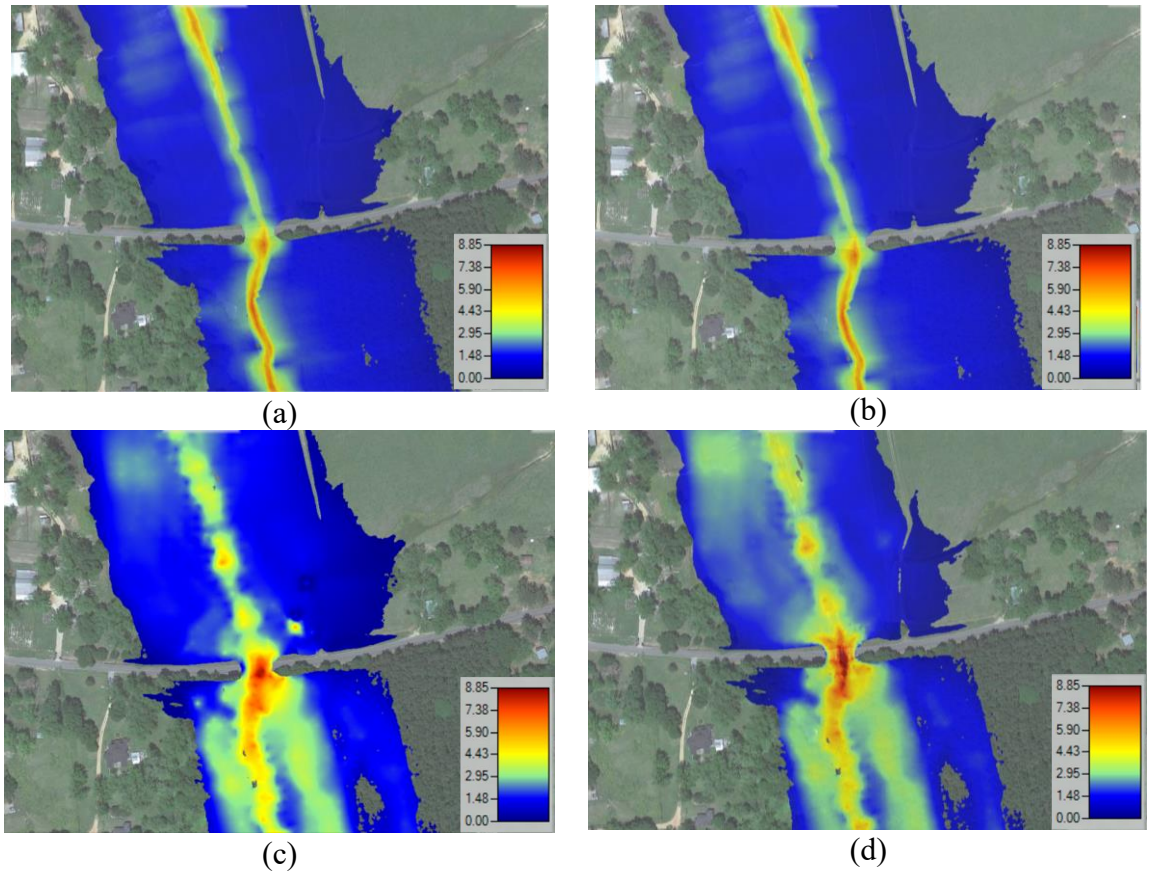

Figure 51. Velocities results for different bridge modeling approaches, Bridge BrM No 010738. (a) WSPRO (b) Energy (c) 2D/SA connection (d) 2D terrain modification with raised piers

Figure 52 shows the velocity differences in each pier according to each bridge modeling approach, showing the higher velocity in the benchmark model followed by 2D-

SA connection, WSPRO and energy, respectively. Table 11 shows the velocity comparison between the benchmark and the other methods, finding percentage velocity average differences from the benchmark to the other methods that that ranged between -1.8% below and 50% above the reference values according to each method. The negative sign shows the cases that the average velocity is above the benchmark.

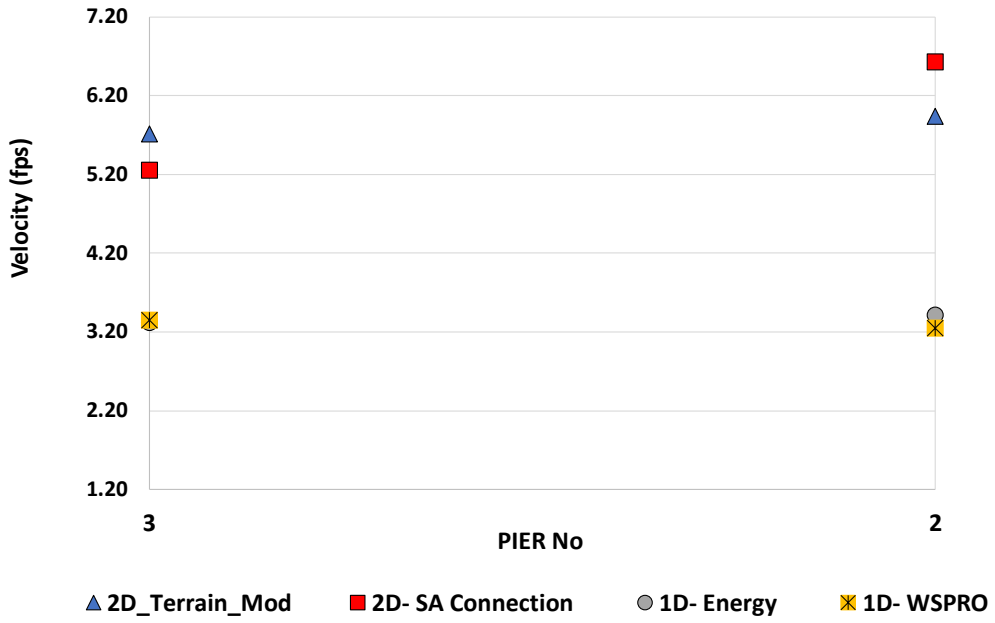

Figure 52.Velocities for the different bridge modeling approach. Bridge BrM010738

Table 11. Velocity comparison between the benchmark model and other approaches for different alternatives to calculate peak flow. BrM 010738

Method	RRE	CN_{II}	CN_{III}
1D WSPRO	50%	43.3%	47%
1D Energy	50%	42.2%	47%
2D Connection	14.9%	-1.8%	6.7%

Also, Figure 53 shows that the water depth in the 1D models, WSPRO (a) and Energy (b), appears notably alike. When contrasting these 1D models (a) and (b) with the 2D/SA

connection (c) model, the floodplain exhibits similarity upstream of the bridge but reveals variations downstream, which are more extensive in the 1D models. Two-dimensional models were compared, and it was found that the 2D/SA connection (c) has a wider floodplain upstream of the bridge (with a yellower tone) than the 2D terrain modification with raised piers model (d), which has a greener tone. This model presents similar behavior to the previous model (Bridge BrM No 015002), when the benchmark illustrates shallow water depths and higher velocity approaches.

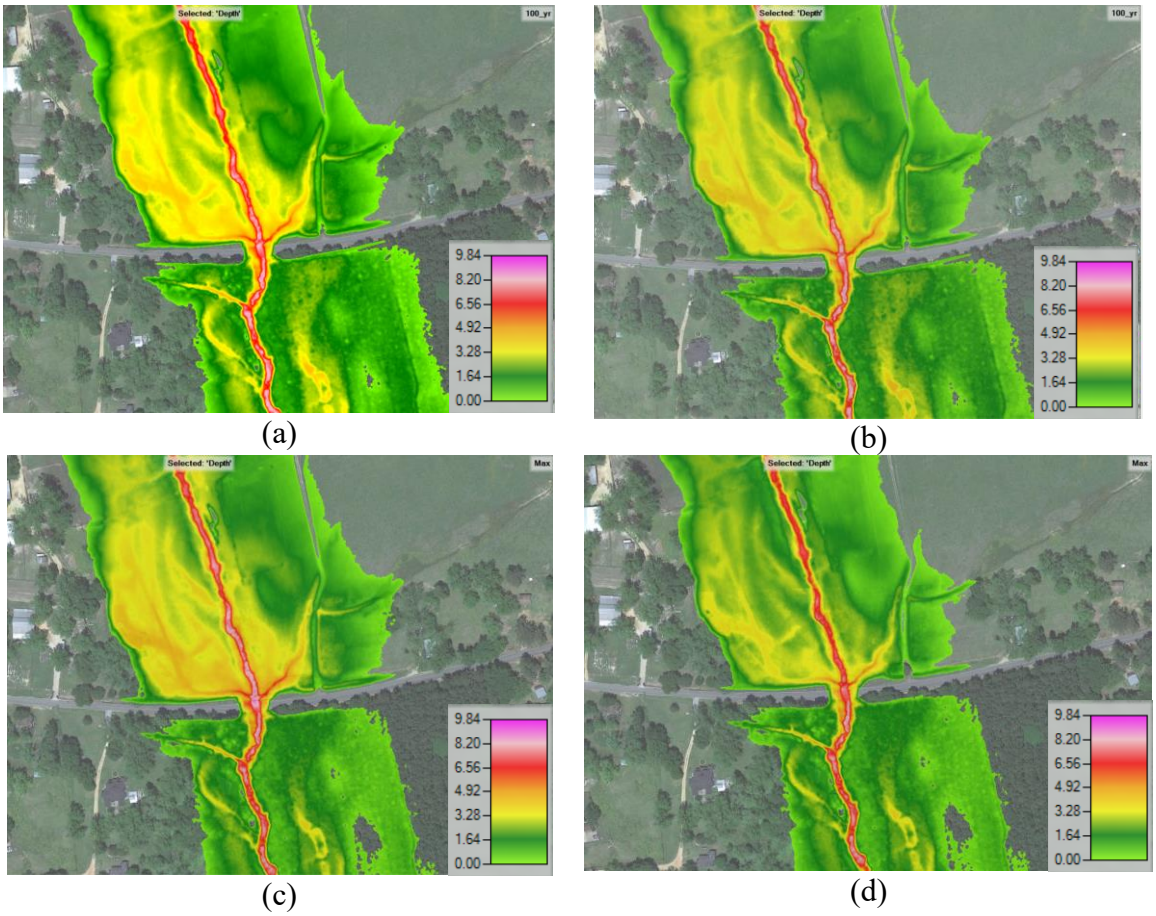

Figure 53. Water depth for different bridge modeling approaches, Bridge BrM No 010738. (a) WSPRO (b) Energy (c) 2D/SA connection (d) 2D terrain modification with raised piers

Furthermore, Figure 54 displays the results for water depths, revealing variations in maximum values in water depth for the 2D-SA connection and minimum values for the

benchmark. Once again, the values of the one-dimensional models behave very similarly, with water depths almost identical. Table 12 presents a comparison of water depths among different modeling approaches, indicating average differences in water depth percentages relative above to the benchmark, which ranged from 9.6% to 33.8% depending on the specific method.

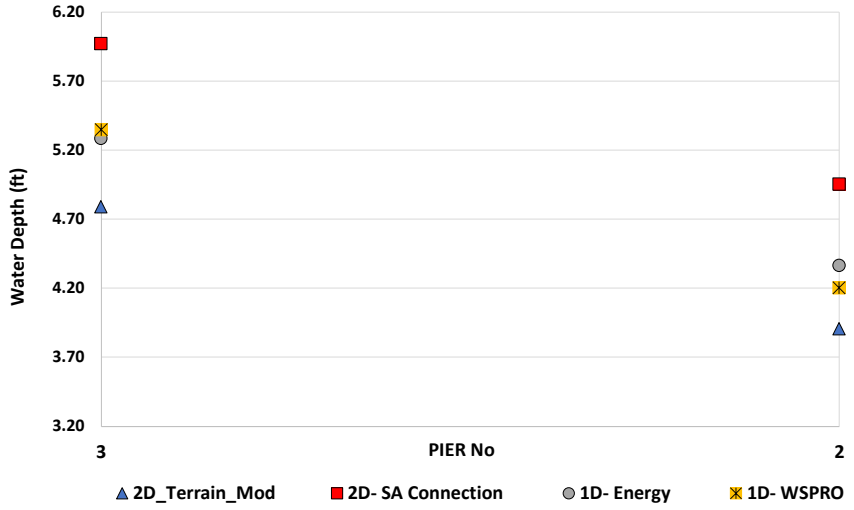

Figure 54.Water depth for the different bridge modeling approach. Bridge BrM010738

Table 12. Water depth comparison between the benchmark model and other bridge modeling approaches for different alternatives to calculate peak flow. BrM 015002

Method	RRE	CN_{II}	CN_{III}
1D WSPRO	14.9%	9.6%	11.9%
1D Energy	15.9%	11%	13.7%
2D Connection	33.8%	25.8%	32.7%

4.2.3 BrM No 013310. Conecuh River and County Road 2243

Similar analyses were conducted for Bridge BrM No. 013310 over the Conecuh River. This river is unique with complex hydraulics, multiple openings and channels and a wider floodplain. Figure 55 shows the results and differences between the 1D models,

WSPRO (a), has lower velocity values at the bridge entrance (more yellow) than energy (b) approach (redder), being the highest velocities among the four models. Comparing the 2D models, it can be observed that the 2D-SA connection (c) (greener), has higher velocities than the 2D terrain modification with raised piers (d) (green, yellow). Looking at the graphs of the 1D models in comparison to the 2D models, the latter display more realistic flow line characteristics.

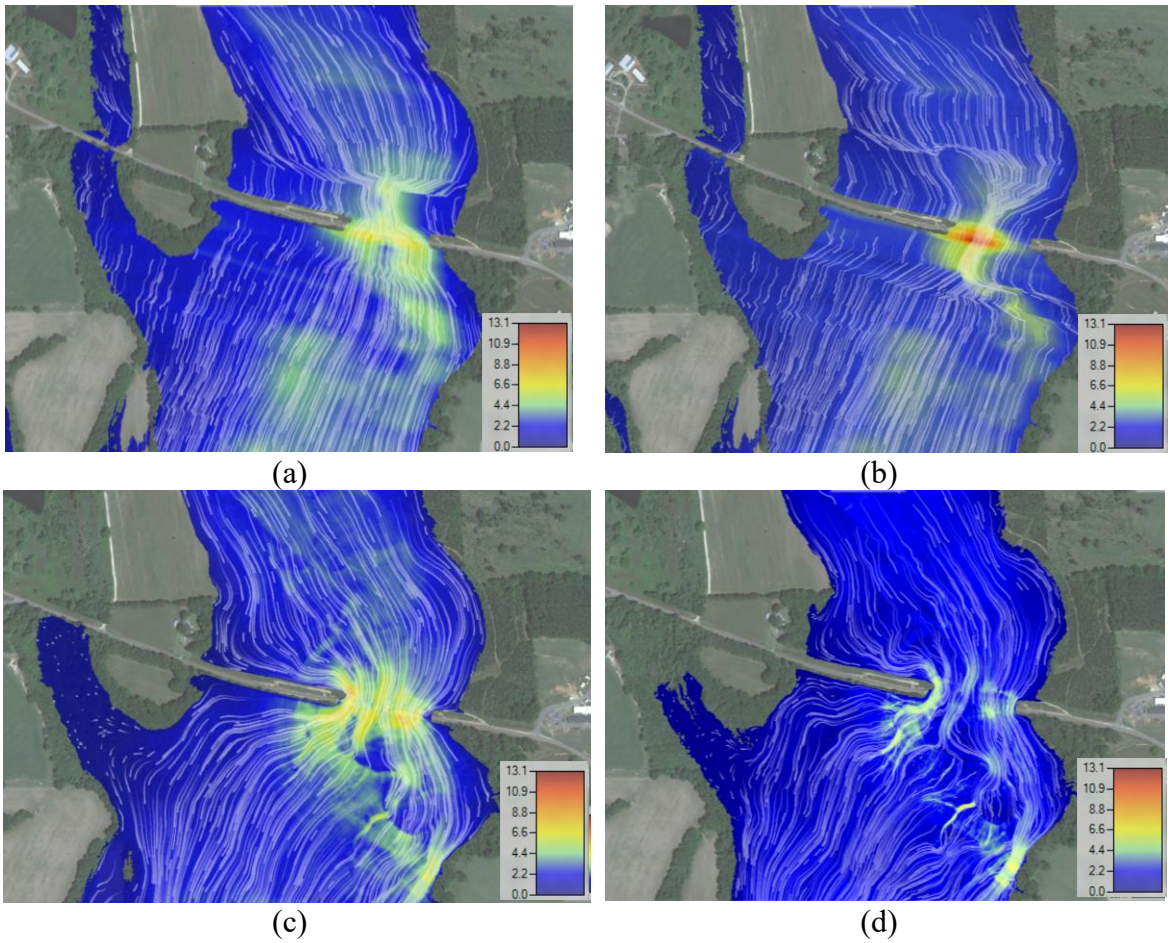

Figure 55. Velocities for different bridge modeling approaches, Bridge BrM No 013310. (a) WSPRO (b) Energy (c) 2D/SA connection (d) 2D terrain modification with raised piers

Figure 56 shows the velocity differences in each pier according to each bridge modeling approach, showing a different behavior compared to the other two analyzed bridges. In this bridge, the 1D energy has a higher velocity compared to the other three

approaches. Nevertheless, the results of this method are concentrated in the main channel, creating high velocities in this part of the cross section, a condition that is considered unrealistic taking into account the assumptions that the 1D models have and observing the results of the benchmark approach. Moreover, Table 13 presents a comparison of velocities between the benchmark and alternative approaches, revealing that the percentage differences in average velocity, vary between 1.6% and 119.6% above depending on the specific method employed. The negative sign indicates that the average water depth percentage is above the benchmark.

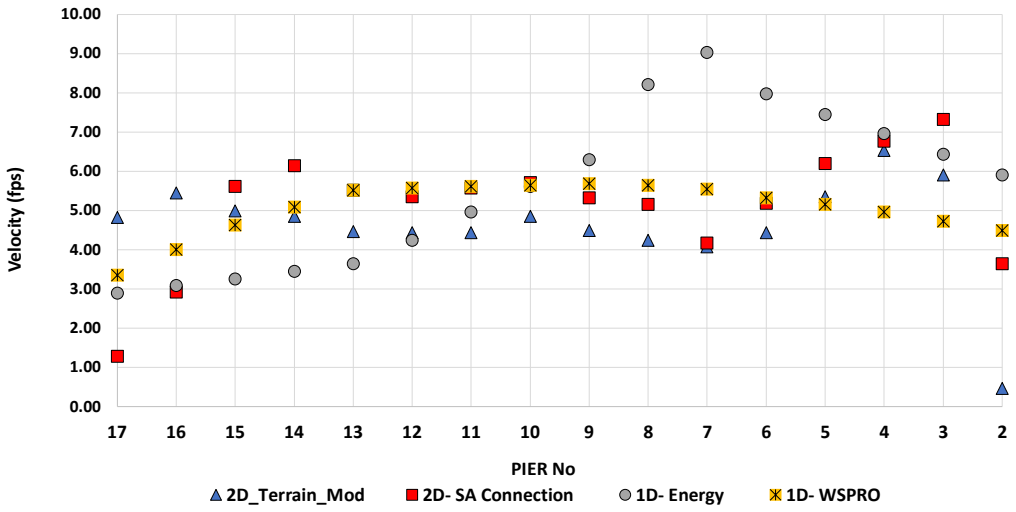

Figure 56.Velocities for the different bridge modeling approach. Bridge BrM013310

Table 13. Velocity comparison between the benchmark model and other approaches for different alternatives to calculate peak flow. BrM No 013310

Method	RRE	CN_{II}	CN_{III}
1D WSPRO	-119.6%	-6.3%	-38.4%
1D Energy	-140.2%	-15.5%	-52.3%
2D Connection	-35.3%	-6.8%	-1.6%

Analogously, Figure 57 presents water depth values for the different bridge modeling approaches concerning Bridge BrM No 013310. The energy model (b) exhibits deeper water depths than the WSPRO model (a). Additionally, it can be observed that the 2D-SA connection model (c) displays a possible pooling effect upstream the bridge section, acting as a flow control (red-magenta tones) due to the contraction. When this model is compared with the benchmark (d), both show significant differences presenting the latter a smooth transition at the bridge entrance. Compared with the other two bridges analyzed before, this bridge behaves differently with the maximum velocities registered for the 1D models and minimum velocity approach for the 2D models at the bridge entrance.

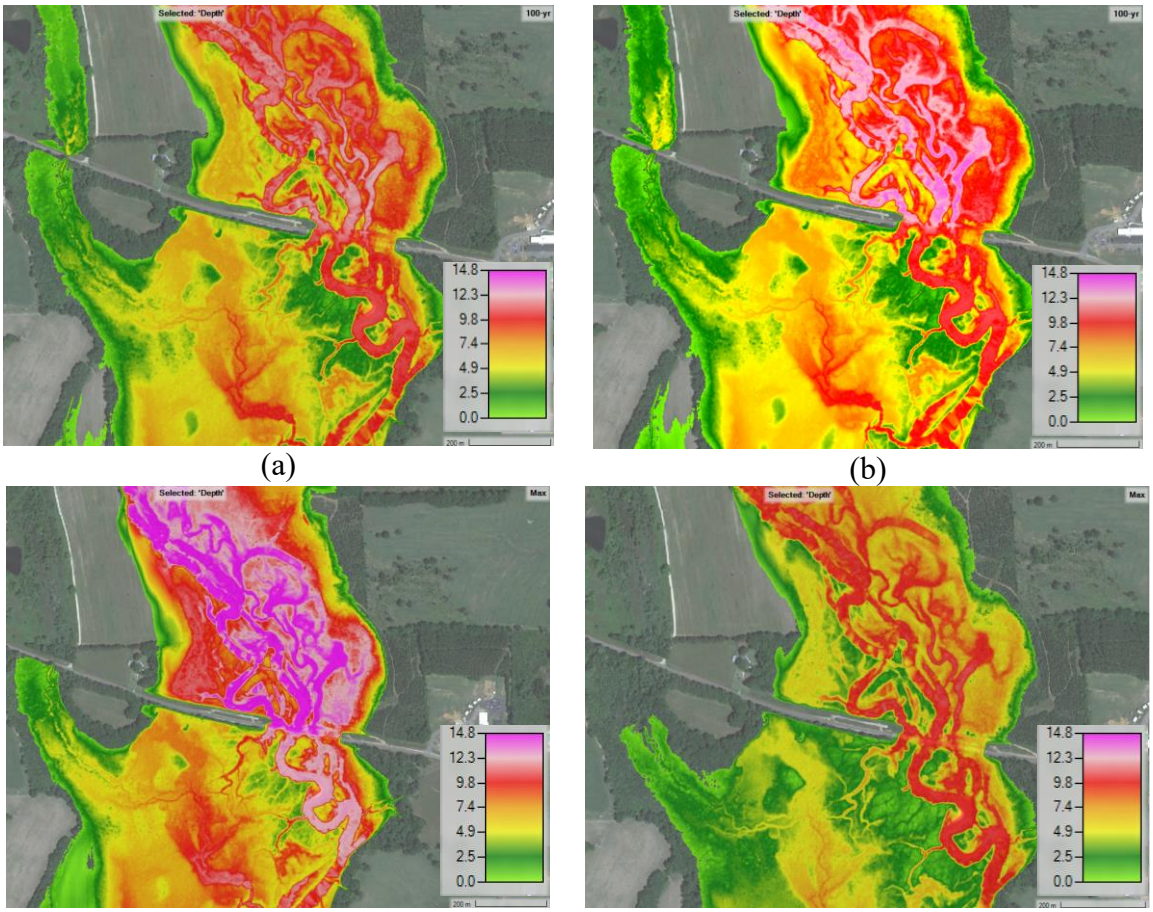

Figure 57. Water depth for different bridge modeling approaches, Bridge BrM No 013310. (a) WSPRO (b) Energy (c) 2D/SA connection (d) 2D terrain modification with raised piers

Besides, Figure 58 shows the results for water depths illustrating maximum values in water depth for the 2D-SA connection and minimum values for the WSPRO. Table 14 presents a comparison of water depth among different modeling approaches, indicating average differences in water depth percentages relative to the benchmark approach, which ranged from -31.4% to 10.6% depending on each specific method. The negative sign indicates that the average water depth percentage is above the benchmark.

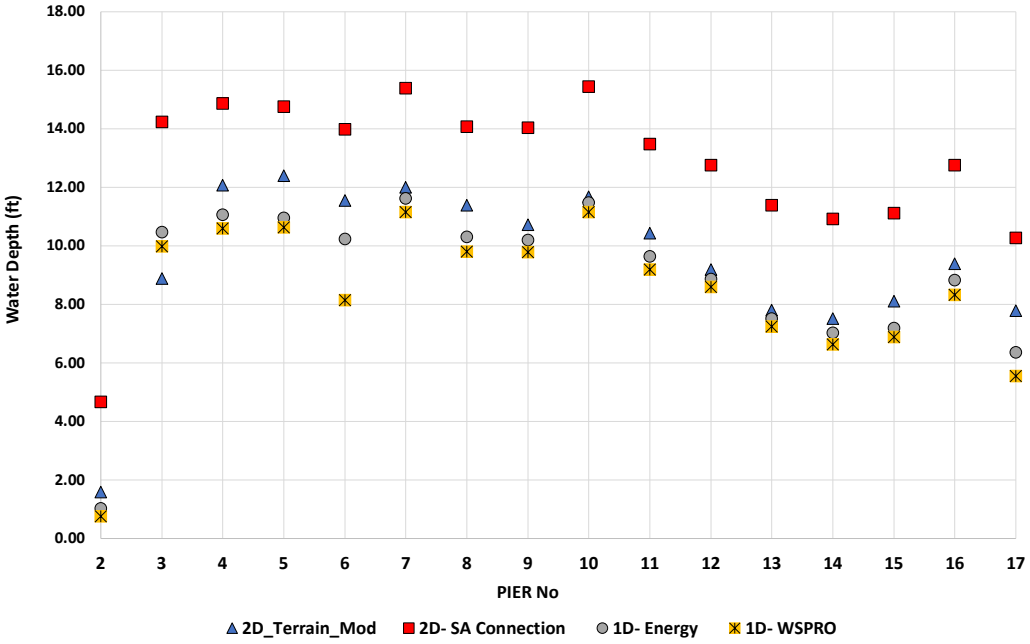

Figure 58.Water depth for the different bridge modeling approach. BrM No 013310

Table 14. Water depth comparison between the benchmark model and other approaches for different alternatives to calculate peak flow. Bridge BrM No 013310

Method	RRE	CN_{II}	CN_{III}
1D WSPRO	-15.8 %	10.6 %	3.4 %
1D Energy	-22.1 %	5.6 %	0.8 %
2D Connection	-3.1 %	-31.4 %	24.3 %

4.2.4 BrM No 007070. French Creek and CO RT No 62

Lastly, comparable results for the velocities for French Creek Bridge BrM No. 07070 are shown in Figure 59. Again, the velocity findings obtained using the 1D energy (b) and 1D WSPRO (a) are almost identical. The two-dimensional models, on the other hand, depict significant variations in velocity near the bridge opening. When comparing the 2D models, the benchmark (d) showed higher upstream velocities (yellow, red) than the 2D-SA connection model (c) (more yellow).

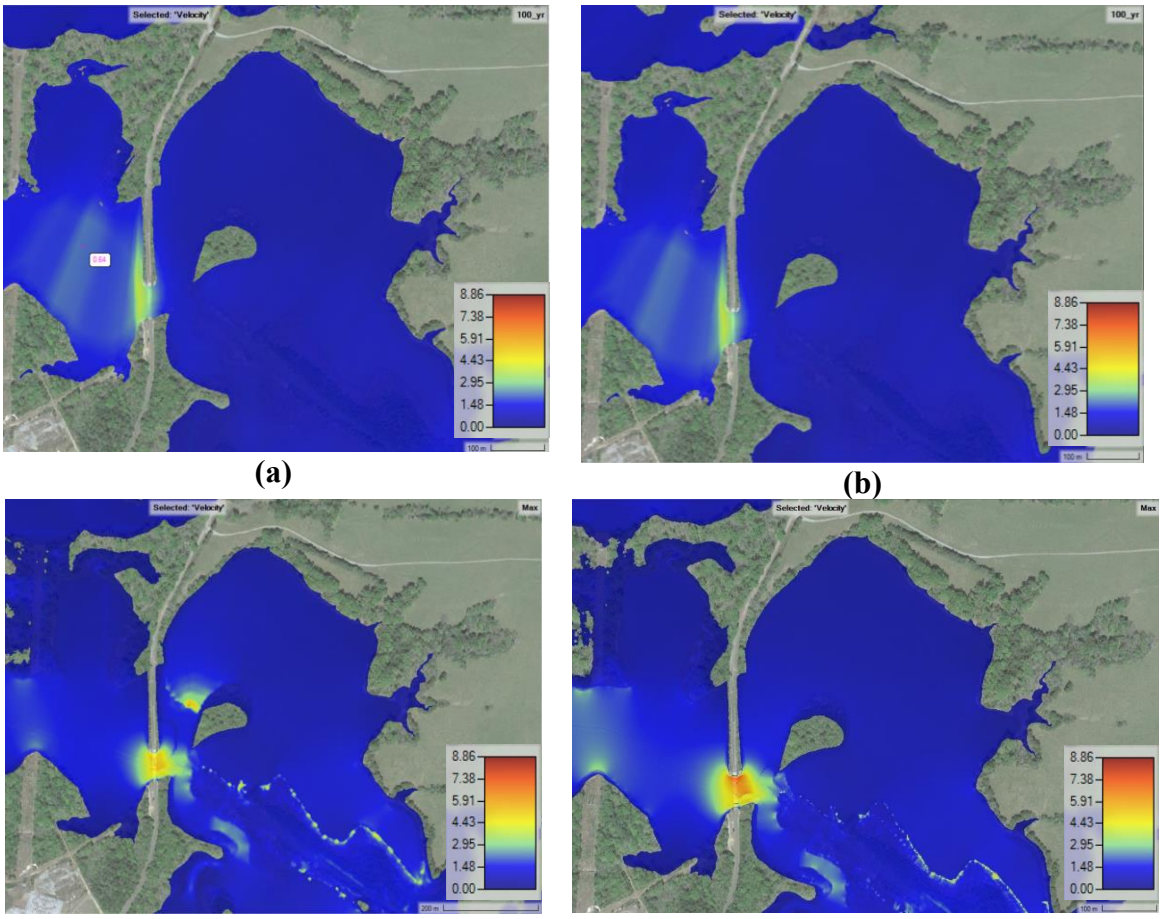

Figure 59. Velocities results for different bridge modeling approaches, Bridge BrM No 007070. (a) WSPRO (b) Energy (c) 2D/SA connection (d) 2D terrain modification with raised piers

Figure 60 shows the velocity differences in each pier according to each bridge modeling approaches, showing the higher velocity in the benchmark model (2D terrain modification with raised piers) followed 2D-SA connection, WSPRO and energy, respectively. The percentage velocity differences between the benchmark and the other approaches vary depending on each approach and the method to calculate the peak flow. Table 15 shows the velocity comparison between the benchmark and the other methods, finding percentage velocity average differences below the benchmark that raging in 16.9% above and 50.1% below the benchmark according to each method. In this specific case, the negative sign indicates that in some cases the average velocity is above the benchmark.

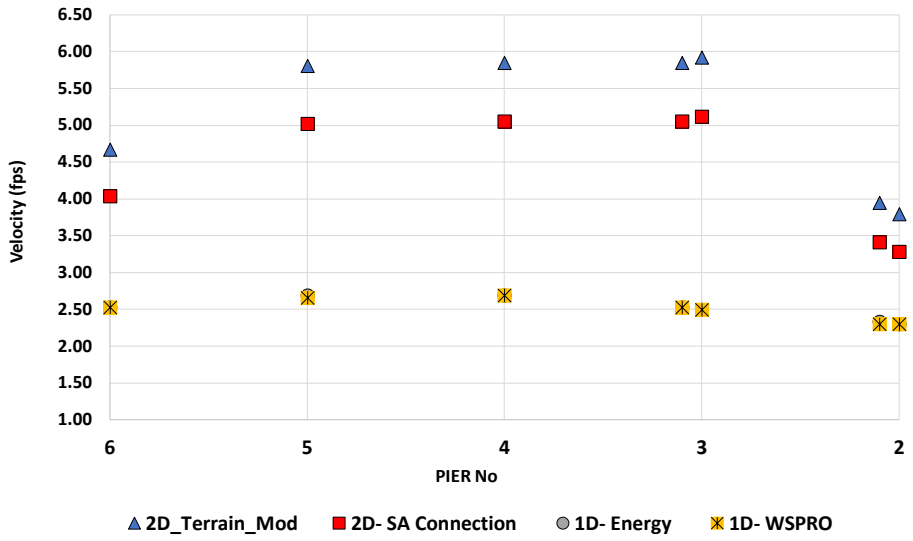

Figure 60. Velocity for the different bridge modeling approach. Bridge BrM No 007070

Table 15. Velocity comparison between the benchmark model and other approaches for different alternatives to calculate peak flow. BrM No 007070

Method	RRE	CN_{II}	CN_{III}
1D WSPRO	35 %	50.1 %	46.4 %
1D Energy	35.2 %	49.9 %	46.4 %
2D Connection	-7.8 %	13.6 %	-16.9 %

Figure 61 the water depth in the 1D models, WSPRO (a) and Energy (b), appears notably alike (same colors). When contrasting these 1D approaches (a) and (b) with the 2D approaches (c) (d), there are notable differences downstream the bridge where the 2D approaches presents deep water depths and broader floodplains. Comparing the 2D models, it was found that the 2D/SA connection (c) has a wider floodplain upstream and downstream than the 2D terrain modification with raised piers model (d).

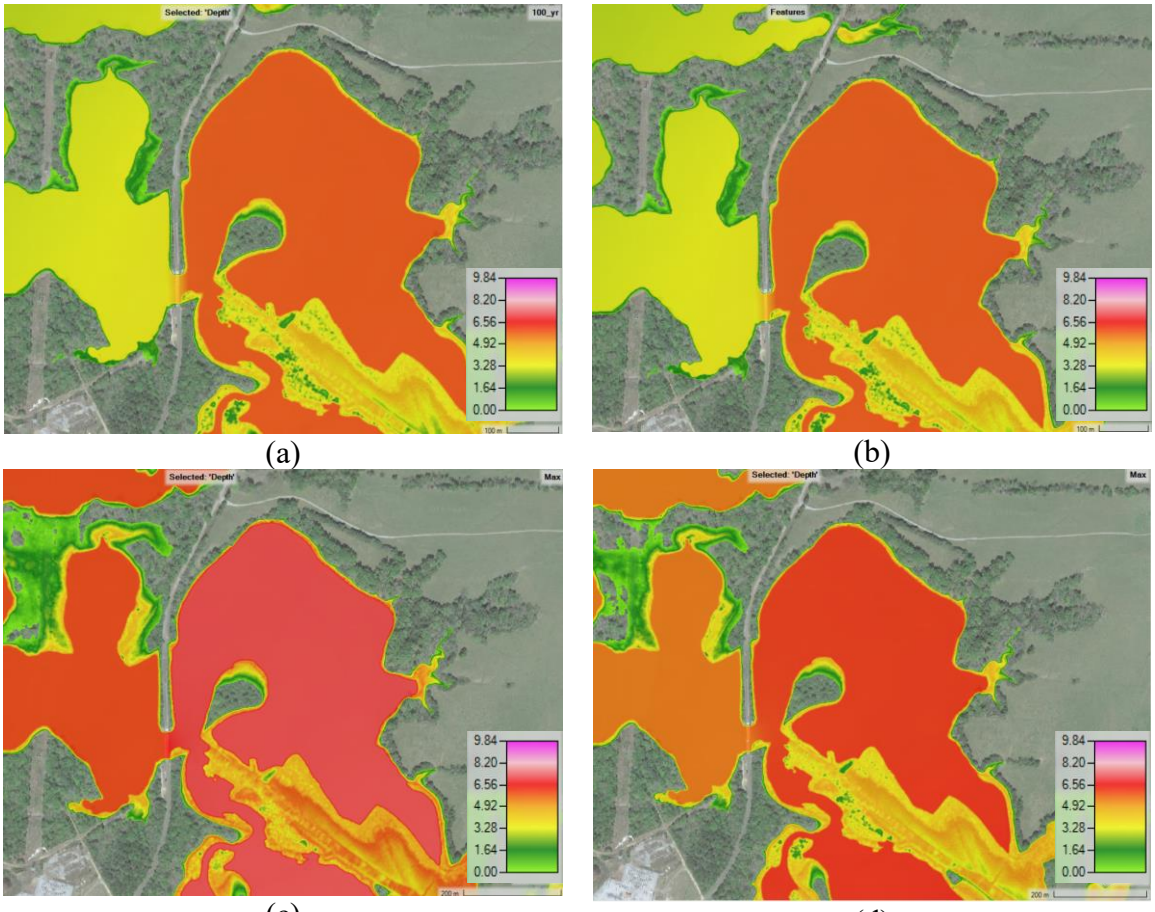

Figure 61. Water depth for different bridge modeling approaches, Bridge BrM No 007070. (a) WSPRO (b) Energy (c) 2D/SA connection (d) 2D terrain modification with raised piers

Moreover, Figure 55 displays the results for water depths, where the benchmark presents the maximum water depths and WSPRO and Energy the minimum values.

One more time, the values of the 1D approaches behave very similarly, with water depths almost identical. Table 16 presents a comparison of water depths among different modeling approaches, indicating average differences in water depth percentages relative above to the benchmark, which ranged from 9.2% to 32.1% depending on the specific method. In this case, the negative value indicates that the average water depth percentage is above the benchmark.

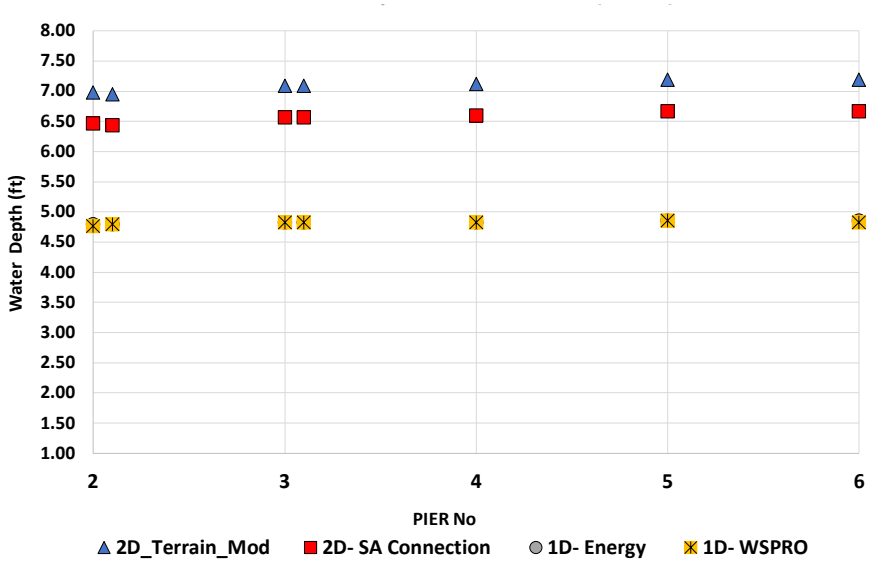

Figure 62.Water depth for the different bridge modeling approach. Bridge BrM007070

Table 16. Water depth comparison between the benchmark model and other approaches for different alternatives to calculate peak flow. BrM No 007070

Method	RRE	CN_{II}	CN_{III}
1D WSPRO	-1.1 %	32.1 %	22.6 %
1D Energy	-1.3 %	31.9 %	22.7 %
2D Connection	-9.2 %	7.4 %	-1.8 %

A peak-to-average analysis was done for velocity, in addition to visual analyses and comparisons between average values for velocities and water depth. This method involves dividing the maximum calculated velocity by the average velocity for each bridge modeling approach. This process helps standardize the values across methods, enabling the determination of which methods exhibit higher velocity that could be related with more potential of scour. The results of this analysis for the four bridges are presented in Figure 63.

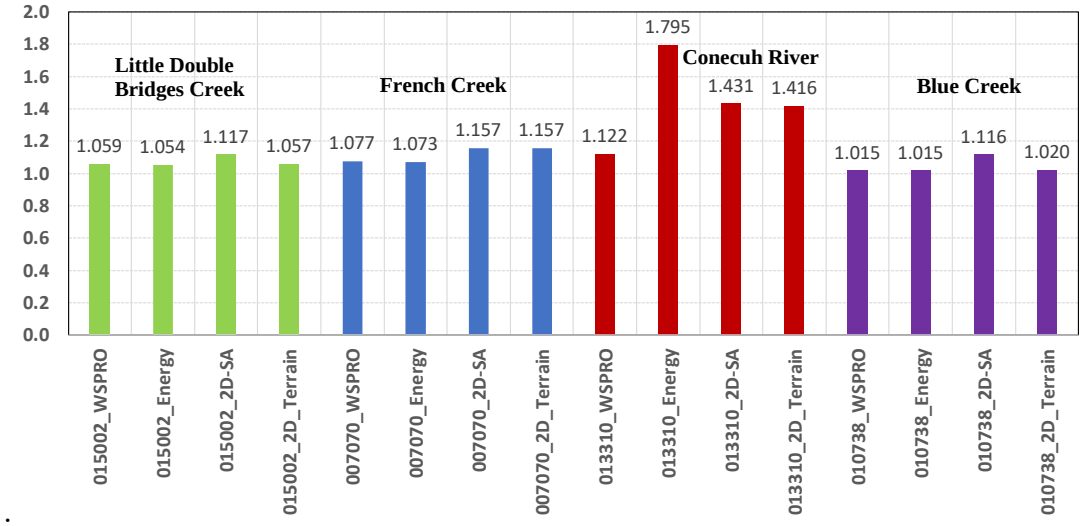

Figure 63.Peak to average velocities by bridge for the different bridge modeling approaches

Figure 63 shows that for Bridge BrM No 015002 (in green), the bridge modeling approach with the highest peak to average value corresponds to 2D SA connection with 1.117, and the lowest value is for 1D energy. Similarly, for Bridge BrM No 010738, the behavior is very similar to Bridge BrM No 015002, with a maximum value of 1.116 for 2D SA connection and a minimum value for energy of 1.015. These two bridges have relatively uniform peak-to-average values with little difference between the bridge modeling approaches. In these bridges, where the sections are well-defined and there are no extensive floodplains, all models generally behave quite similarly, whether in 1D or 2D.

Similarly, Bridge 007070 exhibited a maximum peak-to-average value for the benchmark, but with an almost identical value for 2D-SA connection at 1.157 and a minimum value for energy at 1.073. This also indicates considerable uniformity in water depths upstream of the bridge for those models.

Finally, the same analysis was performed for Bridge BrM No 013310, where there was considerable disparity in the peak to average values. The maximum peak to average value was recorded for the 1D energy approach with a value of 1.795, and the minimum for 1D WSPRO with a value of 1.122. This reflects the lack of uniformity in one-dimensional models when are used in complex geometries and multiple openings and channels. In this bridge, it was found that the peak to average values for the two-dimensional models are quite similar, with 1.413 for 2D SA connection and 1.416 for the benchmark, indicating better hydraulic performance in the vicinity of the bridge.

4.3. Scour calculations

This section presents the scour results for the evaluated methodologies HEC-18 and OMS. The values corresponding to HEC-18 calculations are depicted in graphs that compare the calculated values for each bridge modeling approach to identify how the scour depth calculations behave throughout the different alternatives to calculate the peak flow.

A summary of the ranges for each bridge modeling approach and the analyzed alternatives for peak flow calculation corresponding to RRE, CN_{II}, and CN_{III} is provided, followed for the analysis the peak to average for scour depth when is possible recognize which method produce more peak to scour depth that indirectly relate the modeling approach with the scour depth production. Finally for HEC-18 calculations, the scour values for each

bridge modeling approach are compared against the benchmark, showing the percentage difference between each approach for each of the analyzed bridges.

A summary of the ranges for each bridge modeling approach and the analyzed alternatives for peak flow calculations corresponding to RRE, CN_{II}, and CN_{III} is provided, followed by the analysis by peak to average for scour depth. The latter analysis allows to recognize indirectly which modeling approach is related to more scour depth.

Finally, for HEC-18 calculations, the scour values for each bridge modeling approach are compared against the benchmark, showing the percentage difference between each approach for each of the analyzed bridges sites. Following the HEC 18 calculations, the OMS results for the four studied bridges, using as a maximum observed scour the values consigned in BrM.

4.3.1 HEC-18 Calculations

For the scour analysis using HEC-18, it was used the methodology presented in subsection 3.4.1 of the present document. To develop the methodology, one of the necessary activities was the determination of the D_{50} of riverbed samples, as the methodologies require soil characterization or particle size distribution to assess critical velocity and scour depth. The size particles size per bridge is presented in Figure A1 of the Appendix and the D_{50} results are summarize in Table 17.

Table 17. D_{50} results for the analyzed bridges.

BrM No	River name	D_{50} (mm)
015002	Little Double Bridges Creek	0.2
010738	Blue Creek	0.2
013310	Conecuh river	0.35
007070	French Creek	0.7

Using D_{50} information, Equation 14 and the considerations outlined in section 2.3.4 of this document, pier scour calculations were performed using HEC-18 for the bridge analyzed. These calculations were conducted using various bridge modeling approaches (1D WSPRO, 1D energy, 2D SA-connection, and the benchmark 2D terrain modification with raised piers) for different alternatives to calculate the peak flow (RRE, CN_{II}, and CN_{III}).

The information below presents the results for each of the bridges and the conditions described above. Table 18 shows the ranges for HEC-18 pier scour results for different analyzed methods in Bridge BrM No 015002. This table shows minimum scour values for 1D WSPRO and 1D energy, which behave almost identical with values of 6.9 –7.3 ft, 6.7 – 7.1 ft, 7.5-7.8 ft for RRE, CN_{II} and CN_{III}, respectively. The maximum scour values recorded corresponded to 2D Terrain modification with raised piers (benchmark) with values of 7.6-8.0 feet for the RRE, 7.1 -7.5 feet for CN_{II} and 8.1 – 8.5 feet for CN_{III}. The detailed information of those calculations is presented from Figure A2 to Figure A4 and Table A1 to Table A3 of the Appendix.

Table 18. HEC-18 pier scour results for different alternatives to calculate the peak flow and bridge modeling approach. Bridge BrM No 015002

METHOD	RRE	CN_{II}	CN_{III}
1D WSPRO	6.9 - 7.3 ft	6.7 - 7.1 ft	7.5 - 7.8 ft
1D Energy	6.9 - 7.3 ft	6.5 - 7.0 ft	7.5 - 7.8 ft
2D SA connection	6.9 -7.9 ft	6.3 - 7.3 ft	7.2 - 8.2 ft
2D Terrain_mod	7.6 - 8.0 ft	7.1 - 7.5 ft	8.1 - 8.5 ft

Likewise, Table 19 displays the ranges of HEC-18 pier scour findings for different methods of analysis for Bridge BrM No 010738. The minimum scour values were registered for 1D energy, and they range from 4.4 - 4.5 feet for RRE, 4.2 feet for CN_{II}, and 4.3 feet for

CN_{III}. The maximum scour values estimated corresponded to 2D Terrain modification with raised piers (benchmark) with values of 5.8 feet for the RRE, 5.2 - 5.3 feet for CN_{II} and 5.6 feet for CN_{III}. Nevertheless, some high values are registered for 2D-SA connection using CN_{III} corresponding to values ranging from 5.4 - 5.9 feet. The complete information of those calculations is presented from Figure A5 to Figure A7 and Table A4 to Table A6 of the Appendix. This bridge, in a similar way that the previous one, showed that the maximum scour depths were related to the 2D Terrain modification with raised piers. In this case, the maximum scour did not correspond to the HEC-HMS CN_{III} peak flow, because the RRE peak flow was a little bit above the HEC-HMS CN_{III} peak flow.

Table 19. HEC-18 pier scour results for different alternatives to calculate the peak flow and bridge modeling approach. Bridge BrM No 010738

METHOD	RRE	CN_{II}	CN_{III}
1D WSPRO	4.4 – 4.5 ft	4.1 – 4.3 ft	4.3 ft
1D Energy	4.4- 4.5 ft	4.2 ft	4.3 ft
2D SA connection	5.5 ft	5.2 ft	5.4 – 5.9 ft
2D Terrain_mod	5.8 ft	5.2 – 5.3 ft	5.6 ft

In a similar way, Table 20 presents the HEC-18 pier scour calculations results for all tested methods evaluated for Bridge BrM No 013310. The minimum obtained values for scour calculations were for 2D terrain modification with raised piers (benchmark) with values of 0 - 4.5 feet for the RRE, 1.3 - 6.4 feet for CN_{II} and 1.1 - 6.1 feet for CN_{III}. The maximum obtained values for scour calculations were found for 1D energy with values of 3.4 - 8.7 feet, 3.5 - 8.7 feet and 4.0 - 9.2 feet. This model contrasted to the two previous ones, showing more scour depth for the 1D models than the D models. In this specific case, as was told before in the hydraulic results the hydraulic complexity, the multiple openings and channels

presume the 1D models do not represent appropriately the channel of approach. The complete information of those calculations is presented from Figure A8 to Figure A10 and Table A7 to Table A9 of the Appendix.

Table 20. HEC-18 pier scour results for different alternatives to calculate the peak flow and bridge modeling approach. Bridge BrM No 013310

METHOD	RRE	CN_{II}	CN_{III}
1D WSPRO	2.9 – 7.0 ft	3.2 – 7.0 ft	4.1 – 7.5 ft
1D Energy	3.4 -8.7 ft	3.5 – 8.7 ft	4.0 – 9.2 ft
2D SA connection	0 – 5.2 ft	2.6 – 7.1 ft	2.0 -6.1 ft
2D Terrain_mod	0 - 4.5 ft	1.3 – 6.4 ft	1.1 – 6.1 ft

Finally, Table 21 depicts HEC-18 pier scour calculations results for the various methods assessed for Bridge BrM No 007070. This table shows minimum scour values for 1D energy, of 3.9 - 4.2 ft, 3.4 - 3.9 ft, 3.9 - 4.2 ft for RRE, CN_{II} and CN_{III}, respectively. The maximum scour values recorded corresponded to 2D Terrain modification with raised piers (benchmark) with values of 4.2 - 5.8 feet for the RRE, 4.8 - 5.8 feet for CN_{II} and 4.8 - 6.1 feet for CN_{III}. Nonetheless, certain high values are registered for 2D-SA connection utilizing CN_{III}, corresponding to values ranging from 5.4 to 6.1 feet. The complete information of those calculations is presented from Figure A11 to Figure A13 and Table A10 to Table A12 of the Appendix.

Table 21. HEC-18 pier scour results for different alternatives to calculate the peak flow and bridge modeling approach. Bridge BrM No 007070

METHOD	RRE	CN_{II}	CN_{III}
1D WSPRO	3.6 – 3.9 ft	3.7 – 3.9 ft	4.0 – 4.2 ft
1D Energy	3.9 – 4.2 ft	3.4 – 3.9 ft	3.9 – 4.2 ft
2D SA connection	4.4 – 5.5 ft	4.5 – 5.4 ft	5.4 – 6.1 ft
2D Terrain_mod	4.2 – 5.8 ft	4.8 – 5.8 ft	4.8 - 6.1 ft

The results show a trend where the maximum scour calculations corresponded to the 2D Terrain modification with raised piers (benchmark) and the minimum values corresponded to 1D WSPRO. In some cases, as in Bridge BrM No 013310 the maximum scour calculations correspond to 1D energy but as it was said before due to the complex hydraulics of that river the 1D models do not represent the channel approach.

Another type of analysis conducted was to determine the peak to average scour for the different alternatives to calculate the peak flow and for the analyzed bridge modeling approaches. Figure 64 to Figure 66 show the peak to average for scour for the different bridge modeling approaches when the alternative for calculating the peak flow is RRE, CN_{II}, and CN_{III}, respectively.

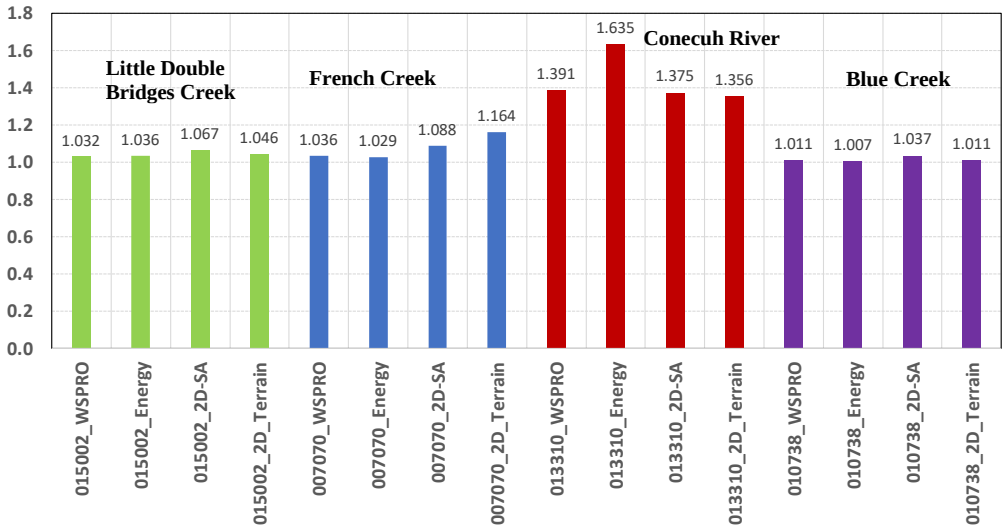

Figure 64.Peak to average for scour depth using RRE

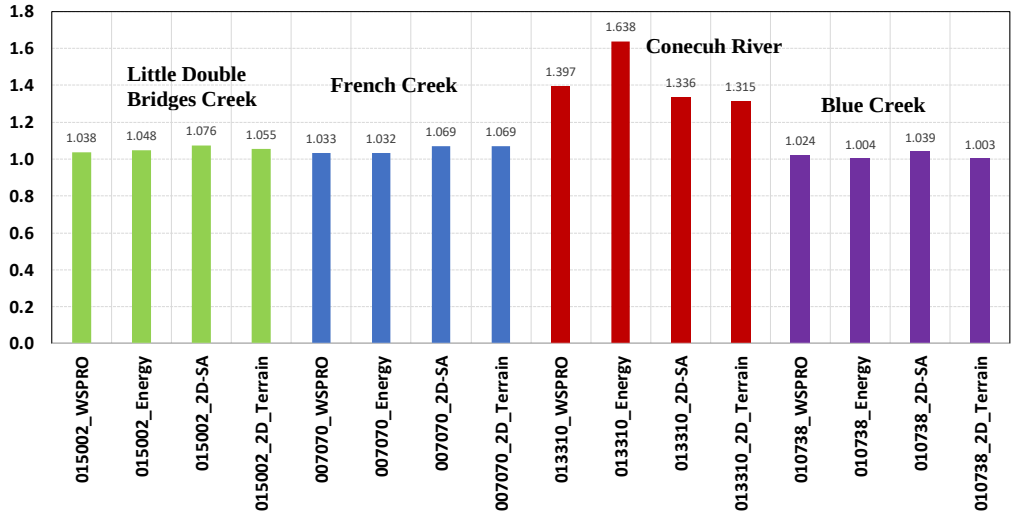

Figure 65. Peak to average for scour depth using CN_{II}

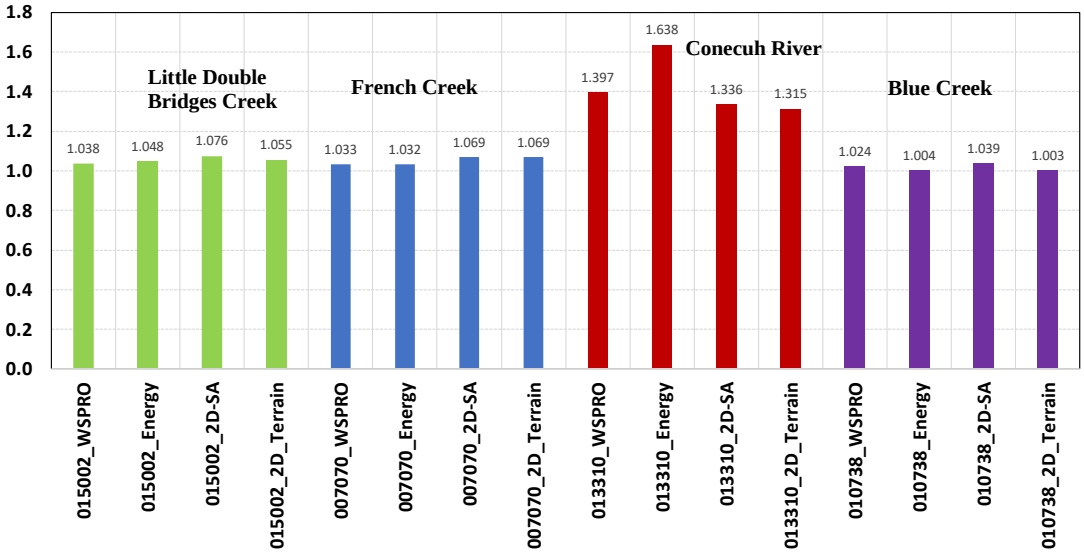

Figure 66. Peak to average for scour depth using CN_{III}

In this graph, it can be observed that, for almost all cases, the 2D-dimensional models exhibit a higher peak to average for scour, which is associated with large velocities (Figure 63) and deeper scour depth. In the same scenarios, the models with a lower peak to average for scour correspond to 1D models, which are related to low velocities and scour depth. The exception to the results mentioned before corresponds to Bridge BrM 013310, whose maximum scour values correspond to the 1D energy and have the maximum peak to average

for scour. Nevertheless, the obtained results were not considered appropriate because those types of models do not appropriately describe the complex hydraulics of the mentioned bridge.

Additionally, in the analyses conducted earlier, a comparison was performed using the 2D terrain modification with raised piers as the bridge modeling approach but varying the alternative for calculating the peak flow. The pier scour values for each of the bridges were averaged to determine which peak flow alternative exhibited the highest average scour. Figure 67 and Table 22 present the results of this procedure for the bridge BrM 015002, showing that the worst-case scenario is represented by the alternative corresponding to CN_{III} with 8.28 ft, followed by RRE with 7.8 ft, and CN_{II} with 7.23 ft. The percentage variation between RRE, CN_{II}, and CN_{III} corresponded to -7.3% and 6.15%, respectively. The negative value indicates that the scour depth is below the corresponding one using the RRE.

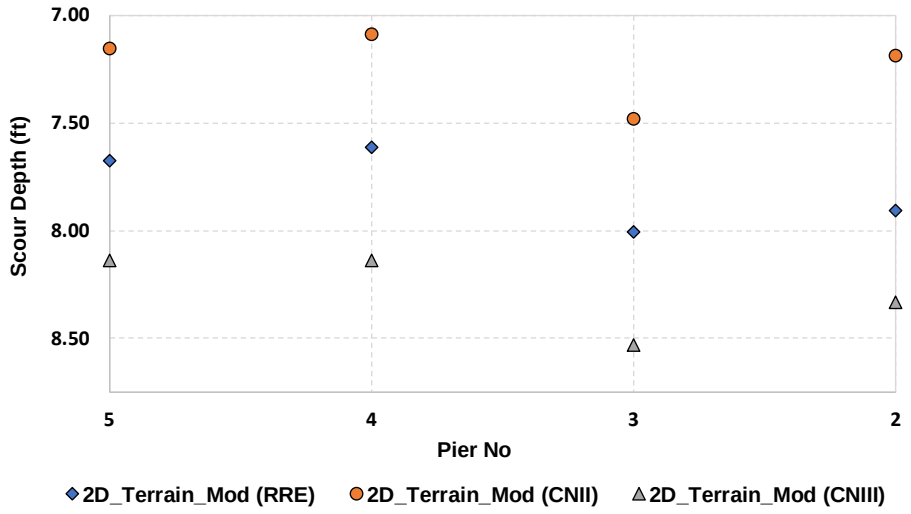

Figure 67. HEC-18 scour comparison values of the different alternatives to calculate the flow using the Bridge modeling approach (benchmark). Bridge BrM No 015002

Table 22. HEC-18 scour comparison values of the different alternatives to calculate the flow using the Bridge modeling approach (benchmark). Bridge BrM No 015002

PIER BrM	2D_Terrain_Mod (RRE)	2D_Terrain_Mod (CN_{II})	2D_Terrain_Mod (CN_{III})
2	7.91	7.19	8.33
3	8.01	7.48	8.53
4	7.61	7.09	8.14
5	7.68	7.15	8.14
Average	**7.80**	**7.23**	**8.28**

Figure 68 and Table 23 present the results of this process for the bridge BrM 010738, indicating that the alternative corresponding to RRE with 5.87 feet is the worst-case scenario for scour, followed by CN_{III} with 5.61 ft and CN_{II} with 5.27 ft. The percentage variation between RRE, CN_{II}, and CN_{III} corresponded to -10.22% and -4.42%, respectively. The negative value indicates that the scour value depth is below the corresponding one computed RRE.

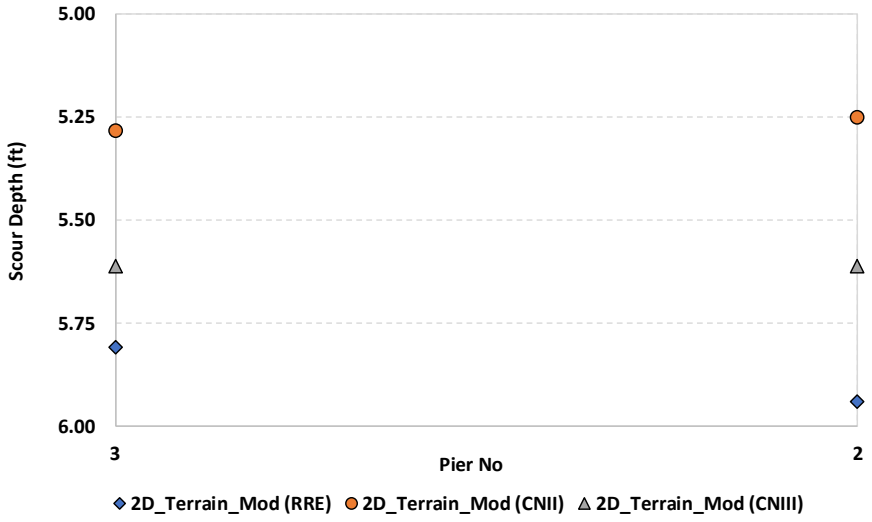

Figure 68. HEC-18 pier scour comparison of the different alternatives to calculate the flow using the Bridge modeling approach (benchmark). Bridge BrM No 010738

Table 23. HEC-18 pier scour comparison values of the different alternatives to calculate the flow using the Bridge modeling approach (benchmark). Bridge BrM No 010738

PIER BrM	2D_Terrain_Mod (RRE)	2D_Terrain_Mod (CN_{II})	2D_Terrain_Mod (CN_{III})
2	5.94	5.25	5.61
3	5.81	5.28	5.61
Average	**5.87**	**5.27**	**5.61**

Analogously, Figure 69 and

Table **24** Table 24 present the results of this procedure for the bridge BrM 013310, showing that the worst-case scenario is represented by the alternative corresponding to CN_{III} with 4.89 ft, followed by RRE 3.34 ft, and CN_{II} with 4.63 ft. The percentage variation between RRE, CN_{II}, and CN_{III} corresponded to 27.86% and 31.69%, respectively. The positive value indicates that the scour value depth is larger than the corresponding one computed using the RRE.

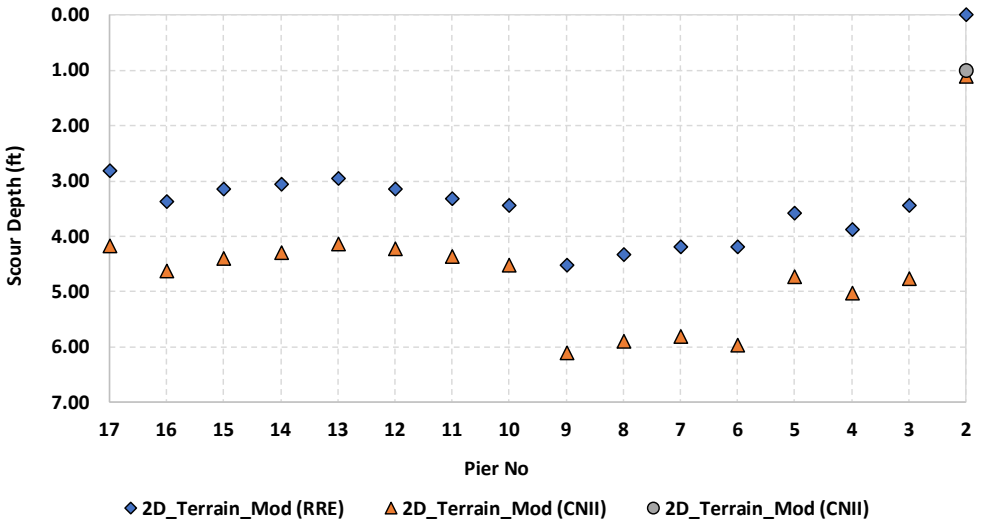

Figure 69. HEC-18 pier scour comparison of the different alternatives to calculate the flow using the Bridge modeling approach (benchmark). Bridge BrM No 013310

Table 24. HEC-18 pier scour comparison values of the different alternatives to calculate the flow using the Bridge modeling approach (benchmark). Bridge BrM No 013310

PIER BrM	2D_Terrain_Mod (RRE)	2D_Terrain_Mod (CN_{II})	2D_Terrain_Mod (CN_{III})
2	0.00	1.12	1.31
3	3.44	4.76	4.95
4	3.87	5.02	5.41
5	3.58	4.72	4.99
6	4.20	5.97	6.43
7	4.20	5.81	6.23
8	4.33	5.91	6.27
9	4.53	6.10	6.40
10	3.44	4.53	4.72
11	3.31	4.36	4.49
12	3.15	4.23	4.40
13	2.95	4.13	4.33
14	3.05	4.30	4.46
15	3.15	4.40	4.56
16	3.38	4.63	4.82
17	2.82	4.17	4.46
Average	**3.34**	**4.63**	**4.89**

Finally, Figure 70 and Table 25 present the results of this procedure for the bridge BrM 07070, depicting that the worst-case scenario is represented by the alternative corresponding to CN_{III} with 7.35 ft, followed by CN_{II} with 7.09 ft and RRE 5.47 ft, The percentage variation between RRE, CN_{II}, and CN_{III} corresponded to 22.85 % and 25.58%, respectively. The positive value indicates that the scour value depth is larger than the corresponding one computed using the RRE.

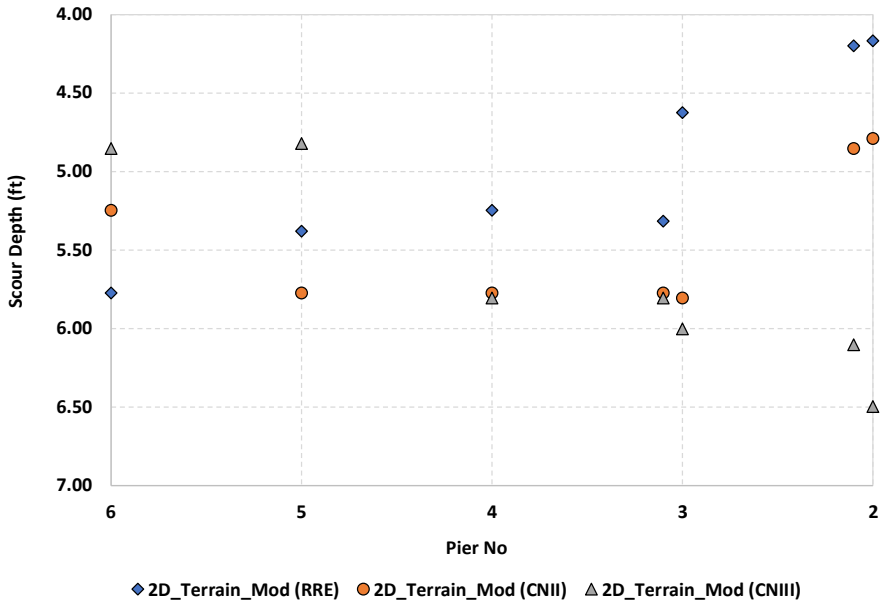

Figure 70. HEC-18 pier scour comparison of the different alternatives to calculate the flow using the Bridge modeling approach (benchmark). Bridge BrM No 007070

Table 25. HEC-18 pier scour comparison values of the different alternatives to calculate the flow using the Bridge modeling approach (benchmark). Bridge BrM No 007070

PIER BrM	2D_Terrain_Mod (RRE)	2D_Terrain_Mod (CN_{II})	2D_Terrain_Mod (CN_{III})
2	5.41	6.98	7.38
2.1	5.41	6.94	7.38
3	5.48	7.09	7.38
3.1	5.48	7.09	7.35
4	5.48	7.12	7.35
5	5.51	7.19	7.32
6	5.54	7.19	7.28
Average	**5.47**	**7.09**	**7.35**

4.3.2 OMS calculations

The following discussion presents the pier scour results using the OMS methodology (Govindasamy et al., 2013). Using TAMU-OMS software (Briaud et. al, 2009), the future scour was calculated for the bridges analyzed. Following the

methodological steps, exposed in section 3.4.2. The first step was to determine the maximum scour depth at the bridge utilizing secondary information based on AASHTOWare Bridge Management BRM for the Bridges. The results of the OMS calculations are presented in Table 26. For Bridge BrM No. 007070, it was not possible to apply the methodology because it was found that since its construction this bridge experienced an aggradation process.

Table 26. OMS pier scour calculations for the analyzed Bridges

BrM ID	Feature Intersected	OMS scour (ft)
015002	Little Double Bridges Creek	5.5 - 5.6
010738	Blue Creek	1.7 - 1.9
007070	French Creek	NA
013310	Conecuh River	5.4 - 5.7

Comparing the outcomes of the HEC-18 and OMS pier scours allowed for comparison. The results show the obtained ranges without taking into account the method used; they only display values within the obtained ranges. For bridge BrM No. 015002, the HEC-18 pier scour depth results showed differences that were 33.7 to 51.7% higher than OMS. For bridge BrM No. 010738, the differences were 164.7 to 210.5% higher than OMS. For bridge BrM No. 013310 and BrM No. 007070, the differences were 20% to 61.4% higher than OMS. It was not possible to evaluate the differences.

4.3.3 Summary of scour results

As a summary of scour the results described above, Table 27 presents the obtained scour depth using HEC-18 calculations for the different hydrological and hydraulic approaches and OMS calculations.

Table 27. Summary of scour results

BRIDGE BrM No	METHOD	RRE	CN_{II}	CN_{III}	OMS
015002	1D WSPRO	6.9 - 7.3 ft	6.7 - 7.1 ft	7.5 - 7.8 ft	5.5-5.6 ft
	1D Energy	6.9 - 7.3 ft	6.5 - 7.0 ft	7.5 - 7.8 ft	
	2D SA connection	6.9 -7.9 ft	6.3 - 7.3 ft	7.2 - 8.2 ft	
	2D Terrain_mod	7.6 - 8.0 ft	7.1 - 7.5 ft	8.1 - 8.5 ft	
010738	1D WSPRO	4.4 – 4.5 ft	4.1 – 4.3 ft	4.3 ft	1.7-1.9 ft
	1D Energy	4.4- 4.5 ft	4.2 ft	4.3 ft	
	2D SA connection	5.5 ft	5.2 ft	5.4 – 5.9 ft	
	2D Terrain_mod	5.8 ft	5.2 – 5.3 ft	5.6 ft	
013310	1D WSPRO	2.9 – 7.0 ft	3.2 – 7.0 ft	4.1 – 7.5 ft	5.4-5.7 ft
	1D Energy	3.4 -8.7 ft	3.5 – 8.7 ft	4.0 – 9.2 ft	
	2D SA connection	0 – 5.2 ft	2.6 – 7.1 ft	2.0 -6.1 ft	
	2D Terrain_mod	0 - 4.5 ft	1.3 – 6.4 ft	1.1 – 6.1 ft	
007070	1D WSPRO	3.6 – 3.9 ft	3.7 – 3.9 ft	4.0 – 4.2 ft	NA
	1D Energy	3.9 – 4.2 ft	3.4 – 3.9 ft	3.9 – 4.2 ft	
	2D SA connection	4.4 – 5.5 ft	4.5 – 5.4 ft	5.4 – 6.1 ft	
	2D Terrain_mod	4.2 – 5.8 ft	4.8 – 5.8 ft	4.8 - 6.1 ft	

5. CONCLUSIONS

This thesis systematically evaluated a number of different ways to compute scour in bridges through the peak flow estimates and hydraulic modeling approaches techniques. The goal is to assess how these different ways can change the results of the pier scour calculations in bridges that use HEC-18 and OMS. These combinations were implemented on four bridges in Alabama, which were identified using the same AASTHOWare BrM identifier and pier nomenclature.

The alternatives evaluated to calculate the peak flow were Regional Regression Equations (RRE), Flood Frequency Analysis (FFA), and models using HEC-HMS using the SCS curve number for different antecedent moisture conditions (CN_I, CN_{II} and CN_{III}). Flood Frequency Analysis was used for BrM 015002, which has streamflow data. The value of the SCS curve number (CN_I) was not used for further analysis because it was considered that it did not represent the worst scenario for scour due to the low flow rates produced. The bridge modeling approaches were 1D-WSPRO, 1D-Energy, 2D SA connection, 2D terrain modification with raised piers, and HEC-RAS 6.1 and 6.2.

Peak flows were estimated for an event based on the return period of a 100-year event. The results showed that for some bridges, when the peak flow estimated using Regional Regression Equations presented similar values than those estimated using the model HEC-HMS CN_{III}, such is the case of BrM No 007070 and BrM No 010738, where the Regional Regression Equations peak flow was 4% and 0.6% smaller than HEC-HMS CN_{III}, respectively. On the other hand, there were some bridges where the peak flows were yielded using the model HEC-HMS CN_{III}, such as BrM 015002 and BrM 013310, where the Regional Regression Equations peak flow was 23% and 70% smaller than the model HEC-HMS CN_{III}. At the same time, Flood Frequency Analysis was conducted for BrM 015002, and it was

found that its peak flow was 89% greater than the Regional Regression Equations peak flow and 50% greater than the HEC-HMS CN_{III} peak flow. Neither RRE nor HEC-HMS CN_{III} represented the maximum peak flow. According to the obtained results, it can be concluded that for those bridges that have stream flow data, it is necessary to perform Flood Frequency Analysis stream flow data. For those that do not have it, HEC-HMS CN_{III} possibly yields a more conservative maximum peak flow estimate for scour calculations than Regional Regression Equations. It is important to mention that the accuracy of the Regional Regression equations is associated with the mean standard error of the model used to determine the equations. Anderson (2020) describes the mean standard error of the model as a measure of how well the regression model fits the input data and represents the standard deviation of the differences between stream gage data and the corresponding prediction from the regression equation. For the state of Alabama, Anderson (2020) also shows that the standard error varies between 12 and 29% for a 1% exceedance probability or 100-Yr return period (analyzed scenario) depending on the flood zone, which can explain in some cases the worst-case scenario in peak flow calculations.

From the hydraulic point of view, it was found that the 1D bridge modeling approaches produced similar values associated with velocity and water depths. These approaches showed a similar floodplain for the different alternatives to calculate the peak flow, Regional Regression Equations, HEC-HMS CN_{II} and HEC-HMS CN_{III}. For the simple channel geometries, the 2D modeling approaches show a wider floodplain, faster water velocities, and shallower water depths than the 1D approaches. These included the 2D SA connection and the 2D terrain modification with raised piers which was considered the benchmark for comparison. For three of the four bridges, the 2D approaches showed a worse-case scenario for scour calculations than the 1D approaches. When the 2D models were

compared with each other, the 2D SA connection behaved like a flow control in a bridge cross section, a situation that was not noticed in the 2D terrain modification with raised piers.

To compare the velocities and water depths, an average velocity and water depth were calculated using the results at each pier. For three of the four bridges, BrM No 015002 over Little Bridges Creek, BrM No. 010738 over Blue Creek, and BrM No. 007070, the benchmark model produced a larger velocity and shallow water depth than the other approaches, scenario related with more scour depth. For the remaining bridge, corresponding to Bridge BrM No. 013310 over the Conecuh River the hydraulic behavior was different, the worst-case scenario was yielded by 1D models, specifically 1D Energy, but it was noticed that for the complex geometry of that channel approach, the 1D models did not reproduce well the hydraulics of the bridge opening.

A peak-to-average analysis was proposed to compare the HEC-18 pier scour results for each bridge modeling approach. The peak-to-average diagram helped to normalize the results of each bridge modeling approach so that they could be compared. Three different diagrams were created to show the peak-to-average for scour, in each hydraulic approach and the alternatives analyzed to calculate the peak flow. The diagrams indicate that 2D models have a higher scour peak-to-average, indicating higher velocities and deeper scour depth. 1D models have a lower peak-to-average, corresponding to low velocities and scour depth. Bridge BrM 013310 had the maximum scour values and peak to average for 1D energy, but these models are not suitable for describing the complex hydraulics of that bridge approach channel, as they do not accurately represent the bridge's hydraulic system.

In addition, a comparison was performed using the 2D terrain modification with raised piers (benchmark) as the bridge modeling approach but varying the alternative for calculating the peak flow. The pier scour values for each of the bridges were averaged to

determine which peak flow alternative exhibited the highest average scour. The results of these models were also compared, and percentage differences were found between the Regional Regression Equations (a method that the DOT often uses) and the other peak flows that were looked at. The result of these analyses showed that, for most of the cases, HEC-HMS CN_{III} presented the worst-case scenario for scour and not for the Regional Regression Equations. Nevertheless, the use of wet antecedent moisture CN_{III} conditions is justifiable in zones such as the southeast of the United States or that exhibit the same behavior as the humid zones of the state of Alabama.

Comparisons were made between the HEC-18 and OMS pier scour. The results display values within the obtained ranges without considering the approach. The HEC-18 pier scour depth results showed differences of 33.7 to 51.7% greater than OMS for bridge BrM No. 015002, 164.7 to 210.5% for bridge BrM No. 010738, 20% to 61.4% for bridge BrM No. 013310, and BrM No. 007070, the differences were unmeasurable.

To sum up, scour estimates using approach HEC-18 depend on the choices for hydrological and hydraulic modeling tools. The 1D models are comparable to one another in some cases but have limited usefulness in complex bridge crossings. For such models, the deserved results indicated larger depths upstream of the modeled bridge, and the bridge acts as a control section at the entrance often reducing velocity and scour. For the 2D models, larger velocities were often noticed, and flow representation is more reasonable for complex stream cross sections which should improve scour estimations in most cases.

5.1 Recommendations

It is important that the state DOTs improve their approaches to scour calculations. This research indicates that there can be significant differences between estimated peak flows, and the most conservative method, albeit justifiable, needs to be selected. The errors associated with RRE can be too significant, and due to the importance of bridge structures, hydrological modeling needs to be used more frequently. Likewise, when complex bridge cross sections are considered, 2D hydraulic models should be the selected approach, as the assumptions used in 1D modeling tools may not lead to representative velocity and depths during peak flow conditions near these structures.

The obtained results where HMS CN_{III} presented the worst-case scenario for scour makes sense only in humid areas, but such an assessment needs to be validated if a similar study is performed for bridges in arid states.

5.2 Futures studies

A subsequent investigation is suggested to analyze more bridges in comparison in order to have a representative sample of the hydraulic and hydrological behavior. This study could identify trends in the different hydraulic approaches, grouping the bridges according to characteristics as slope, similar geometry, type of piers, an alignment of the approach channel and identifying why some differences were found in the present research.

Additionally, it is important to consider in future studies more combinations of 1D models for the main channel and 2D models for the floodplain and analyze if those models have similar behavior to the benchmark. Finally, it would be important to incorporate other

2D models, such as SRH-2D which is sponsored by the Federal Highway Administration (FHWA).

6. REFERENCES

Anderson, B.T. (2020) Magnitude and frequency of floods in Alabama, 2015: U.S. Geological Survey Scientific Investigations Report 2020–5032, 148 p.

Arneson, L. A., & Shearman, J. O. (1998). User's Manual For WSPRO: A Computer Model for Water Surface Profile Computations (No. FHWA-SA-98-080). United States. Federal Highway Administration. Office of Technology Applications.

Bergendahl, B. S., and L. A. Arneson. FHWA hydraulic toolbox (version 4.2): Federal Highway Administration, accessed March 3, 2021. (2014).

Beven, K. J., & Kirkby, M. J. (1979). A physically based, variable contributing area model of basin hydrology. Hydrological Sciences Journal, 24(1), 43-69.

Briaud, J.L., F.C.K. Ting, H.C. Chen, R. Gudavaiii, K. Kwak, B. Philogene, S.W. Han., S. Perugu, G. Wei, P. Nurtjahyo, Y. Cao, Y. Li, (1999), "SRICOS Prediction of Scour Rate at Bridge Piers," Report 2937-F, Texas Depart. of Transportation, Texas A&M University, Civil Engineering, College Station, TX 77843-3136.

Briaud, J.-L., Govindasamy, A. V., Kim, D., Gardoni, P., Olivera, F.,Chen, H., Mathewson, C. C., and Elsbury, K. (2009).“Simplified method for estimating scour at bridges.” Rep. 0 5505-1, Texas De-partment of Transportation, Austin, TX

Briaud, J.L., H.C. Chen, K.A. Chang, S.J. Oh, S. Chen, J. Wang, Y. Li, K. Kwak, P. Nartjaho, R. Gudaralli, W. Wei, S. Pergu, Y.W. Cao, and F. Ting. (2011) "The Sricos – EFA Method" Summary Report, Texas A&M University.

Brown, S. A., Schall, J. D., Morris, J. L., Stein, S., & Warner, J. C. (2009). Urban drainage design manual: hydraulic engineering circular 22 (No. FHWA-NHI-10-009). National Highway Institute (US).

Brunner G. W., CEIWR-HEC, (2020) HEC-RAS River Analysis System User's Manual Version 6.0, US Army Corps of Engineers–Hydrologic Engineering Center, Davis, CA 703

Brunner, G. W. (2016). HEC-RAS River Analysis System: Hydraulic Reference Manual, Version 5.0. US Army Corps of Engineers–Hydrologic Engineering Center, 547.

Brunner, G. W. (2020). HEC-RAS River Analysis System: Hydraulic Reference Manual, Version 6.0 Beta. US Army Corps of Engineers–Hydrologic Engineering Center, 520.

Brunner, G. W., & CEIWR-HEC, (2016). HEC-RAS River Analysis System, 2D Modeling User's Manual Version 5.0. US Army Corps of Engineers, Institute for Water Resources, Hydrologic Engineering Center, Davis, CA, USA.

Brunner, G. W., Hunt, J. H., & Hydrologic Engineering Center, Davis CA. (1995). A Comparison of the One-Dimensional Bridge Hydraulic Routines from HEC-RAS, HEC-2 and WSPRO.

Brunner, G., Savant, G., & Heath, R. (2020). Modeler application guidance for steady vs unsteady, and 1D vs 2D vs 3D hydraulic modeling. Hydrologic Engineering Center, Davis, California, USA.

Carswell Jr., & William J.(2013), The 3D Elevation Program: summary for AlabamA, U.S. Geological Survey, Report 2013-3105, Reston, VA

Chabert, J., & Engeldinger, P. (1956). Study of scour around bridge piers. Rep. Prepared for the Laboratoire National d'Hydraulique, Chatou, France.

Chang, F. M., & Yevjevich, V. M. (1962). Analytical study of local scour (Doctoral dissertation, Colorado State University. Libraries).

Chen, Y. (2018). Distributed Hydrological Models. In: Duan, Q., Pappenberger, F., Thielen, J., Wood, A., Cloke, H., Schaake, J. (eds) Handbook of Hydrometeorological Ensemble Forecasting. Springer, Berlin, Heidelberg

Chow, V. T. (1953) Frequency analysis of hydrologic data with special application to rainfall intensities, bulletin no. 414, University of Illinois Eng. Station.

Chow, V.T., Maidment, D.R., and Mays, L.W. (1988). Applied hydrology. McGraw-Hill, New York, NY.

Clark, C.O. 1945. "Storage and the Unit Hydrograph." Transactions of the American Society of Civil Engineers 110, pp. 1419-1446.

Cohn, T.A., England, J.F., Berenbrock, C.E., Mason, R.R., Stedinger, J.R., and Lamontagne, J.R., 2013, A generalized Grubbs-Beck test statistic for detecting multiple potentially influential low outliers in flood series: Water Resources Research, v. 49, no. 8, p. 5047–5058

Cohn, T.A., Lane, W.L., and Baier, W.G., 1997, An algorithm for computing moments-based flood quantile estimates when historical flood information is available: Water Resources Research, v. 33, no. 9, p. 2089–2096.

Dewitz, J., and U.S. Geological Survey. 2021. National Land Cover Database (NLCD) 2019 Products (ver. 2.0, June 2021): U.S. Geological Survey data release. June 4

Einstein, H. A. (1950). The bed-load function for sediment transportation in open channel flows No. 1026). US Department of Agriculture.

England Jr, J. F., Cohn, T. A., Faber, B. A., Stedinger, J. R., Thomas Jr, W. O., Veilleux, A. G., ... & Mason Jr, R. R. (2019). Guidelines for determining flood flow frequency—Bulletin 17C (No. 4-B5). US Geological Survey.

Ettema, R. (1976). Influence of bed gradation on local scour: Report No. 124. University of Auckland, School of Engineering, New Zealand. Ettema, R. (1980). Scour at bridge piers: Report No. 216. University of Auckland, School of Engineering, New Zealand

Ettema, R., 1980, "Scour at Bridge Piers," Report 215, Dept. of Civil Engineering, University of Auckland, Auckland, New Zealand.

Feaster, T.D., Kolb, K.R., Painter, J.A., and Clark, J.M. (2020) Methods for estimating selected low-flow frequency statistics and mean annual flow for ungaged locations on Streams in Alabama: U.S. Geological Survey Scientific Investigations Report 2020–5099, 21 p.

Federal Highway Administration, 1988, "Scour at Bridges," Technical Advisory T5140.20, updated by Technical Advisory T5140.23, October 28, 1991, "Evaluating Scour at Bridges," U.S. Department of Transportation, Washington, D.C.

Feldman, A. D. (2000). Hydrologic modeling system HEC-HMS: technical reference manual [report documentation page–us army corps of engineers]. Computer Software Techical Reference Manual. USA: HQ US Army Corps of Engineers.

Fleming, M. J., & Doan, J. H. (2009). HEC-GeoHMS geospatial hydrologic modelling extension: User's manual version 4.2. US Army Corps of Engineers, Institute for Water Resources, Hydrologic Engineering Centre, Davis, CA.

Flynn, K.M., Kirby, W.H., and Hummel, P.R., 2006, User's manual for program PeakFQ, Annual Flood Frequency Analysis Using Bulletin 17B Guidelines: U.S. Geological Survey Techniques and Methods Book 4, Chapter B4, 42 pgs.

Froehlich, D. C., & Pilarczyk, K. W. (2017). Bridge scour and stream instability countermeasures: experience, selection, and design guidance. CRC Press.

Ghelardi, V. "FHWA hydraulic toolbox (version 5.1): Federal Highway Administration, accessed March 3, 2021." (2021).

Goudriaan, J., & Monteith, J. L. (1990). A mathematical function for crop growth based on light interception and leaf area expansion. Annals of Botany, 66(6), 695-701.

Govindasamy, A. V., Briaud, J. L., Kim, D., Olivera, F., Gardoni, P., & Delphia, J. (2013). Observation method for estimating future scour depth at existing bridges. Journal of Geotechnical and Geoenvironmental Engineering, 139(7), 1165-1175.

Green, W. H., & Ampt, G. A. (1911). Studies on Soil Phyics. The Journal of Agricultural Science, 4(1), 1-24.

Hamill, L. (1999). Bridge Hydraulics, E and FN Spon. Routledge, London. Khosronejad, A., S. Kang, and F. Sotiropoulos (2012), Experimental and computational investigation of local scour around bridge piers, Adv. Water Resour, 37, 73-85.

Hedgecock, T. S., & Lee, K. G. (2010). Magnitude and frequency of floods for urban streams in Alabama, 2007 (Vol. 2010). US Department of the Interior, US Geological Survey.

Hedgecock, T.S. (2004) Magnitude and Frequency of Floods on Small Rural Streams in Alabama: U. S. Geological Survey Scientific Investigations Report 2004-5135, 10 p.

Hydrologic Engineering Center (2023) HEC-RAS, HEC-RAS Mapper User's Manual Modeling User's Manual Version 6.0. US Army Corps of Engineers, Davis, CA, USA.

Interagency Committee on Water Data (IACWD). (1982). "Guidelines for determining flood flow frequency." Bulletin 17B (revised and corrected), Hydrol. Subcomm., Washington, D.C.

Jones, J.S. (1983), Comparison of Prediction Equations for Bridge Pier and Abutment Scour, Transportation Research Board, Transportation Research Record 950, Second Bridge Engineering Conference, Vol. 2, Transportation Research Board, Washington, D.C.

Jones, J.S. and D.M. Sheppard, (2000) Local Scour at Complex Pier Geometries, Proceedings of the ASCE 2000 Joint Conference on Water Resources Engineering and Water Resources Planning and Management, July 30 - August 2, Minneapolis, MN

L.A. Arneson, L.W. Zevenbergen, P.F. Lagasse, P.E. Clopper. (2012) Evaluating scour at bridges. No. FHWA-HIF-12-003. Hydraulic Engineering Circular 18, United States. Federal Highway Administration

Lagasse, P. F., Clopper, P. E., Pagan-Ortiz, J. E., Zevenbergen, L. W., Arneson, L. A., Schall, J. D., & Girard, L. G. (2009). Bridge scour and stream instability countermeasures: experience, selection, and design guidance: Volume 2 (No. FHWA-NHI-09-112). National Highway Institute (US).

Lagasse, P.F., L.W. Zevenbergen, W.J. Spitz, and L.A. Arneson, Federal Highway Administration, 2012, "Stream Stability at Highway Structures," Hydraulic Engineering Circular No. 20, Fourth Edition, HIF-FHWA-12-004, Federal Highway Administration, Washington, D.C.

Laursen, E. M. (1956). The Application of Sediment-Transport Mechanics to Stable-Channel Design. Journal of the Hydraulics Division, 82(4), 1034-1.

Liu, H. K., Chang, F. M., & Skinner, M. M. (1961). Effect of bridge constriction on scour and backwater (Doctoral dissertation, Colorado State University. Libraries).

Maidment, D. R. (1993). Handbook of hydrology. McGraw-Hill, New York

Melville, B. W., & Sutherland, A. J. (1988). Design method for local scour at bridge piers. Journal of Hydraulic Engineering, 114(10), 1210-1226.

Melville, B.W. and Coleman, S.E. (2000). Bridge Scour. Water Resources Publications, LLC, Colorado, USA.

Mockus, V. (1972). Section 4 Hydrology, Chapter 21. Design Hydrographs. National Engineering Handbook Section, 4.

Monteith, J., & Unsworth, M. (2013). Principles of environmental physics: plants, animals, and the atmosphere. Academic Press.

Mueller, D.S., 1996, "Local Scour at Bridge Piers in Nonuniform Sediment Under Dynamic Conditions," Dissertation in partial fulfillment of the requirements for the Degree of Doctor of Philosophy, Colorado State University, Fort Collins, CO

Mulvaney, T. J. (1851). On the use of self-registering rain and flood gauges in making observations of the relations of rain fall and flood discharges in a given catchment. Transactions of the Institution of Civil Engineers of Ireland , Vol. IV, pt. II, 18-33.

Neitsch, S. L., Arnold, J. G., Kiniry, J. R., & Williams, J. R. (2011). Soil and water assessment tool theoretical documentation version 2009. Texas Water Resources Institute.

Penman, H. L. (1948). Natural evaporation from open water, bare soil and grass. Proceedings of the Royal Society of London. Series A. Mathematical and Physical Sciences, 193(1032), 120-145.

Perica, S., Martin, D., Pavlovic, S., Roy, I., St Laurent, M., Trypaluk, C., ... & Bonnin, G. (2013). Precipitation-Frequency Atlas of the United States. Volume 9, Version 2.0. Southeastern States; Alabama, Arkansas, Florida, Georgia, Louisiana, Mississippi.

Pokharel, Sudan. Evaluating and Understanding of Bridge Scour Calculation. Master Thesis, Auburn University, 2017.

Prendergast, L. J., & Gavin, K. (2014). A review of bridge scour monitoring techniques. Journal of Rock Mechanics and Geotechnical Engineering, 6(2), 138-149.

Priestley, C. H. B. and Taylor, R. J.: 1972, 'On the Assessment of Surface Heat Flux and Evaporation Using Large-Scale Parameters', Mon. Wea. Rev. 100, 81–92.

Richardson, E. V., & Davis, S. R. (1993). Evaluating scour at bridges (No. HEC 18). United States. Federal Highway Administration. Office of Technology Applications.

Richardson, E. V., & Davis, S. R. (2001). Evaluating scour at bridges (No. HEC-18). U.S. Army Engineer Research and Development Center, Coastal and Hydraulics Laboratory.

Richardson, E.V. and Davis, S.R. (1995). Evaluating scour at bridges. Third edition. Publication No. FHWA IP 90-017, Hydraulic Engineering Circular No. 18. National Highway Institute, U. S. Department of Transportation, Federal Highway Administration.

Richardson, E.V. and Davis, S.R. (2001). Evaluating scour at bridges. Fourth edition. Publication No. FHWA NHI 01-001, Hydraulic Engineering Circular No. 18. National Highway Institute, U. S. Department of Transportation, Federal Highway Administration.

Richardson, E.V., P.F. Lagasse, J.D. Schall, J.F. Ruff, T.E. Brisbane, and D.M. Frick, 1987, "Hydraulic, Erosion and Channel Stability Analysis of the Schoharie Creek Bridge Failure, New York," Resource Consultants, Inc. and Colorado State University, Fort Collins, CO.

Ries III, K. G., and J. B. Atkins. (2007) The national streamflow statistics program: A computer program for estimating streamflow statistics for ungaged sites. DIANE Publishing, 2007.

Ries III, K. G., Steeves, P. A., Coles, J. D., Rea, A. H., & Stewart, D. W. (2004). StreamStats: a US Geological Survey web application for stream information (No. 2004-3115).

Ries III, K.G., Steeves, P.A., Coles, J.D., Rea, A.H., and Stewart, D.W., 2004, StreamStats: A U.S. Geological Survey web application for stream information: U.S.

Geological Survey Fact Sheet 2004–3115, 4 p. Ries III, K.G., and Dillow, J.J.A., 2006, Magnitude and frequency of floods on nontidal streams in Delaware: U.S. Geological Survey Scientific Investigations Report 2006–5146, p. 3

Robinson, Dusty, Alan Zundel, Casey Kramer, Royd Nelson, Will deRosset, John Hunt, Scott Hogan, Yong Lai, and L. L. C. Aquaveo. (2019) Two-Dimensional Hydraulic Modeling for Highways in the River Environment: Reference Document. No. FHWA-HIF-19-061. Federal Highway Administration (US)

Rossman, L. A. (2010). Storm water management model user's manual, version 5.0 (p. 276). Cincinnati: National Risk Management Research Laboratory, Office of Research and Development, US Environmental Protection Agency.

Salim, M. and J.S. Jones, 1995, "Effects of Exposed Pile Foundations on Local Pier Scour," Proceedings ASCE Water Resources Engineering Conference, San Antonio, TX.

Salim, M. and J.S. Jones, 1996, "Scour Around Exposed Pile Foundations," Proceedings ASCE North American and Water and Environment Congress, '96, Anaheim, CA (also issued as FHWA Memo).

Salim, M. and J.S. Jones, 1999, Scour Around Exposed Pile Foundations," ASCE Compendium, Stream Stability and Scour at Highway Bridges, Richardson and Lagasse (eds.), Reston, VA.

Sharp P., Mohamed K., Kerenyi K., Krolak, J. (2021) Scour Considerations within AASHTO LRFD Design Specifications, U.S. Federal Highway Administration. Office of Bridges and Structures, FHWA-HIF-19-060

Sheppard, D. M., & Renna, R. (2005). Bridge scour manual. Florida department of transportation. 605 Suwannee Street. Tallahassee. Florida.

Sheppard, D.M. (1999). Conditions of maximum local scour. Proceedings of Stream Stability and Scour at Highway Bridges, E. V. Richardson and P. F. Lagasse, eds., Reston, Va.

Sheppard, D.M. and Renna, R. (2010). Florida bridge scour manual. Florida Department of Transportation, Tallahassee.

Sheppard, D.M., (2001) "A Methodology for Predicting Local Scour Depths Near Bridge Piers with Complex Geometries," unpublished design procedure, University of Florida, Gainesville, FL.

Snyder, F. F. (1938). Synthetic unit-graphs. Eos, Transactions American Geophysical Union, 19(1), 447-454.

Soil Survey Staff, NRCS, USDA. 2015. Soil Survey Geographic Database (SSURGO). 12 29.

USACE (2000). HEC-HMS hydrological modeling system user's manual. Hydrologic Engineering Center, Davis, CA

Wang, C., Yu, X. & Liang, F. (2017). A review of bridge scour: mechanism, estimation, monitoring and countermeasures. Nat Hazards 87, 1881–1906

Zevenbergen, L. W., Arneson, L. A., Hunt, J. H., & Miller, A. C. (2012). Hydraulic design of safe bridges (No. FHWA-HIF-12-018). United States. Federal Highway Administration.

7. APPENDIX

7.1 Particle Size distribution

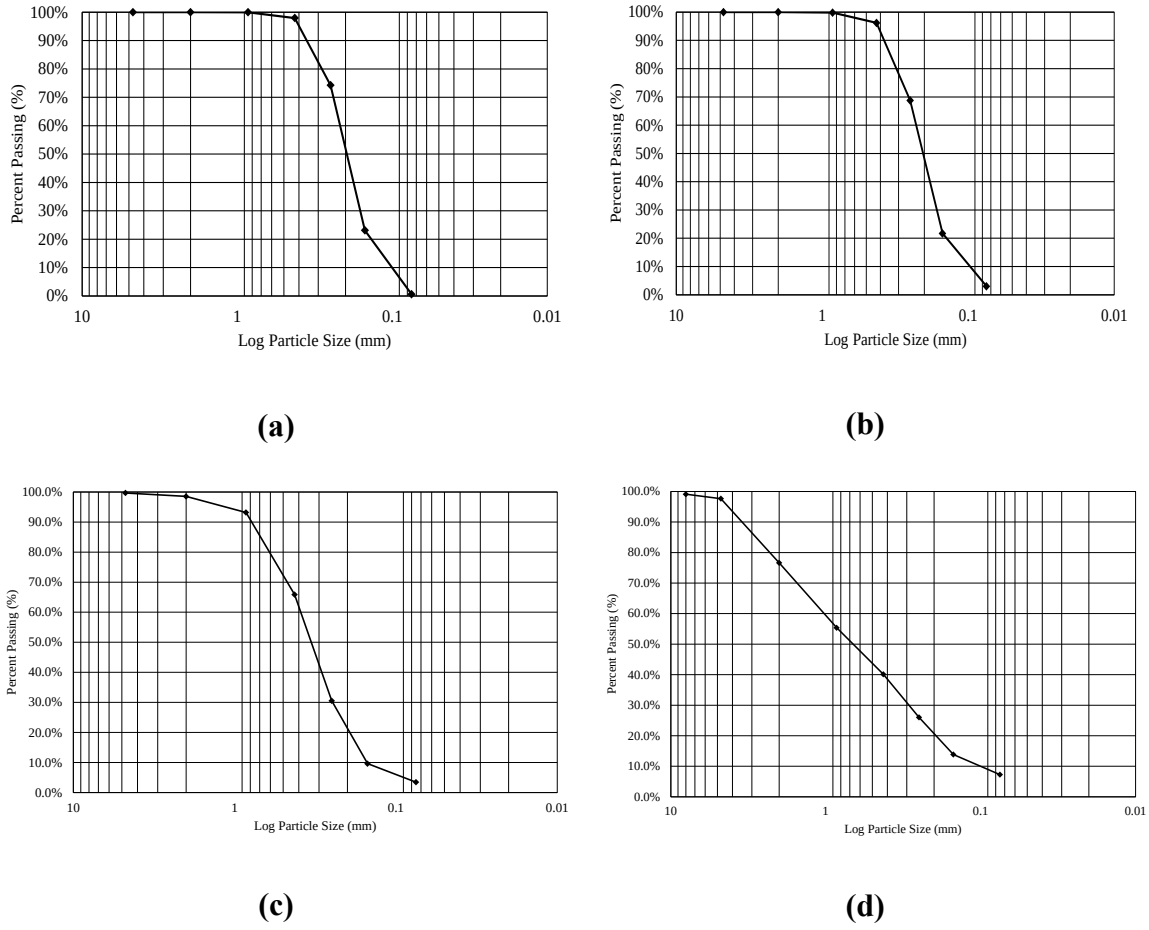

Figure A1 .Particle site distribution for the analyzed bridges (a) BrM No 015002, (b) BrM No 010738, (c) BrM No 013310, (d) BrM No 007070

7.2 Scour results calculations using HEC-18

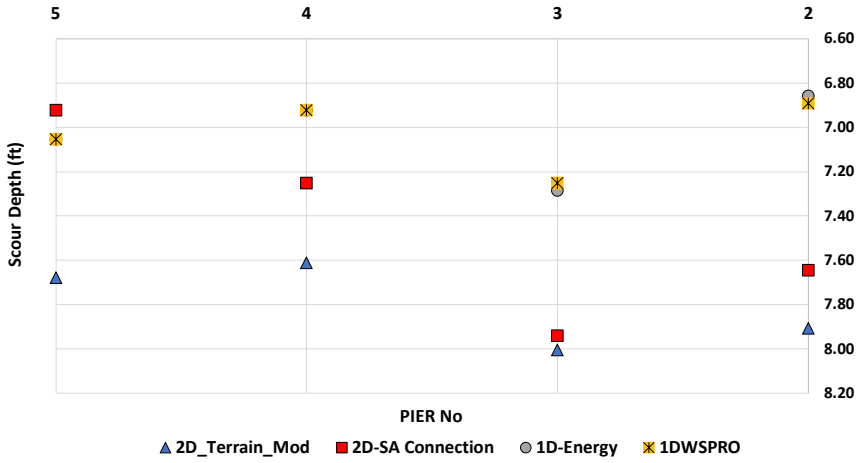

Figure A2. Scour results for Bridge BrM 015002 using HEC-18. Different Bridge modeling approaches. Peak Flow RRE

Table A1. Scour values for Bridge BrM 015002 using HEC-18. Different Bridge modeling approaches. Peak Flow RRE

PIER BrM	1D- WSPRO	1D- Energy	2D- SA Connection	2D_Terrain_Mod
2	6.9 ft	6.9 ft	7.6 ft	7.9 ft
3	7.3 ft	7.3 ft	7.9 ft	8.0 ft
4	6.9 ft	6.9 ft	7.3 ft	7.6 ft
5	7.1 ft	7.1 ft	6.9 ft	7.7 ft

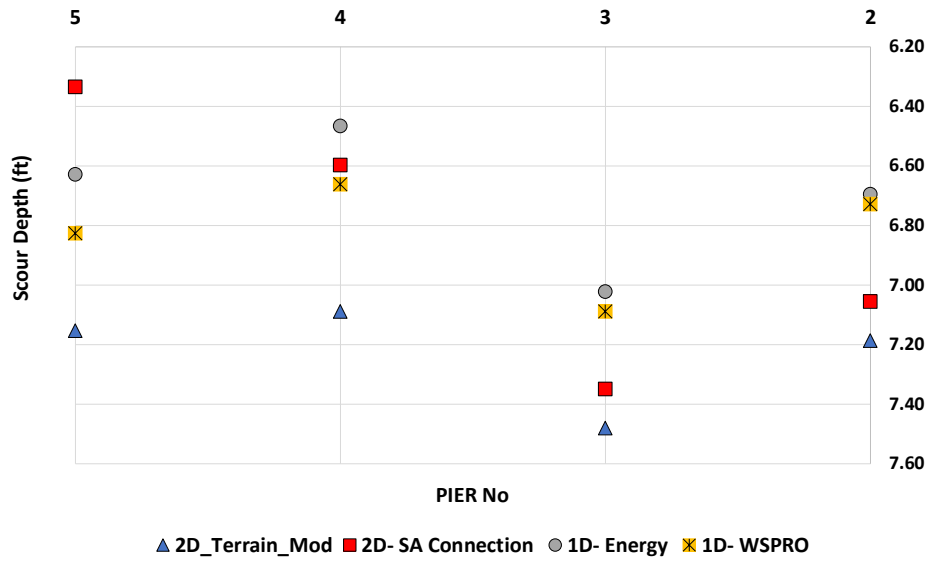

Figure A3. Scour results for Bridge BrM 015002 using HEC-18. Different Bridge modeling approaches. Peak Flow CN_{II}

Table A2. Scour values for Bridge BrM 015002 using HEC-18. Different Bridge modeling approaches. Peak Flow CN_{II}

PIER BrM	1D- WSPRO	1D- Energy	2D- SA Connection	2D_Terrain_Mod
2	6.7 ft	6.7 ft	7.1 ft	7.2 ft
3	7.1 ft	7.0 ft	7.3 ft	7.5 ft
4	6.7 ft	6.5 ft	6.6 ft	7.1 ft
5	6.8 ft	6.6 ft	6.3 ft	7.2 ft

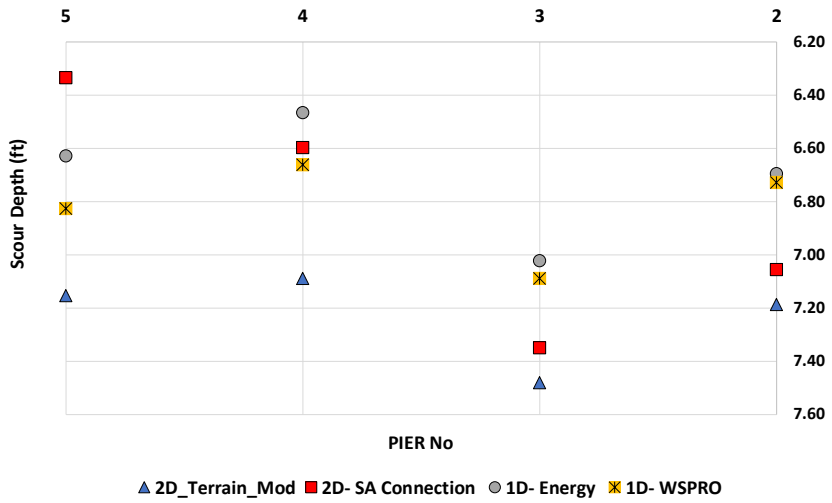

Figure A4. Scour results for Bridge BrM 015002 using HEC-18. Different Bridge modeling approaches. Peak Flow CN_{III}

Table A3. Scour values for Bridge BrM 015002 using HEC-18. Different Bridge modeling approaches. Peak Flow CN_{III}

PIER BrM	2D_Terrain_Mod	2D- SA Connection	1D- Energy	1D- WSPRO
2	8.3 ft	7.9 ft	7.6 ft	7.6 ft
3	8.5 ft	8.2 ft	7.8 ft	7.8 ft
4	8.1 ft	7.5 ft	7.5 ft	7.5 ft
5	8.1 ft	7.2 ft	7.6 ft	7.7 ft

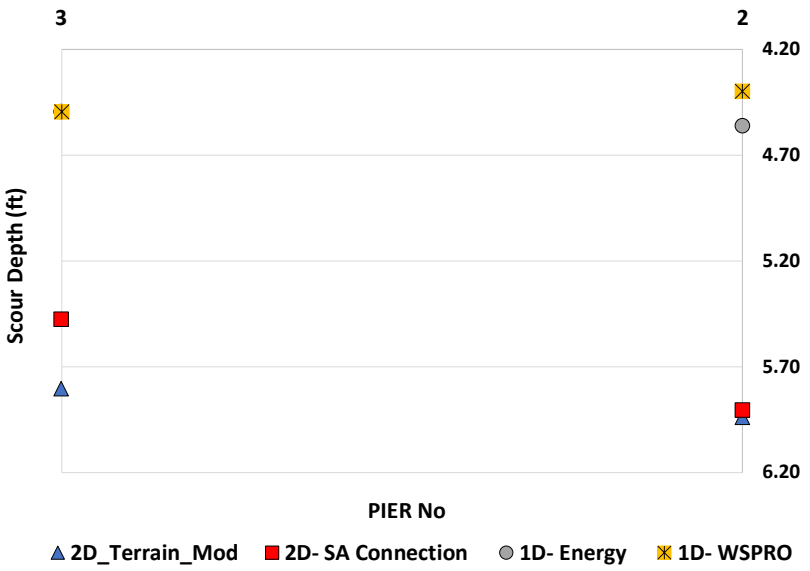

Figure A5. Scour results for Bridge BrM 010738 using HEC-18. Different Bridge modeling approaches. Peak Flow RRE

Table A4. Scour values for Bridge BrM 010738 using HEC-18. Different Bridge modeling approaches. Peak Flow RRE

Pier BrM	1D- WSPRO	1D- Energy	2D- SA Connection	2D_Terrain_Mod
2	4.4 ft	4.6 ft	5.9 ft	5.9 ft
3	4.5 ft	4.5 ft	5.5 ft	5.8 ft

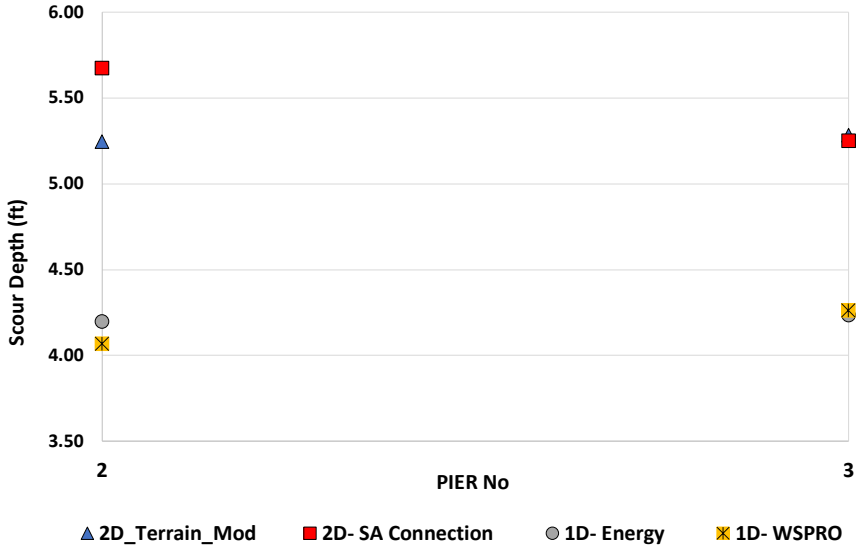

Figure A6. Scour results for Bridge BrM 010738 using HEC-18. Different Bridge modeling approaches. Peak Flow CN_{II}

Table A5. Scour values for Bridge BrM 010738 using HEC-18. Different Bridge modeling approaches. Peak Flow CN_{II}

Pier BrM	1D- WSPRO	1D- Energy	2D- SA Connection	2D_Terrain_Mod
2	4.1 ft	4.2 ft	5.7 ft	5.2 ft
3	4.3 ft	4.2 ft	5.2 ft	5.3 ft

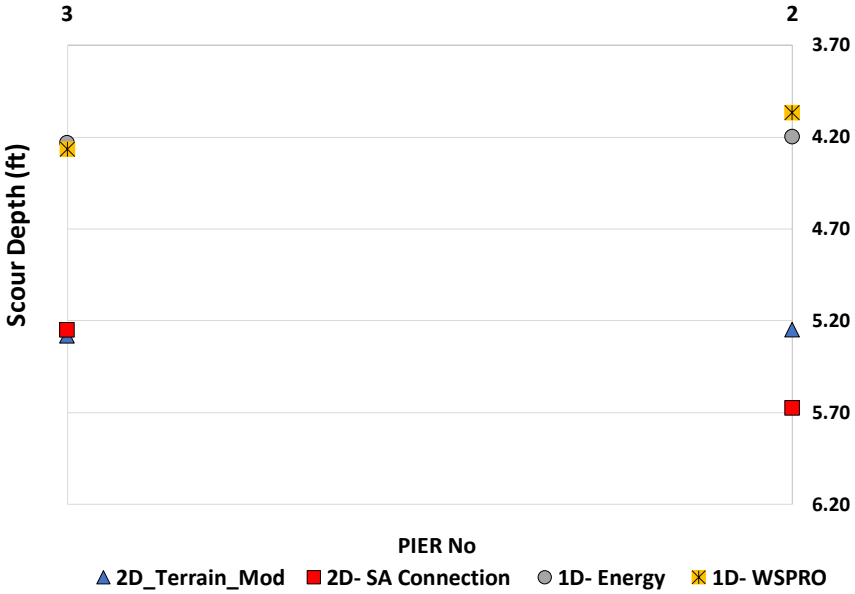

Figure A7. Scour results for Bridge BrM 010738 using HEC-18. Different Bridge modeling approaches. Peak Flow CN_{III}

Table A6. Scour values for Bridge BrM 010738 using HEC-18. Different Bridge modeling approaches. Peak Flow CN_{III}

Pier BrM	1D- WSPRO	1D- Energy	2D- SA Connection	2D_Terrain_Mod
2	4.3 ft	4.4 ft	5.4 ft	5.6 ft
3	4.3 ft	4.3 ft	5.9 ft	5.6 ft

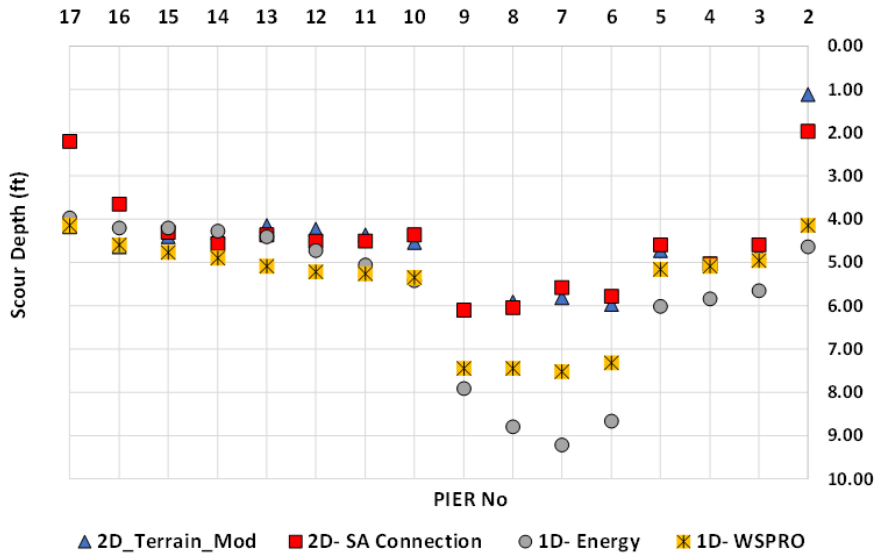

Figure A8. Scour results for Bridge BrM 013310 using HEC-18. Different Bridge modeling approaches. Peak Flow RRE

Table A7. Scour values for Bridge BrM 013310 using HEC-18. Different Bridge modeling approaches. Peak Flow RRE

Pier BrM	1D- WSPRO	1D- Energy	2D- SA Connection	2D_Terrain_Mod
2	2.9 ft	3.6 ft	0.0 ft	0.0 ft
3	4.6 ft	5.2 ft	4.8 ft	3.4 ft
4	4.6 ft	5.5 ft	4.3 ft	3.9 ft
5	4.8 ft	5.6 ft	3.9 ft	3.6 ft
6	6.8 ft	8.1 ft	4.9 ft	4.2 ft
7	7.0 ft	8.7 ft	4.7 ft	4.2 ft
8	7.0 ft	8.2 ft	5.1 ft	4.3 ft
9	7.0 ft	7.3 ft	5.2 ft	4.5 ft
10	5.0 ft	5.0 ft	3.8 ft	3.4 ft
11	4.9 ft	4.6 ft	3.9 ft	3.3 ft
12	4.8 ft	4.3 ft	3.8 ft	3.1 ft
13	4.7 ft	3.9 ft	3.6 ft	3.0 ft
14	4.5 ft	3.8 ft	3.8 ft	3.1 ft
15	4.3 ft	3.7 ft	3.7 ft	3.1 ft
16	4.2 ft	3.7 ft	2.8 ft	3.4 ft
17	3.7 ft	3.4 ft	1.9 ft	2.8 ft

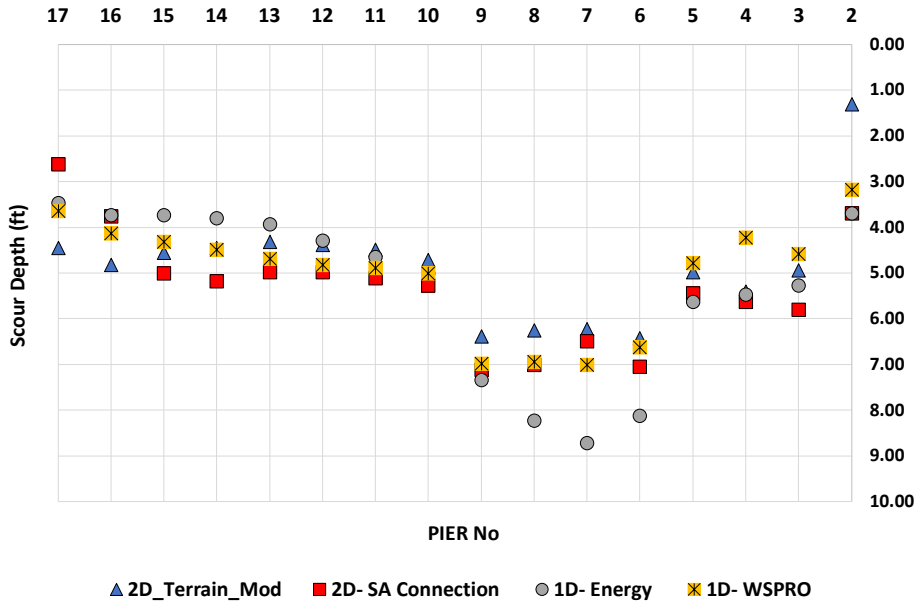

Figure A9. Scour results for Bridge BrM 013310 using HEC-18. Different Bridge modeling approaches. Peak Flow CN_{II}

Table A8. Scour values for Bridge BrM 013310 using HEC-18. Different Bridge modeling approaches. Peak Flow CN_{II}

Pier BrM	1D- WSPRO	1D- Energy	2D- SA Connection	2D_Terrain_Mod
2	3.2 ft	3.7 ft	3.7 ft	1.3 ft
3	4.6 ft	5.3 ft	5.8 ft	5.0 ft
4	4.2 ft	5.5 ft	5.6 ft	5.4 ft
5	4.8 ft	5.6 ft	5.4 ft	5.0 ft
6	6.6 ft	8.1 ft	7.1 ft	6.4 ft
7	7.0 ft	8.7 ft	6.5 ft	6.2 ft
8	7.0 ft	8.2 ft	7.0 ft	6.3 ft
9	7.0 ft	7.3 ft	7.1 ft	6.4 ft
10	5.0 ft	5.0 ft	5.3 ft	4.7 ft
11	4.9 ft	4.7 ft	5.1 ft	4.5 ft
12	4.8 ft	4.3 ft	5.0 ft	4.4 ft
13	4.7 ft	3.9 ft	5.0 ft	4.3 ft
14	4.5 ft	3.8 ft	5.2 ft	4.5 ft
15	4.3 ft	3.7 ft	5.0 ft	4.6 ft
16	4.1 ft	3.7 ft	3.8 ft	4.8 ft
17	3.6 ft	3.5 ft	2.6 ft	4.5 ft

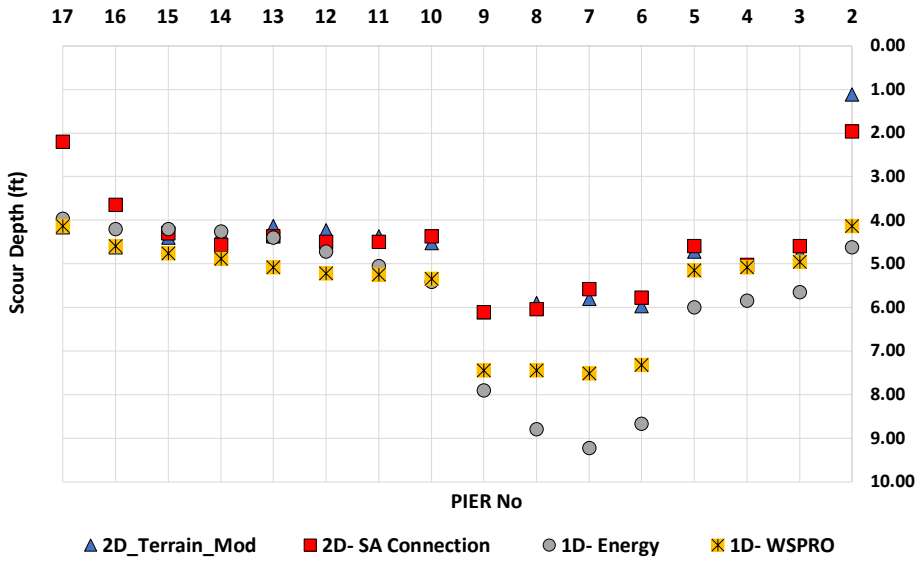

Figure A10. Scour results for Bridge BrM 013310 using HEC-18. Different Bridge modeling approaches. Peak Flow CN_{III}

Table A9. Scour values for Bridge BrM 013310 using HEC-18. Different Bridge modeling approaches. Peak Flow CN_{III}

Pier BrM	1D- WSPRO	1D- Energy	2D- SA Connection	2D_Terrain_Mod
2	4.13 ft	4.63 ft	1.97 ft	1.12 ft
3	4.95 ft	5.64 ft	4.59 ft	4.76 ft
4	5.09 ft	5.84 ft	5.02 ft	5.02 ft
5	5.15 ft	6.00 ft	4.59 ft	4.72 ft
6	7.32 ft	8.66 ft	5.77 ft	5.97 ft
7	7.51 ft	9.22 ft	5.58 ft	5.81 ft
8	7.45 ft	8.79 ft	6.04 ft	5.91 ft
9	7.45 ft	7.91 ft	6.10 ft	6.10 ft
10	5.35 ft	5.41 ft	4.36 ft	4.53 ft
11	5.25 ft	5.05 ft	4.49 ft	4.36 ft
12	5.22 ft	4.72 ft	4.49 ft	4.23 ft
13	5.09 ft	4.40 ft	4.36 ft	4.13 ft
14	4.89 ft	4.27 ft	4.56 ft	4.30 ft
15	4.76 ft	4.20 ft	4.30 ft	4.40 ft
16	4.59 ft	4.20 ft	3.64 ft	4.63 ft
17	4.13 ft	3.97 ft	2.20 ft	4.17 ft

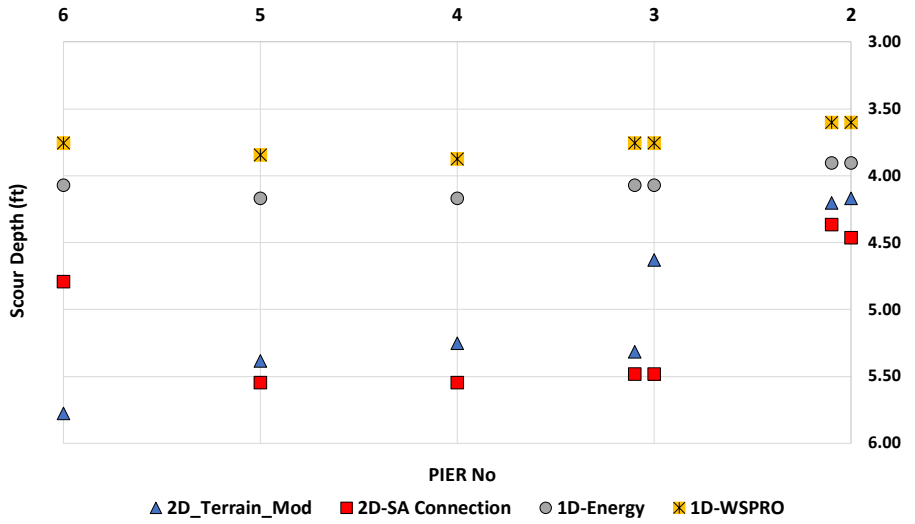

Figure A11. Scour results for Bridge BrM 007070 using HEC-18. Different Bridge modeling approaches. Peak Flow RRE

Table A10. Scour values for Bridge BrM 007070 using HEC-18. Different Bridge modeling approaches. Peak Flow RRE

Pier BrM	1D- WSPRO	1D- Energy	2D- SA Connection	2D_Terrain_Mod
2	3.6 ft	3.9 ft	4.5 ft	4.2 ft
2.1	3.6 ft	3.9 ft	4.4 ft	4.2 ft
3	3.8 ft	4.1 ft	5.5 ft	4.6 ft
3.1	3.8 ft	4.1 ft	5.5 ft	5.3 ft
4	3.9 ft	4.2 ft	5.5 ft	5.2 ft
5	3.8 ft	4.2 ft	5.5 ft	5.4 ft
6	3.8 ft	4.1 ft	4.8 ft	5.8 ft

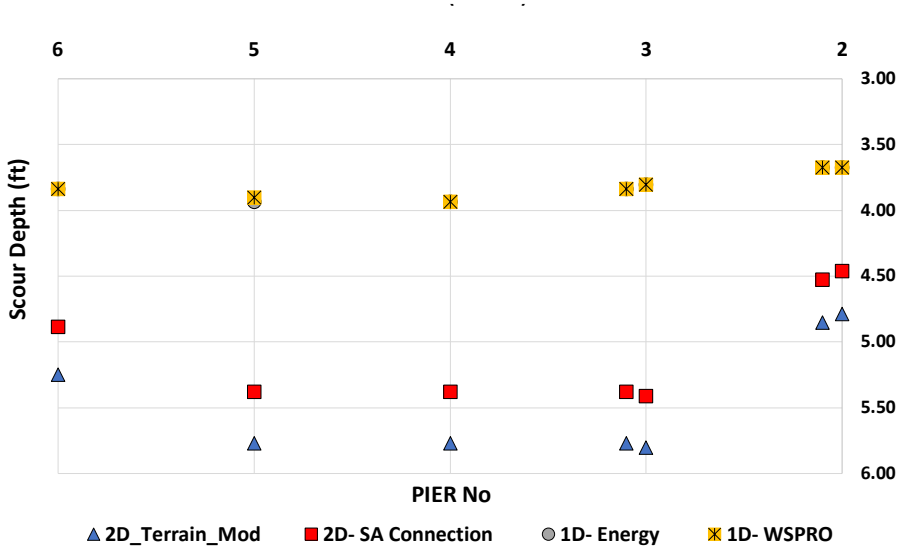

Figure A12.Scour results for Bridge BrM 007070 using HEC-18. Different Bridge modeling approaches. Peak Flow CN_{II}

Table A 11. Scour values for Bridge BrM 007070 using HEC-18. Different Bridge modeling approaches. Peak Flow CN_{II}

Pier BrM	1D- WSPRO	1D- Energy	2D- SA Connection	2D_Terrain_Mod
2	3.7	3.7	4.5	4.8
2.1	3.7	3.7	4.5	4.9
3	3.8	3.8	5.4	5.8
3.1	3.8	3.8	5.4	5.8
4	3.9	3.9	5.4	5.8
5	3.9	3.9	5.4	5.8
6	3.8	3.8	4.9	5.2

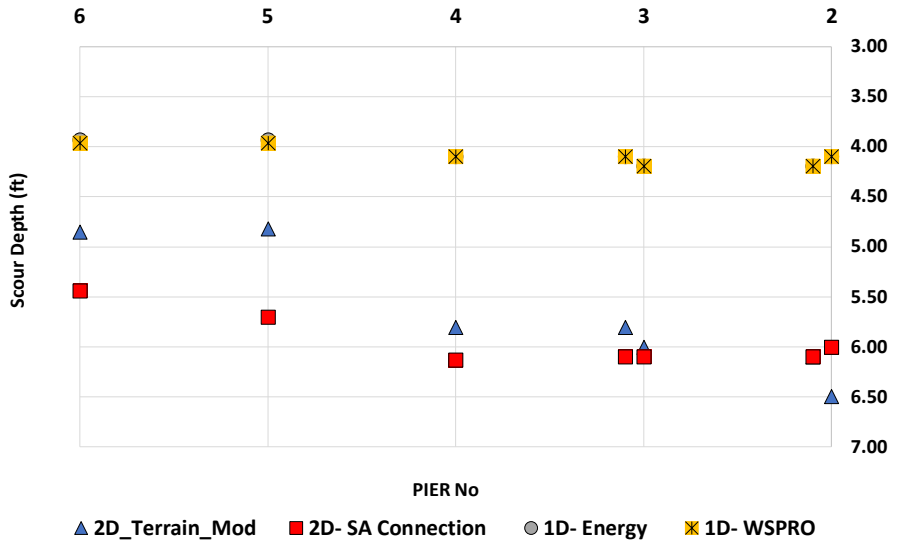

Figure A13. Scour results for Bridge BrM 007070 using HEC-18. Different Bridge modeling approaches. Peak Flow CN_{III}

Table A12. Scour values for Bridge BrM 007070 using HEC-18. Different Bridge modeling approaches. Peak Flow CN_{III}

Method	1D- WSPRO	1D- Energy	2D- SA Connection	2D_Terrain_Mod
2	4.1 ft	4.1 ft	6.0 ft	6.5 ft
2.1	4.2 ft	4.2 ft	6.1 ft	6.1 ft
3	4.2 ft	4.2 ft	6.1 ft	6.0 ft
3.1	4.1 ft	4.1 ft	6.1 ft	5.8 ft
4	4.1 ft	4.1 ft	6.1 ft	5.8 ft
5	4.0 ft	3.9 ft	5.7 ft	4.8 ft
6	4.0 ft	3.9 ft	5.4 ft	4.9 ft

7.3 Example of pier scour calculations using OMS for the Bridge 0133310

Step 1: Determine Z_{mo} using BrM (Figure C1)

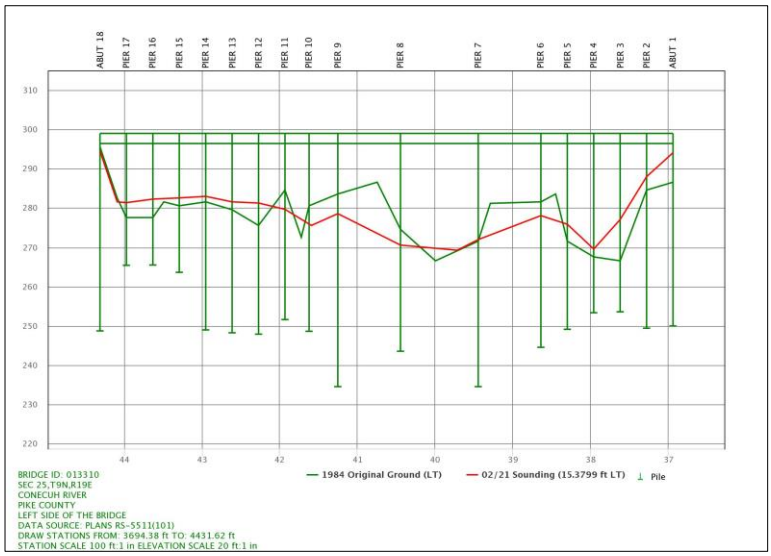

Figure C1. Sounding profile in BrM (Bridge BrM 015002)

En la Figure C1 se observa que la pila No 9 presenta una diferencia entre el terreno original y el terreno del último sondeo correspondiente a 5 ft. Este valor es escogido como valor de Z_{mo}.

Step 2: Determine de Recurrence Interval (RI)

To determine the recurrence interval (RI) was used the software TAMU Flood (Briaud et al, 2011), based on nearby stream gauges and rain gages. shows the input parameters for the software and Figure 3 illustrates the obtained values.

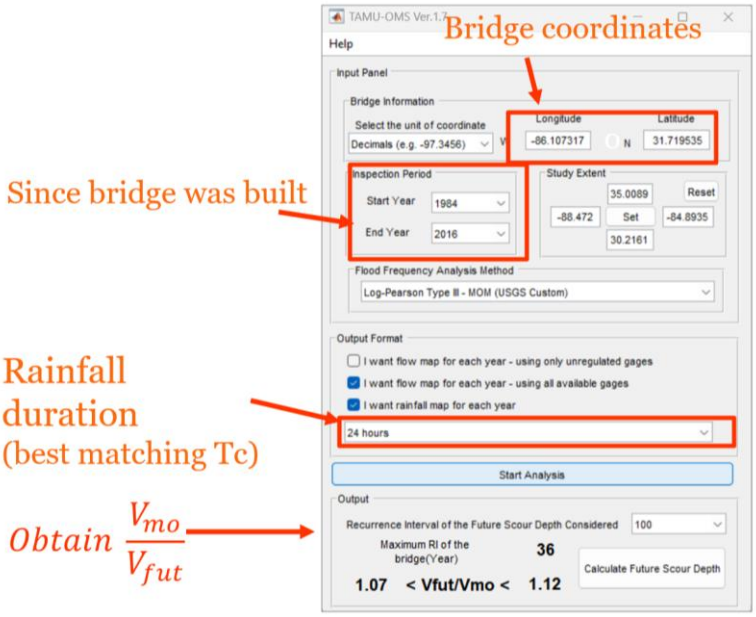

Figure C2. Input values in Tamu Flood (Briaud et. al, 2011)

The recurrence interval calculated was 36 years for the analyzed bridge.

Step 3: Obtain the ratio $Qmo/Qfut$ as a function of the recurrence interval.

$$1.07 < \frac{V_{mo}}{V_{fut}} < 1.12$$

$$\left(\frac{Q_{mo}}{Q_{fut}}\right)^{1/4} = 1.07 \qquad \left(\frac{Q_{mo}}{Q_{fut}}\right)^{2/5} = 1.12$$

Step 4: Future scour estimate

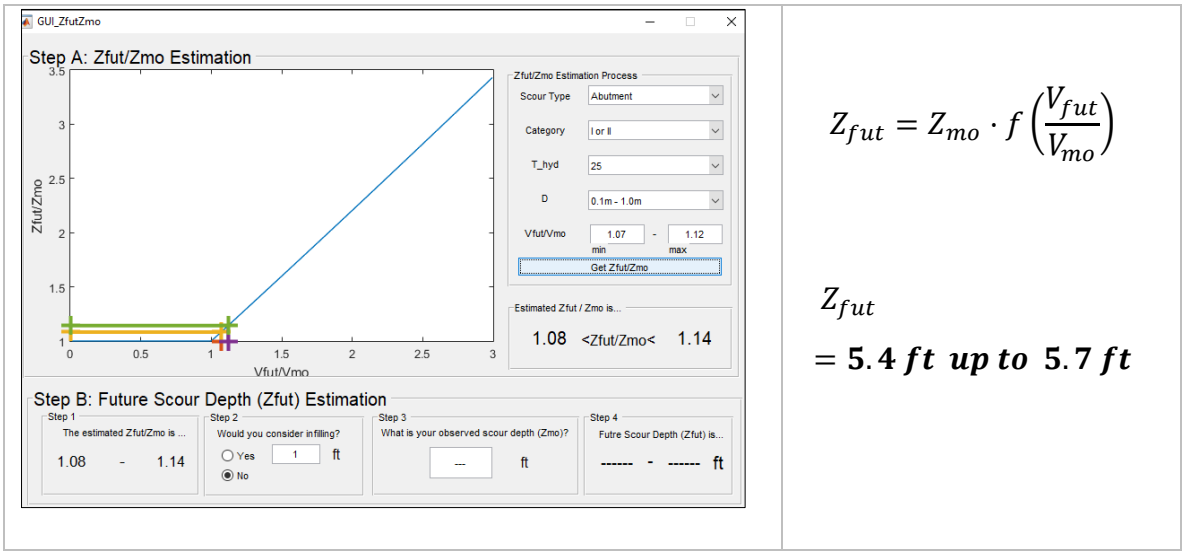

Figure C3. Future scour depth using Tamu Flood (Briaud et. al, 2011)

The obtained value for the future scour (Z_{mo}) corresponds to a value between 5.4 and 5.7 ft.